INSTATIONARY MODAL ANALYSIS FOR IMPULSE-TYPE STIMULATED STRUCTURES

Vom Fachbereich Produktionstechnik

der

UNIVERSITÄT BREMEN

zur Erlangung des Grades

Doktor- Ingenieur

genehmigte

Dissertation

von

Dipl-Ing. Linghan Li

Gutachter: Prof. Dr.-Ing. Bernd Kuhfuß

Prof. Dr. Peter Maaß

Tag der mündlichen Prüfung: 08.Mai. 2015

Vorwort

Die vorliegende Arbeit mit dem Titel *Instationary modal analysis for impulse-type stimulated structures* entstand während meiner Tätigkeit als Doktorand am Bremer Institut für Strukturmechanik und Produktionsanlagen an der Universität Bremen. Diese Arbeit basiert auf den Forschungen im Projekt „Scientific Computing in Engineerging“ unter der Leitung des Zentrums für Technomathematik von Herrn Prof. Dr. Peter Maaß. Hiermit möchte ich mich bei ihm für die Organisation des Projektes und die Begutachtung meiner Arbeit bedanken.

Mein besonderer Dank gilt meinem Doktorvater Herr Prof. Dr.-Ing. Bernd Kuhfuß, der meine Studien-, Diplom- sowie Doktorarbeit konstruktiv und technologisch betreut und die Arbeit begutachtet hat. Mit seinen kreativen Anregungen und wertvollen Diskussionen hat er dazu beigetragen diese Arbeit zu unterstützen. Durch seine sehr guten Vorlesungen habe ich bei ihm sehr viel gelernt.

Ganz besonders möchte ich mich bei Herrn Dr.-Ing. Christian Schenck bedanken. Während der gesamten Promotionsphase zeigte er sich hilfebereit. Auch die intensiven fachlichen und auch persönlichen Diskussionen und die daraus abgeleiteten Anregungen haben maßgeblich zum Gelingen meiner Arbeit beigetragen.

Weiterhin danke ich allen Mitarbeiterinnen und Mitarbeitern des Fachgebiets, insbesondere Frau Brigit Taeger, Dipl.-Ing. Frank Lichthorn, Dr.-Ing. Mohamed Nassef, Dipl.-Ing Eric Moumi, die mich, jeder auf seine Art, hilfsbereit unterstützten. Nicht vergessen möchte ich den Kollegen Dr. Bastian Kanning vom Zentrum für Technomathematik, dem ich für seine Zusammenarbeit einen besonderen Dank aussprechen möchte. Auch allen Studenten, die im Rahmen der Masterarbeiten und Bachelorarbeiten zum Fortschritt der Arbeit beigetragen haben, möchte ich mich an dieser Stelle bedanken.

Abschließend danke ich meiner ganzen Familie, insbesondere meiner Frau Dipl.-Kauffrau Songhui Han. Sie hat mir jederzeit hilfreich zur Seite gestanden und für das Gelingen der Arbeit unterstützt.

Stuttgart, im September 2015 Linghan Li

CONTENTS

Abstract

In order to determine modal parameters, classical experimental modal analysis can be used in engineering application. This method finds a system frequency response function using fast Fourier Transform (FFT). The Fourier Transform is one type of global data analysis method. The frequency resolution is equal to the reciprocal of the total sample time. So applying the FFT is not suitable for any transient signal to reveal local characteristics. However, in modern manufacturing industries, processing forces are rapidly changing. The dynamic behavior may vary rapidly in a short time due to variations in the machining parameters and changes in boundary conditions. These nonlinear and non-stationary dynamic parameters are not constant during machining operations identification using FFT.

In this research, an innovative transient signal analysis approach has been developed, which is based on an application of the least squares estimation. The proposed method provides transient information with high resolution and to identify the time-varying modal parameters during machining. Least squares estimation can be augmented with a sliding-window operation (SWLSE) to reveal the actual system dynamic behavior at any moment. The accuracy of this method depends on the window size, the noise ratio and the sampling rate etc. The estimation accuracy of modal parameters is discussed in this work.

To examine the efficiency of the SWLSE method experimental tests are performed on a laboratory beam system and the results are compared with the classical experimental modal analysis (CEMA) method. The laboratory beam system is designed and assembled that the stiffness and damping ratio of the structure can be adjusted. Additionally, the proposed method is applied to the identification of the actual modal parameters of machine tools during machining operations. In another application, the proposed method provides also the process varied damping information in a process monitoring.

Abstract in German

Zur Bestimmung des dynamischen Verhaltens eines mechanischen Systems werden experimentelle Modalanalysen durchgeführt. Das wesentliche Werkzeug der experimentellen Modalanalyse ist die Fast Fourier-Transformation (FFT). Mit ihr kann aus der Anregung und der Systemantwort die Übertragungsfunktion berechnet werden. Ein Nachteil der Fourier-Transformation ist, dass transiente Schwingungen nicht oder nur schlecht erfasst werden können. Da die Überführung des Problems in den Frequenzbereich mittels Fourier-Transformation erfolgt, hängt die erreichbare Auflösung von der Messdauer ab. Moderne Fertigungsprozesse werden häufig mit der Zielsetzung hoher Produktionsleistungen optimiert und weisen dementsprechend zeitlich schnell wechselnde und unregelmäßige oder impulsförmige Krafteinleitungen auf. Die modalen Parameter können mit Hilfe der klassischen Modalanalyse in diesem Fall schlecht oder nur unvollständig identifiziert werden.

Im Rahmen dieser Arbeit wird die Grundlage einer Least Squares Methode in Verbindung mit einer Fernsterfunktion (SWLSE) zur Identifikation der aktuellen modalen Parameter entwickelt und praktisch erprobt. Die Genauigkeit der Methoden ist abhängig von der Länge der Fernsterfunktion, der Rauschamplitude und der Abtastrate des Signals. Die Einflüsse werden in dieser Arbeit diskutieren.

Zur Überprüfung der entwickelte SWLSE Methode werden die experimentellen Untersuchungen sowohl an einem Versuchsträger mit einstellbarer Steifigkeit und Dämpfung als auch an einer realen Werkzeugmaschine durchgeführt. Die aktuellen Modalen Parameter werden in diesen Untersuchungen mit Hilfe der SWLSE Methode bestimmt. Die Ergebnisse werden auch mit den Ergebnissen der klassischen experimentellen Modalanalyse verglichen. Die Potentiale der vorgestellten Methode zur Prozessüberwachung werden beispielhaft an den Fertigungsverfahren Fräsen und Rundkneten demonstriert.

List of Abbreviations

AMP	Amplitude
ARMAV	Autoregressive Moving Average Vector
CEMA	Classical Experimental Modal Analysis
CPU	Central Processing Unit
dB	Decibel
DRY	Dry Milling
EMA	Experimental Modal Analysis
EMD	Empirical Mode Decomposition
Eq	Equation
ERA	Eigenvalue Realization Algorithm
ESPRIT	Estimation of Signal Parameters via Rotational Invariance Technique
FCP	Four Column Press
FDD	Frequency Domain Decomposition
FFS	Frequency Family Separation
FFT	Fast Fourier Transform
FT	Fourier transform
FRF	Frequency Response Function
HHT	Hilbert-Huang Transform
IFFT	Inverse Fast Fourier Transformation
IMFs	Intrinsic Mode Functions
ITD	Ibrahim Time Domain Method
KFD	Kernel Function Decomposition
LMD	Local Mean Decomposition
LQL	Little Quantity of Lubrication
LSCE	Least Squares Complex Exponential Method
LSE	Least Squares Estimation
LSM	Least Squares Method

MDOF	Multi-Degree of Freedom
MIMO	Multiple Inputs Multiple Outputs
MQL	Minimum Quantity of Lubrication
NExT	Natural Excitation Technique
OMA	Operational modal analysis
OOIM	Output-Only Identification Method
PF	Product Functions
PI	Parametric Identification
PP	Peak Picking Method
rpm	revolutions per minute
RAM	Random-Access Memory
RD	Random Decrement
SDOF	Single Degree of Freedom
SIMO	Single Input Multiple Outputs
SISO	Single Input Single Output
SNR	Signal to Noise Ratio
SPEC	Spectrogram
STFT	Short Time Fourier Transform
SVD	Singular Value Decomposition
SWLSE	Sliding-Window Least Squares Estimation
TARMA	Time-Dependent Autoregressive Moving Average
TCP	Tool Center Point
WT	Wavelet Transform
WPFR	Workpiece Frequency Response
WQL	Wet Quantity of Lubrication
WVD	Wigner-Ville Distribution

List of symbols

a , b		wavelet scale and translation parameter
f_n	Hz	natural frequency
r		mode order
t	s	time
$a(t)$		continuous envelop
$b(t)$, $u(t)$		bottom and upper envelop
$h(t)$		fixed-size moving window
$m(t)$		local mean function
$r(t)$		residue
$s(n)$		sinusoidal signal part
$w(n)$		zero-mean white noise
$x(t)$	mm	displacement vector (time domain), or time history
$\dot{x}(t)$	mm/s	velocity vector (time domain)
$\ddot{x}(t)$	mm/s^2	acceleration vector (time domain)
$x^*(t)$		complex conjugate of $x(t)$
$y(t)$		output signal
y_{noise}		a narrowband white Gaussian noise
A_k		complex amplitude
A_{signal}		magnitude of signal
$D(t)$		free vibration response
$E[x]$		mathematical expectation
$F(t)$	N	force vector (time domain)
D_A , D_E		initial part diameter, diameter after swaging
K_{er}	N/mm	equivalent stiffness
R_{xx}		auto-correlation matrix
R_{xy}		cross-correlation matrix
X	mm/s^2	amplitude

$X(\omega)$	mm	displacement vector (frequency domain)
$F(\omega)$	N	force vector (frequency domain)
$H(\omega)$	(mm/s^2)/Hz	frequency response function
$G_{xy}(\omega)$		cross power spectrum between input and output
$G_{xx}(\omega)$		auto power spectrum of input signal
$G_{yy}(\omega)$		auto power spectrum of output signal
α		decay constant
β_k		decay constant
ω , f	rad/s, Hz	frequency of vibration
φ		eigenvector
φ_k	°	initial phase
φ_{st}		incremental deformation degree
$\varphi_r\varphi_r^T$		the mode constant for mode r
$\gamma^2(\omega)$		coherence function
σ^2		standard deviation
$\triangle t$	s	time interval
$\bar{\omega}_r$	rad/s	natural frequency of r^{th} mode
ζ_r		viscos-damping ratio
δ		eigenvalue
Φ		rotation matrix
$\Psi(t)$		wavelet function
$\Psi^*(t)$		complex conjugate of $\Psi(t)$
$[C]$	(N·s)/mm	damping matrix
$[K]$	N/mm	stiffness matrix
$[M]$	Kg	mass matrix
$[I]$		identity matrix

Chapter 1

Introduction

1.1 Background

Modern machinery builds steadily towards a high-speed, lightweight, low power and high-performance development [KUH08a]. Mechanical and structural vibration problems are becoming more and more serious. This leads to master the vibration characteristics of structure necessarily in designing and manufacturing of machine tools.

Machine tools are complex dynamic systems that are made of many different machine elements and are generally considered as multi-degree of freedom damped oscillator systems [WEC90]. It is well known that a dynamic force or shock results in vibrations. Resonance is considered as one of the main problems that engineers face in the field of tool machinery. It occurs when the excitation frequency matches one of the natural frequencies of the structure, and then the maximum value of displacement amplitude of the system is reached. The dynamic behavior of the system determines the reliability of machine tools, the quality of the workpiece surface, and the tool wear. Therefore, the dynamic behavior of a machine structure should be known.

Modal analysis is one of the most important technologies of dynamic analysis that detects the dynamic model of a structure using numerical or experimental data. It has been developed very fast in the past 30 years and has been widely applied in aviation, aerospace, shipbuilding, automobile, machinery and civil architecture industries [HEY98]. In most practical situations experimental modal analysis (EMA) can be used to determine modal parameters which involves the determination of natural frequencies, damping ratios and mode shapes by measuring the vibration data of the structure. The EMA is necessary to estimate the modal parameters of structure in order to predict the structural dynamic behavior [NAS11], improving workpiece quality by cutting processing [DIN10, DIN12], fault diagnosis [ZEN12], optimization design [LED06] and life prediction [DAM07].

1.2 Problem Statement

The classical EMA studies the free vibration behavior of a system and finds the system frequency response function using a fast Fourier Transform (FFT). The main drawback of FFT consists in the following:

- The Fourier Transform cannot reveal the local frequency contents of the signal. The frequency resolution is equal to the reciprocal of the total sample time. A shorter sampling time corresponds to a poorer frequency resolution.
- Applying the FFT is not suitable for any transient signal to reveal local characteristics. It can be seen in Figure 1 that the higher frequency component (about 1000 Hz) is overwhelmed by the lower frequency component (about 100 Hz) which occurred over the entire time of the analysis.

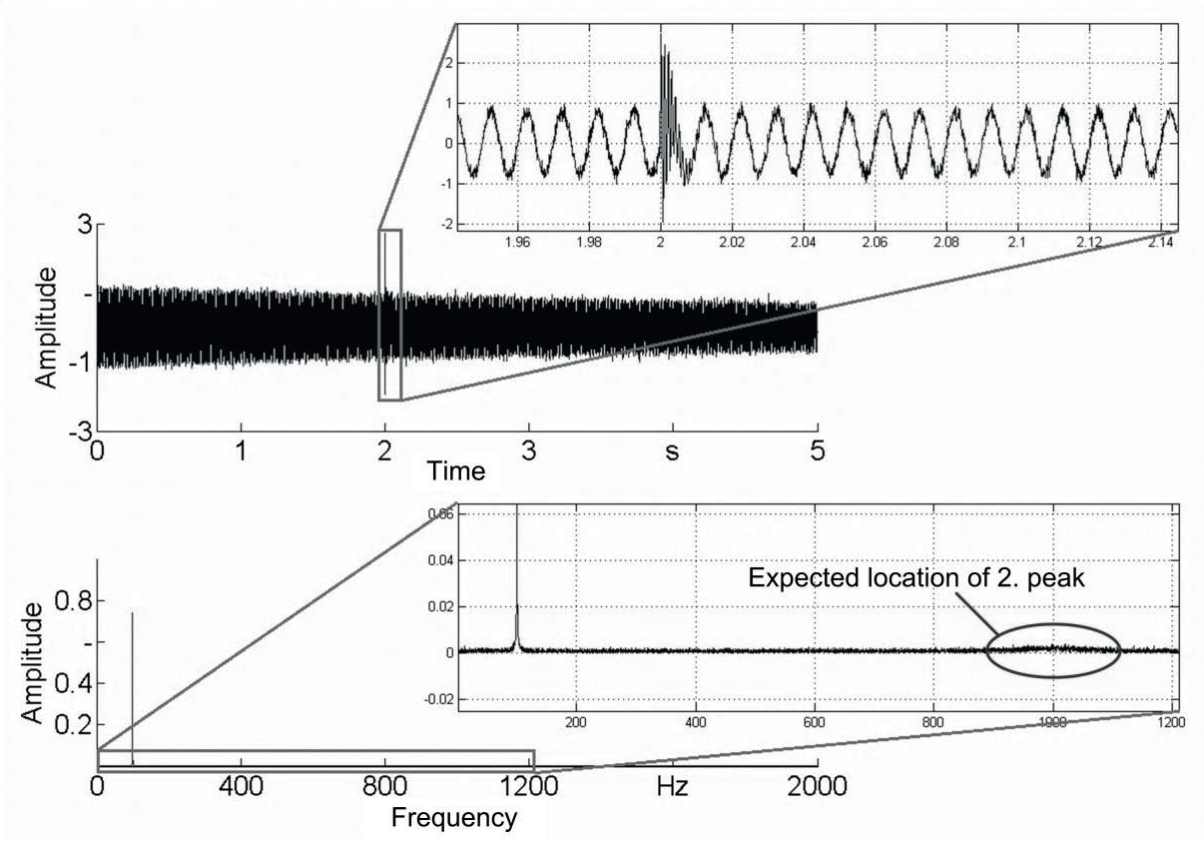

Figure 1: Spectrum of a transient signal occurring within a harmonic oscillation data.

In modern manufacturing industries, processing forces are rapidly changing. The dynamic behavior may vary rapidly in a short time due to variations in the cutting parameters and changes in boundary conditions [SPI09]. The natural frequency and the damping ratio might be changed during the actual machining operation. In rotating machinery, the dynamic modal parameters shift between the 0 rpm state (non-running spindle) and the machining operation state [OUY10]. In the area of high-speed

machining, time- and frequency-varying events and transient and complex harmonic interactions arise from complicated machining processes [GU02]. The dynamic modal parameters also shift due to changing geometric configuration, such as in robotic devices [PET00], flexible mechanisms [ZHO07], cranes [PIN06] and others. For example, the natural frequencies of a machine tool that are observed for variations of between 2 % and 8 % and the damping ratios are also changed between 2 and 10 times during the machining operation test [ZAG09]. These nonlinear and non-stationary dynamic characteristics during machining operations cannot be accurately identified using classical EMA.

In order to obtain the local characteristics of time-varying systems, some time-frequency analysis methods have been developed in the last two decades. They can provide information about the frequency occurring instantly. The signal energies are also represented in a frequency-time plane. Among a number of time-frequency analysis, short time Fourier transform (STFT) [HAM96], the Wigner-Ville distribution of Cohen class [COH95] and the wavelet transform (WT) [HEI89] have been widely used in the analysis of frequency modulated signals. These methods are bound to the Heisenberg's uncertainty principle and thus, the resolution in the time-frequency domain is restricted. Hilbert-Huang transform (HHT) [HUA98] is an improved time-frequency analysis method for non-stationary signals. However, the identification accuracy is limited by some shortcomings [LIU06] and side effects of empirical mode decomposition (EMD) which is the core of HHT.

Operational modal analysis (OMA) [IBR77 MOH04] is considered a powerful tool for modal parameter identification during a machining process. OMA is also recognized as one kind of the non-parametric output-only identification methods (OOIM). This method is applied to big civil structures where it is extremely difficult to measure the excitation forces. The identification procedure is based on experimental modal analysis with the assumption of a stationary white-noise excitation. However, the OMA does not provide transient information of the vibrational behaviour.

Parametric output-only identification is based on time-dependent autoregressive moving average (TARMA) representations [POU06]. The major parametric method consists in the least squares estimation (LSE) which is successfully applied to low-frequency oscillation parameters estimation for power systems by Yang et al. [YAN05 YAN08]. The modal parameters can be obtained by fitting the time window data with a damped oscillating function using a least squares estimation.

1.3 Motivations of the Work

Goal of the work:

To reveal the dynamic characteristic of machining operations and the corresponding effect on the shifting of modal parameters, a transient modal analysis method is required. The goal of this thesis is to propose a short time modal analysis method in order to identify the actual modal parameters of transient non-stationary signals or time varying systems with high resolution. The actual modal parameters consist of actual natural frequency and damping ratio. Mode shapes are not discussed in depth in this work. The proposed algorithm is applicable in real-time control system to estimate the system parameters in order to help the machining operation more effectively.

Hypothesis:

Thought briefly discussing of the existing modal parameter identification methods in the previous chapter, two main hypotheses circumventing the analysis of non-stationary transient data are suggested:

- The classical modal analysis based on the FFT cannot identify transient modal parameters accurately. Therefore, this method is not suitable for real-time control system.
- The actual modal parameters for transient or non-stationary data that occur in a short time can be identified efficiently using a sliding-window least squares estimation method (which is detailed in chapter 4)

In order to prove these hypotheses, this study addresses recent approaches to the modal analysis technique and sets up a new modal analysis method for actual modal parameters of transient non-stationary systems. This thesis does not focus on the improvement of analyzing algorithm, but emphasizes the performance or applicability of the proposed method using numerical and experimental tests, to be finally applied in some real machining operational processes in order to reveal the actual modal parameters. The proposed method allows the accurate extraction of the modal parameters of the analyzed systems.

1.4 Scope of the Work

This thesis is organized as follows: chapter 2 briefly reviews modal analysis techniques and approaches of signal processing. Unfortunately, the state of the art does not provide a high precise estimation method suitable for transient modal parameters identification with high frequency resolution. In following a sliding-window least squares estimation method (SWLSE) is demonstrated and studied in this work. The concept of SWLSE methods is introduced in chapter 3 as well as the theoretical background of the method to identify the modal parameters. Chapter 4 shows the identification performance of the proposed method using numerical simulations. In order to verify the proposed method the SWLSE method is then demonstrated in chapter 5 and 6 using laboratory experimental examples and several real industrial machining processes, respectively. Finally, the thesis concludes with a summary of all theoretical and experimental results. The method's limitations as well as further works are outlined in the conclusions of chapter 7.

In this section, the main procedure of this work is introduced. According to the discussion in chapter 2, the algorithms, which are more suitable for the modal parameters identification with transient or time-varying systems, are tested firstly using several numerical examples. The performance or applicability of the proposed algorithms is discussed. By further experimental tests, the procedure is demonstrated to estimate the modal parameters of a laboratory beam and several real industrial machining processes using the proposed algorithm.

Numerical Tests

In chapter 2, all current developed methods to identify the modal parameters are introduced. Least squares estimation (LSE) and estimation of signal parameters via rotational invariance technique (ESPRIT) are more suitable for the actual modal parameter identification of transient signal with high resolution. The identification accuracy might be dependant on the window size, the noise level, the applied filtering and the sampling rate of the acquired signals and this is discussed in chapter 4. The performance or applicability of these methods is examined under various window size and signal-to-noise ratio (SNR) assumptions using several numerical examples. The accuracy of natural frequency and damping ratio identification of the methods are compared with the classical experimental modal analysis (CEMA) method and the advantages of each method are figured out.

Tests based on a Laboratory Structure

According to the numerical tests, the performance of the proposed method with higher identification accuracy is further investigated with a laboratory beam structure. This beam system is set up with two coupling assemblies, with which the stiffness and

damping can be independently adjusted thus changing the dynamic behavior of the beam system. The procedure of this work then consists of two main steps: Firstly, stationary testing is performed under various stiffness and damping ratio of the beam system. The obtained modal parameters are compared with the results of the CEMA method. Second, the instantaneous modal parameters are also estimated using the proposed method while an inertia is moving on the beam system. Similarly, the results are compared also with the classical EMA (in chapter 5).

Tests based on Engineering Application

All of the developed algorithms are in the service of the engineering application. The real machine tools or machining processes are more complicated than the laboratory cases. For this reason, it is necessary to evaluate how the proposed method can be industrially exploited. In this work, the time dependant actual modal parameters are estimated on a high-speed machining center and a four column press machine. On the other hand, this proposed algorithm is not only for the transient modal parameter identification but also for other process parameter estimation. For instance a process damping ratio during a machining milling process with various lubricant conditions is investigated using this method. In another engineering application in chapter 6, the process damping ratios are identified on a micro rotary swaging machine considering different revolution speed.

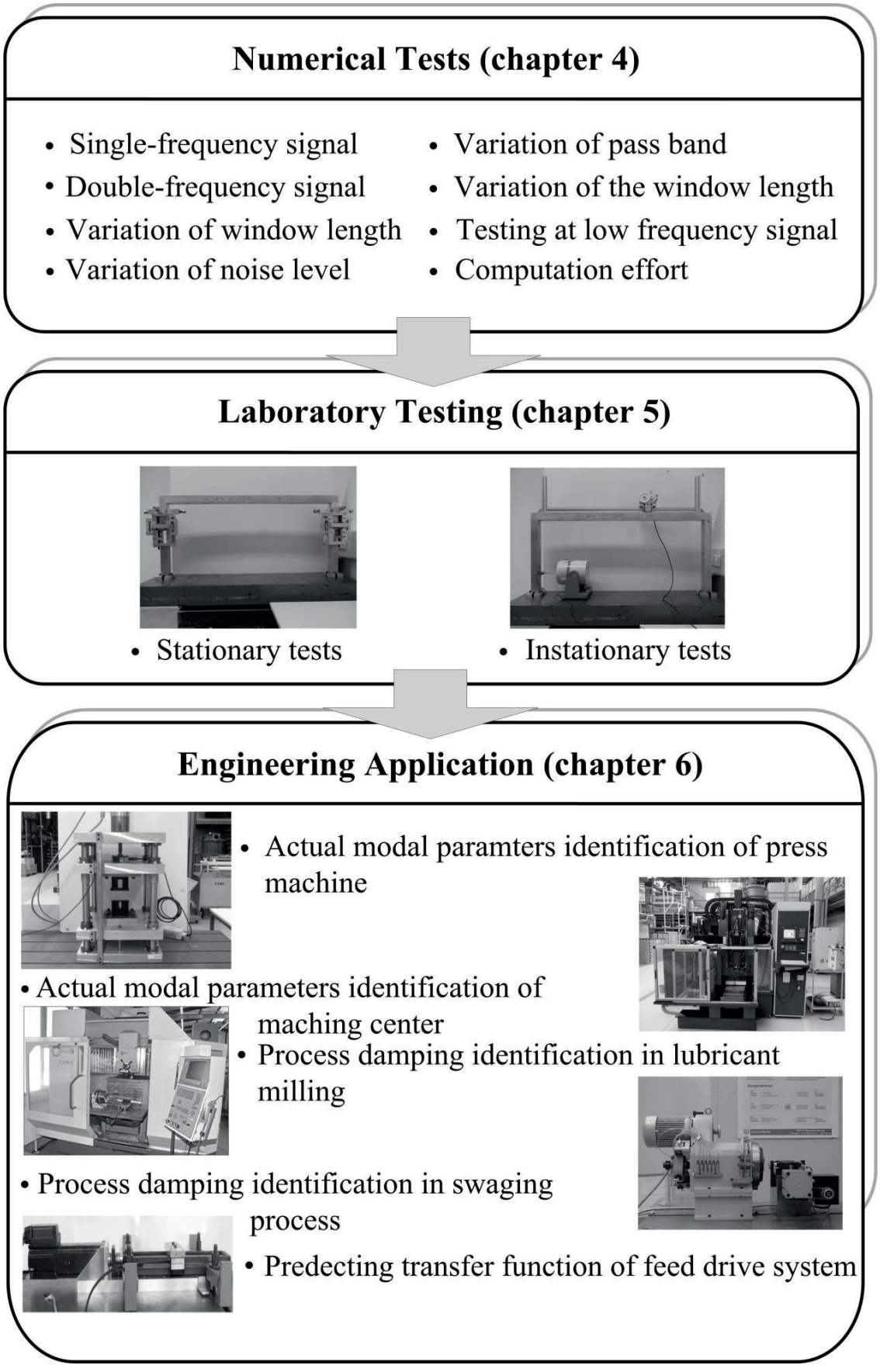

Figure 2: Procedure of testing

Chapter 2

Theoretical background and related works

2.1 Classical Experimental Modal Analysis

The procedure of an experimental modal analysis essentially originates from parameter identification. Over the last 50 years, a lot of parameter identification methods have been developed and are generally classified as time domain, frequency domain and time-frequency domain analysis. According to their algorithmic characteristic, these parameter identification methods have been also classified into three new categories: kernel function decomposition (KFD), frequency family separation method (FFS) and parametric identification method (PI). Their mathematical background and characteristics are discussed in this section.

2.1.1 Transfer function

Modal analysis involves the determination of modal parameters from the sampled vibration data of a structure for all modes in the frequency range of interest. Modal Parameters are natural frequencies, damping ratios and mode shapes which are related to the material of structures and the boundary conditions [EWI00]. In order to determine modal parameters, experimental modal analysis can be used in engineering applications. Following, the mathematical background and the practical measuring technique of experimental modal analysis are introduced.

A dynamical system with multi-degrees of freedom can be expressed as a second-order differential equation:

$$M\ddot{x}(t) + C\dot{x}(t) + Kx(t) = F(t) \tag{2.1}$$

where M, C and K are the inertia matrix, damping matrix and elasticity matrix. $x(t)$ is the displacement vector and $F(t)$ is the excitation force.

After applying the Fourier Transform to the differential equation (2.1) follows the transition from the time domain into the frequency domain, and the function can be written as [EWI00]:

$$(K - \omega^2 M + j\omega C)X(\omega) = F(\omega) \tag{2.2}$$

$$F(\omega) = Fourier\ transform\ of\ F(t)\ (systsem\ excitation)$$
$$X(\omega) = Fourier\ transform\ of\ x(t)\ (system\ response)$$

In order to calculate a digital finite signal, Cooley and Tukey [COO65] formulated the Fast-Fourier-Transform (FFT) in 1965, which is a fast and memory efficient algorithm. With FFT it is possible to examine a time signal and to divide it into its spectral <components that it determines the signal inherent frequencies of the sinusoidal portions and transmits this as a function of their amplitudes in a diagram [BRI82].

The transfer matrix is described from the excitation and the response by the following equation:

$$H(\omega) = \frac{F(\omega)}{X(\omega)} = \frac{1}{K - \omega^2 M + j\omega C} \tag{2.3}$$

Each element in the matrix $H(\omega)$ is called frequency response function (FRF). The FRF describes the input-output relationship between two measured points on the structure.

The FRF has two implications (Superposition and Homogeneity) with the assumption that a measured system behaves linearly which means that a measured FRF is independent of the type of excitation and of the excitation level. Furthermore it is assumed that the system damping is proportional to the velocity of motion (viscous-damping).

To calculate the required modal parameters of this equation system with multi-degrees of freedom, the solving of an eigenvector φ is applied [EWI00, WAN05, CUR88, SER00] (see Appendix A.1 for details). The equation (2.3) can be reconstructed in modal coordinate system as follows:

$$\bar{h}_{lp}(\omega) = \frac{\bar{x}_l(\omega)}{\bar{f}_p(\omega)} = \sum_{r=1}^{N} \frac{\varphi_{lr}\varphi_{pr}}{K_r - \omega^2 M_r + j\omega C_r} \tag{2.4}$$

where l and p indicate the item of response point (output) and excitation point (input). $\bar{h}_{lp}(\omega)$ is the member of FRFs and explain the system response at the position l when the excitation is located at the position p. The equation (2.4) can also be reformed by:

$$\bar{h}_{lp}(\omega) = \sum_{r=1}^{N} \frac{1}{K_{er}((1 - \bar{\omega}_r^2) + j2\zeta_r\bar{\omega}_r} \tag{2.5}$$

the natural frequency ratio $\bar{\omega}_r$, the viscous-damping ratio ζ_r and the equivalent stiffness K_{er} for the r - order mode can be expressed, respectively:

$$\begin{aligned} \bar{\omega}_r &= \frac{\omega}{\omega_r} \\ \zeta_r &= \frac{C_r}{2M_r\omega_r} \\ K_{er} &= \frac{K_r}{\varphi_{lr}\varphi_{pr}} \end{aligned} \tag{2.6}$$

Modal shape is a group of the ratio without units which represents the relative displacement between the structural measured points. The modal shape vector $\{\varphi_r\} = \{\varphi_{1r} \quad \varphi_{2r} \quad \cdots \quad \varphi_{Nr}\}^T (r = 1,2,\cdots,N)$ can be normalized with the maximum element of the modal shape vector equal to 1. Here, all of the modal parameters can be obtained from the second-order differential equations of the MDOF system.

From the equations (2.1) to (2.6), the core of the modal analysis is to measure the FRFs of structure. According to geometry and dimension of the measured structure, one or more fixed inputs and outputs are used. The three most common methods are the single input single output (SISO), the single input multiple outputs (SIMO) and the multiple inputs multiple outputs (MIMO) methods.

The most common acquisition type of output signal is done with a triaxial accelerometer instead of displacement transducers, although the displacement motion of the structure is of more concern. This is because the installation of displacement transducer is restricted for many industrial applications. The FRF in form acceleration / force ($(m/s^2)/N$) can be translated into the FRF in form displacement / force (m/N) using an algorithm of the frequency domain quadratic integral [WEC90] (see Appendix A.2).

There are two most common excitation methods in engineering tests: Impact-testing using an impact hammer and shaker-testing using an electromagnetic shaker. When using the SISO method, there are basically two techniques for measuring with the impact testing. First, the response transducer is fixed at one measurement point and the structure is impacted at every measurement point with impact hammer. This method is called roving hammer test. A second method is the opposite of the latter, it is called roving sensor test where the structure is impacted at just one measurement point and the responses are measured at each measurement points. Both methods generally result in measuring one of the rows or columns of the FRF matrix. Theoretically, there is

no difference between the roving hammer test and the roving sensor test, this is because the FRF matrix describing the system is characterized by reciprocity and is a square symmetric matrix [WÖL05]. This can be seen in equation (2.7) where the first row of the FRF matrix is exactly the same as the first column. Practically, the mass distribution of the whole structure might be affected from the weight of the accelerometer by roving sensor test, which leads to uncertainty in the measurement [PET01]. One way to correct this problem is to choose a lightweight sensor.

$$\varphi_r\varphi_r^T = \underbrace{\begin{bmatrix} \varphi_{1r}\varphi_{1r} & \varphi_{1r}\varphi_{2r} & \cdots & \varphi_{1r}\varphi_{nr} \\ \varphi_{2r}\varphi_{1r} & \varphi_{2r}\varphi_{2r} & \cdots & \varphi_{2r}\varphi_{nr} \\ \vdots & \vdots & \ddots & \vdots \\ \varphi_{nr}\varphi_{1r} & \varphi_{nr}\varphi_{2r} & \cdots & \varphi_{nr}\varphi_{nr} \end{bmatrix}}_{\begin{bmatrix} \varphi_r\varphi_{1r} & \varphi_r\varphi_{2r} & \cdots & \varphi_r\varphi_{nr} \end{bmatrix}} = \begin{bmatrix} \varphi_{1r}\varphi_r^T \\ \varphi_{2r}\varphi_r^T \\ \vdots \\ \varphi_{nr}\varphi_r^T \end{bmatrix} \tag{2.7}$$

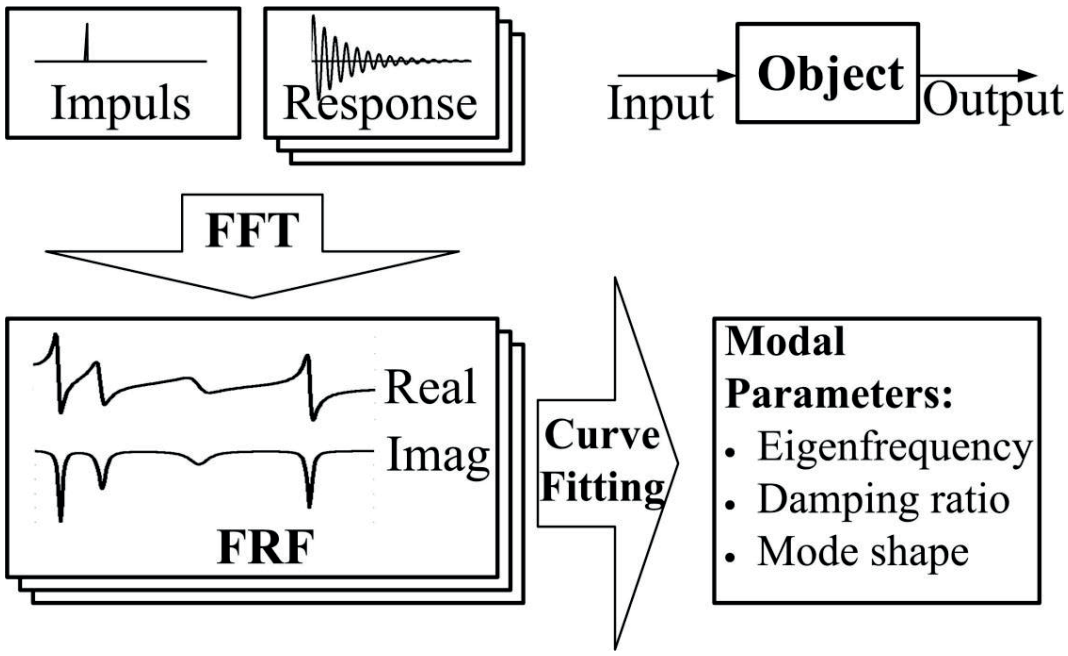

Figure 3: sketch of the experimental modal analysis procedure

After constructing the FRF matrix, the dynamic characteristics of SDOF can be obtained using the Curve-Fitting technique, in which the natural frequency is detected in terms of a spectral peak response (Peak picking method [WEC90]), the modal damping ratio is estimated using the half power bandwidth method [MAI97] (see Appendix A.4) and the mode shape is extracted from quadrature peaks [KJA88]. The Figure 3 shows the procedure of the experimental modal analysis.

2.1.2 Coherence function

In practice, the measured response or excitation signal is often mixed with noise. In order to determine the quality of the measured FRFs, a coherence function is used which is defined as [WEC90, WEL67, CAR73]:

$$\gamma^2(\omega) = \frac{\left|G_{xy}(\omega)\right|^2}{G_{xx}(\omega)G_{yy}(\omega)} \tag{2.8}$$

$G_{xy}(\omega) = \text{cross power spectrum between the input and output signal}$

$G_{xx}(\omega) = \text{auto power spectrum of input signal}$

$G_{yy}(\omega) = \text{auto power spectrum of output signal}$

The coherence function indicates how much of the output signal $y(t)$ is determined by the input signal $x(t)$ through a linear relationship. The coherence value is somewhere between 0 and 1 without units. The values below 0.8 means that the measured FRF is corrupted by noise; or the measured structure has a non-linear behavior strongly; or the signal should be achieved with a suitable windowing operation in the time domain in order to reduce the spectrum leakage [EWI00].

2.2 Operational Modal Analysis

In many industrial applications, it is very difficult to measure the excitation forces during machining process. Especially, some large civil engineering structures like bridge, building, spacecraft, and others are not suitable performed with artificial excitation. For this reason, over the last few decades, an operational modal analysis (OMA) has been developed for extracting modal parameters from structural response data only without knowing the input signal.

The OMA requires only the outputs, such as accelerations to be measured with the assumption of a stationary white noise excitation during operational conditions or ambient excitation like wind, traffic, etc. Then, the modal parameters can be estimated from the output data using parameter identification approach. Many different approaches to estimate modal parameters have been developed.

These approaches can be broadly classified into two categories: time domain and frequency domain identification method. One of the most famous approaches is the Ibrahim time domain method (ITD) [IBR77, PAP81]. There are other time domain methods such as, the natural excitation technique (NExT) [JAM95], the least squares complex exponential method (LSCE) [BRO79], the eigenvalue realization algorithm (ERA) [JUA85] and autoregressive moving average vector (ARMAV) [GER70]. Generally, the OMA with time domain method is suitable for estimating modal damping but unfavorable in extracting of natural frequencies and mode shapes [THA09].

For the frequency domain method, McLamore et al. [MCL70] utilized the FFT to analyze the response signal of two suspension bridges under the ambient excitation and identify the modal parameters using peak picking (PP) method. On that basis, Brinker has proposed a Frequency Domain Decomposition (FDD) method [BRI07], in which the exponential fit technique to the response function in time domain is applied to estimate the damping ratio instead of the half power bandwidth method. The OMA with frequency domain identification is advantageous on natural frequencies and mode shapes estimation, but uncertainty for damping ratios due to bias involved in the spectral analysis [JIM01, LIT95].

Such methods are only applicable to the vibration system with the assumption that the input of the system is a stationary white noise excitation. In fact, most machinery applications do not meet this requirement. Therefore, the identification accuracy is not high enough.

2.3 Parameter Identification Technique

During the past two decades there has been a lot of research in order to determine the modal parameters. There are many methods to classify the parameter identification technique. According to the operation process of the algorithm, in this thesis they have been divided into three groups: Kernel function decomposition， Frequency Family Separation Method and Parametric Identification Method.

2.3.1 Kernel function decomposition

As it has been mentioned above, the Fourier Transformation cannot reveal local information of transient signals. Kernel function decomposition can provide the local information of the transient signal. This is due to the fact that the KFD divides the time data into a lot of blocks and adds a window using kernel function for the analysis [GRÖ00].

2.3.1.1 Short time Fourier transform

The time-frequency analysis was proposed by Gabor [GAB46] in 1946. It expands a one-dimension data to a two-dimension area (time-frequency domain) in order to directly describe the slight variation of a signal varying with time. Several time-frequency representation techniques have been developed. One of the most well-known time-frequency analysis is the Short Time Fourier Transform (STFT) which was introduced by R.K.Potter [HAM96]. The STFT based on the Fourier Transform (FT) can be obtained by applying a fixed-size moving window on the signal, calculating its FT and proceeding in the same way for each instance. The square of this transform is called spectrogram (SPEC) and represents the spectral energy density of the signal in the time-frequency domain. It is defined by:

$$SPEC(t,f) = \left|STFT(t,f)\right|^2 = \left|\int_{-\infty}^{+\infty} x(\tau)\cdot h^*(\tau - t)e^{-j2\pi f\tau}d\tau\right|^2 \quad (2.9)$$

where $x(t)$ is the signal and $h(t)$ is a fixed-size moving window.

The STFT or SPEC time and frequency resolutions are determined by the width of the sliding window. If the segment of signal is decreased in order to increase the time resolution, the frequency resolution is decreased simultaneously. These resolutions are bound to the Heisenberg's uncertainty principle [BOA03], therefore the resolution in the time-frequency domain is restricted. Other limitation of the SPEC or STFT is that it cannot provide the damping ratio of the signal [ZAG09].

2.3.1.2 Wigner-Ville distribution

The Wigner-Ville Distribution (WVD) as an extension to the STFT has been confirmed to provide a theory about 2 times higher time-frequency resolution [COH95, PAD04, COH89]. The WVD of the signal $x(t)$ is defined as:

$$WVD(t,f) = \int_{-\infty}^{+\infty} x(t+\frac{\tau}{2})\cdot x^*(t-\frac{\tau}{2})e^{-j2\pi f\tau}d\tau \quad (2.10)$$

where $x^*(t)$ means the complex conjugate of $x(t)$. Due to the quadratic nature of WVD there is a cross-interference problem, where the cross term for multicomponent signal has a large magnitude [JEO92]. To overcome the cross-interference of WVD several improvements have been proposed, such as the smoothed pseudo WVD [FLA99, BOA92].

2.3.1.3 Wavelet transform

Due to restrictions of time-frequency resolution the STFT or WVD analysis does not fit any frequency signal with one fixed window width. In the 1990s a wavelet transform (WT) was successfully applied in the field of signal processing [MAL99, MEY93].The WT shows the signal over the time-scale plane in which the scale parameter is proportional to the duration and inverse to the peak frequency of the complex wavelet function. It is defined in a continuous form as follows:

$$W_{\psi}^{X}(a,b) = \frac{1}{\sqrt{a}} \int_{-\infty}^{+\infty} X(t) \cdot \Psi^{*}(\frac{t-b}{a}) dt \tag{2.11}$$

where $\Psi^{*}(t)$ indicates complex conjugate of wavelet function (mother wavelet) $\Psi(t)$, a and b are wavelet scale and translation parameters.

By changing the scale and translation parameters, a series of son wavelets can be generated from the mother wavelet shown as follows [HEI89]:

$$\Psi_{a,b}^{*}(t) = \frac{1}{\sqrt{a}} \Psi(\frac{t-b}{a}), a > 0, b \in R \tag{2.12}$$

Therefore, the WT can be seen as a self-adaptive filter that has a narrow time window for high frequency components and a wide time window for low frequency components of the analyzed time series date. So, WT can obtain the best energy density distribution in the time-scale plan. The accurate analysis of different signals depends on the selected mother wavelet. A number of the wavelet functions were developed. Among the wavelet family, the Morlet wavelet function is widely used [GRO90]. The WT has been extended into many fields. However, identification of mode shapes using WT is very difficult [ZAG09].

In order to avoid the complexity about the choice of wavelet function and the derived parameters artificially, the papers [KUH08b, SCH13] introduce a method based on analyzed signal to choose the wavelet function itself. And this effective self-adaptive technology is applied successfully to monitoring of machining processing.

2.3.2 Frequency Family Separation Method

Frequency Family separation (FFS) method presents a time domain identification method, which can decompose the multi-frequency signals adaptively into a set of mono-frequency or narrow-band frequency signals. One of the advantages of the FFS method consists in the absence of any restrictions of FFT, but the method can construct

the adaptive frequency-bands according to the original signal with its own characteristics.

2.3.2.1 Empirical mode decomposition

Empirical mode decomposition (EMD) is one of the FFS methods which is proposed by Huang et al. [HUA98]. It looks as a shifting process, which can divide a width band time series into a set of narrow band time series or mono-component called intrinsic mode functions (IMFs). The shift process for modal parameter identification consists of three main steps [POO07].

1) Find the local minima and maxima from the original time history and obtains the upper $u(t)$ and bottom $b(t)$ envelope using a cubic-splines fitting technique. Then the mean of the envelopes is computed:

$$m_1(t) = (u(t) + b(t)) / 2 \tag{2.13}$$

2) Subtract the $m_1(t)$ from the original time history $x(t)$ to get the first component:

$$h_1(t) = x(t) - m_1(t) \tag{2.14}$$

According to the following two conditions, whether $h_1(t)$ belongs to IMFs can be determined [HUA03]:

- The number of extrema and the number of zero crossings may differ by no more than one.
- The local average is zero.

If these conditions are not met, then repeat this shift process for signal $h_1(t)$ until getting the first $imf_1(t)$.

3) Now the residue is computed using

$$r_1(t) = x(t) - imf_1(t) \tag{2.15}$$

and the EMD procedure continues with the residue $r_1(t)$ until the residue becomes a monotonic function. So, the original time history $x(t)$ is finally divided into a set of intrinsic mode functions and the final residual

$$x(t) = \sum_{i=1}^{n} imf_i + r_n \tag{2.16}$$

Approximately every IMF is a narrow band signal that meets the demands of Hilbert transform. According to the order of the decomposition, all IMFs are arrayed from high to low. This method has been investigated in [LIU06], it has an obvious advantage to deal with the illusive components and mode confusion.

2.3.2.2 Local mean decomposition

Similar to the EMD, Smith [SMI05] puts forward a kind of new adaptive non-stationary signal processing method: local mean decomposition (LMD). Essentially the LMD decomposes a complex multi-component modulated signal into a set of product functions (PF), each of which is the product of a frequency modulated signal and amplitude modulated envelope signal. For a given signal $x(t)$, the decomposition steps are shown as follows.

1) Identify the extrema $n_i(i=1,2,\cdots,M)$ of each half-wave oscillation of the signal, M indicates the extrema points number.
2) Calculate the local mean value m_i and the local magnitude a_i via the two successive extrema.

$$\begin{aligned} m_i &= \frac{n_i + n_{i+1}}{2}, i = 1,2,\cdots,M-1 \\ a_i &= \frac{|n_i + n_{i+1}|}{2}, i = 1,2,\cdots,M-1 \end{aligned} \tag{2.17}$$

3) Obtain the continuous local mean function $m(t)$ und the continuous envelope function $a(t)$ using moving averaging ($m_{11}(t)$ and $a_{11}(t)$ for first loop).
4) Compute the assessment function $s_{1n}(t)$.
   $m_{11}(t)$ is substracted from the original signal $x(t)$,

$$h_{11}(t) = x(t) - m_{11}(t) \tag{2.18}$$

   $h_{11}(t)$ is then amplitude demodulated by dividing it by $a_{11}(t)$, $s_{11}(t)$ can be obtained:

$$s_{11}(t) = \frac{h_{11}(t)}{a_{11}(t)} \tag{2.19}$$

   If the envelope $a_{12}(t)$ of $s_{11}(t)$ does not meet the condition $a_{12}(t)=1$, $s_{11}(t)$ as the original data the iterative procedure needs to be repeated, like formula (2.20),

until its envelope function meets the condition $a_{1(n+1)}(t)=1$, a purely frequency modulated signal $s_{1n}(t)$ is obtained.

$$\begin{aligned} h_{11}(t) &= x(t) - m_{11}(t) \\ h_{12}(t) &= s_{11}(t) - m_{12}(t) \\ &\vdots \\ h_{1n}(t) &= s_{1(n-1)}(t) - m_{1n}(t) \end{aligned} \tag{2.20}$$

Accordingly, the envelop signal is given by:

$$a_1(t) = a_{11}(t)a_{22}(t)\cdots a_{1n}(t) = \prod_{q=1}^{n} a_{1q}(t), \lim_{n\to\infty} a_{1n}(t) = 1 \tag{2.21}$$

The envelope $a_1(t)$ is expressed as the instantaneous amplitude. The instantaneous frequency can be defined as:

$$f_1(t) = \frac{1}{2\pi} \cdot \frac{d(\arccos(s_{1n}(t)))}{dt} \tag{2.22}$$

5) Obtain the PFs. Multiplying $s_{1n}(t)$ by the envelope function $a_1(t)$ gives a PF.

$$PF_1(t) = a_1(t) \cdot s_{1n}(t) \tag{2.23}$$

This $PF_1(t)$ is then subtracted from the original signal resulting in a new function $u_1(t)$. $u_1(t)$ now is considered as a new original signal and the above whole procedure is repeated k times until $u_k(t)$ is a constant or contains no more oscillations. Finally, the original signal $x(t)$ can be reconstructed according to

$$x(t) = \sum_{p=1}^{k} PF_p(t) + u_k(t) \tag{2.24}$$

The LMD method is applied in diagnosis of gearbox fault [WAN12] and in analysis of scalp electroencephalogram visual perception data [SMI05]. The analysis results demonstrate that LMD improve the accuracy of diagnosis, compared to EMD.

2.3.2.3 Random decrement technique

The random decrement (RD) technique is also a FFS approach, where the free decaying response of a vibration structure is extracted from its random excited stationary response. It was first proposed by Cole [COL68, COL73] to identify the damping of an aerospace structure using stationary random response. After that, Vandiver et al. have given the strict theoretical proof for the RD technique [VAN82].

The forced displacement responses $y(t)$ of a linear structure under an assumption of Gaussian white noise excitation (a zero-mean and stationary force) can be written as [HE11]:

$$y(t) = y(0)D(t) + \dot{y}(0)v(t) + \int_0^t h(t-\tau)f(\tau)d(\tau) \tag{2.25}$$

where $D(t)$ is the free vibration response with initial displacement being 1 and initial velocity being 0; $v(t)$ is the free vibration response with initial displacement being 0 and initial velocity being 1; $y(0)$ and $\dot{y}(0)$ are the initial displacement and velocity of system, respectively; $h(t)$ is the unit impulse response function and $f(t)$ is the external excitation of the zero mean stationary Gaussian stochastic process. The extraction procedure is shown as follows.

1) Selecting a triggering level A (constant value) to intercept the sample data $y(t)$, a set of time corresponding to the crossing point can be obtained as $t_i(i = 1,2,3,\cdots)$. For a SDOF vibration system this triggering level can be selected to be 1.5 times the standard deviation of the sample data as an experience value. For a MDOF system it has another triggering condition [BRI92, ASM97, IBR01].

2) For a linear system, the dynamic response $y(t-t_i)$ from time t_i is given by the combination of three contributions: the free vibration response due to the initial displacement at the time $t = t_i$, the free vibration response due to the initial velocity at the time $t = t_i$ and the forced vibration response caused by the random excitation $f(t)$. $y(t-t_i)$ can be expressed as follows:

$$y(t-t_i) = y(0)D(t-t_i) + \dot{y}(0)v(t-t_i) + \int_{t_i}^t h(t-\tau)f(\tau)d(\tau) \tag{2.26}$$

3) Due to the stationary random excitation, the time starting point does not affect its stochastic characteristics. Thus, the many subsample function $y(t-t_i)$ can form a

set of the sub-response process $x_i(t)$ $(i=1,2,3,...,N)$, if each subsample function is moved to the origin of coordinates ($t=0$). And then

$$x_i(t) = AD(t) + \dot{y}(t_i)v(t) + \int_0^t h(t-\tau)f(\tau)d(\tau) \tag{2.27}$$

4) For the limited sample length, the arithmetic mean value can be approximately equal to the mathematical expectation of the sampled date. Then, the arithmetic mean value of the sub-response process is given by

$$\begin{aligned}\delta(t) = \frac{1}{N}\sum_{i=1}^{N} x_i(t) &\approx E\left[AD(t) + \dot{y}(t_i)v(t) + \int_0^t h(t-\tau)f(\tau)d(\tau) \right] \\ &\approx AD(t) + E\left[\dot{y}(t_i)v(t)\right] + \int_0^t h(t-\tau)E\left[f(\tau)\right]d(\tau)\end{aligned} \tag{2.28}$$

Due to the mean value of excitation $f(t)$ being zero and the initial velocity $\dot{y}(t)$ also being zero, then $E[f(t)]=0$ and $E[\dot{y}(t)]=0$. Hence, the free vibration response with initial displacement being A and initial velocity being 0 can be obtained from the arithmetic mean value of the sub-response process, $\delta(t)=AD(t)$.

The RD technique as a preprocessing has been successfully used to many engineering application, such as the detection or prediction of a damage occurrence in civil and offshore structures [ZUB00, YAN84]. Most of the applications of the RD technique have been developed in association with operational modal analysis to identify the modal parameters [IBR77].

2.3.3 Parametric Identification Method

Parametric Identification method is based on the structure of the measured data to establish a mathematical model and through some optimization algorithm to estimate the parameters of the mathematical model [SPI09, POU06].

2.3.3.1 Least squares estimation techniques

Least squares method is one of regression or curve fitting technique. It finds the best fit curve which has a minimal sum of the deviation squared from a measured set of data [BJÖ96, KUT04]. The LSE is successfully applied to low-frequency oscillation parameters estimation and the theoretical basis for these results is outlined in [YAN08]. Further modal parameter identification using LSE is described in detail in chapter 4.

2.3.3.2 Estimation of signal parameters via rotational invariance technique

Other PI method is an estimation of signal parameters via rotational invariance technique (ESPRIT) [ROY89, BAD05], which is based on the short time subspace method. The original signal can be transferred to the two signal subspaces. The signal parameters are obtained by computing the eigenvector of two sets of linearly independent vectors in the signal subspaces.

Consider a damped sinusoid with additive white noise, defined as follows:

$$x(n) = s(n) + w(n) = \sum_{k=1}^{K} A_k e^{(-\beta_k + j\omega_k)n} + w(n) \tag{2.29}$$

here, $s(n)$ is the sinusoidal signal part and $w(n)$ is the zero-mean white noise. $A_k = (a_k / 2) \cdot e^{j\varphi_k}$ is the complex amplitude, β_k is the decay constant, φ_k is the initial phase, $\omega_k = 2\pi f_k$ is the angular frequency, K is the number of sinusoids, and n is the number of samples.

Suppose M to be the length of the signal, then define the signal subspaces X (from 1st to $M-1$) and Y (2nd to M) as the arrays:

$$\begin{aligned} X &= AS + w_x \\ Y &= A\Phi S + w_y \end{aligned} \tag{2.30}$$

where $\Phi = diag\left\{ e^{-\beta_1 + j\omega_1} \quad e^{-\beta_2 + j\omega_2} \quad \dots \quad e^{-\beta_k + j\omega_k} \right\}$

is the rotation matrix, $A = \left[A_1 \quad A_2 \quad \cdots \quad A_k \right]^T$ and S is defined as:

$$S = \begin{bmatrix} 1 & 1 & \cdots & 1 \\ e^{-\beta_1 + j\omega_1} & e^{-\beta_2 + j\omega_2} & \dots & e^{-\beta_k + j\omega_k} \\ \vdots & \vdots & \ddots & \vdots \\ e^{-\beta_1 + j(M-1)\omega_1} & e^{-\beta_2 + j(M-1)\omega_2} & \dots & e^{-\beta_k + j(M-1)\omega_k} \end{bmatrix} \tag{2.31}$$

By computing the auto-correlation matrix R_{xx} and cross-correlation R_{xy}, it follows:

$$R_{xx} = E\left\{XX^H\right\} = SAS^H + \sigma_w^2 I$$
$$R_{xy} = E\left\{XX^H\right\} = SA\Phi^H S^H + \sigma_w^2 Z \tag{2.32}$$

where E denotes the expectation, σ_w^2 is the standard deviation of the noise, I is the identity, and Z is defined as:

$$Z = \begin{bmatrix} 0 & & & 0 \\ 1 & 0 & & \\ & \ddots & \ddots & \\ 0 & & 1 & 0 \end{bmatrix} \tag{2.33}$$

According to the eigenvalue decomposition of (2.32), these matrices are obtained:

$$R_1 = R_{xx} - \lambda_{\min} I = R_{xx} - \sigma_w^2 I = SAS^H$$
$$R_2 = R_{xy} - \lambda_{\min} Z = R_{xy} - \sigma_w^2 Z = SA\Phi^H S^H \tag{2.34}$$

here the singular value decomposition (SVD) of R_1 can be expressed as:

$$R_1 = U\Sigma V^H = \begin{bmatrix} U_1 & U_2 \end{bmatrix} \begin{bmatrix} \Sigma_1 & 0 \\ 0 & \Sigma_2 \end{bmatrix} \begin{bmatrix} V_1^H \\ V_2^H \end{bmatrix} \tag{2.35}$$

then by computing the eigenvalue decomposition of the matrices $\left\{\Sigma_1 \quad U_1^H R_2 V_1\right\}$, the eigenvalues Υ for $R_1 - \Upsilon R_2$ can be obtained:

$$\Upsilon = e^{-\beta_k + j\omega_k}, k = 1, 2, \cdots K \tag{2.36}$$

The frequency and damping ratio are obtained from:

$$f_k = \mathrm{Im}(\ln(\Upsilon_k)) / 2\pi$$
$$\zeta_k = \beta_k / \sqrt{\beta_k^2 + \omega_k^2} \tag{2.37}$$

where $\beta_k = -\mathrm{Re}(\ln(\Upsilon_k))$, $k = 1,2,\cdots K$, Re and Im denote the real and imaginary part, respectively.

2.4 Summary of Current Identification Methods

Each identification method has its own advantage and limitation. The selection of algorithm is based on different industrial cases application. None of the identification methods is the ideal for all applications [HER99]. Generally, output-only identification with time domain method is suitable for estimating modal damping but it is not convenient to extract natural frequencies and mode shapes accurately [THA09]. The classical experimental modal analysis with frequency domain identification such as the Peak-picking method advantages on natural frequencies and mode shapes estimation, but identifies for the damping ratios uncertainly [JIM01]. As a new kind of frequency family Separation Method, LMD etc. are just suitable for the non-stationary frequency modulated signals [CHE09].

In order to apply the algorithm in close to real-time control system, a faster computation of the algorithm is requested. On the other hand, the algorithm must provide high resolution, high accuracy estimation of the modal parameters. By comparing those algorithms to each other the performances are evaluated from “bad” to “good”. Figure 4 summarizes the performance of the mentioned algorithms considering the frequency and damping identification, mode shape identification, and computation effort.

The computation effort of the LSE method can be significantly reduced by high identification accuracy. This method is more suitable for the purpose of this work and is investigated in detail by comparing to that of the standard CEMA through simulations. ESPRIT method provides high modal parameters estimation accuracy and it is also compared with LSE in this thesis.

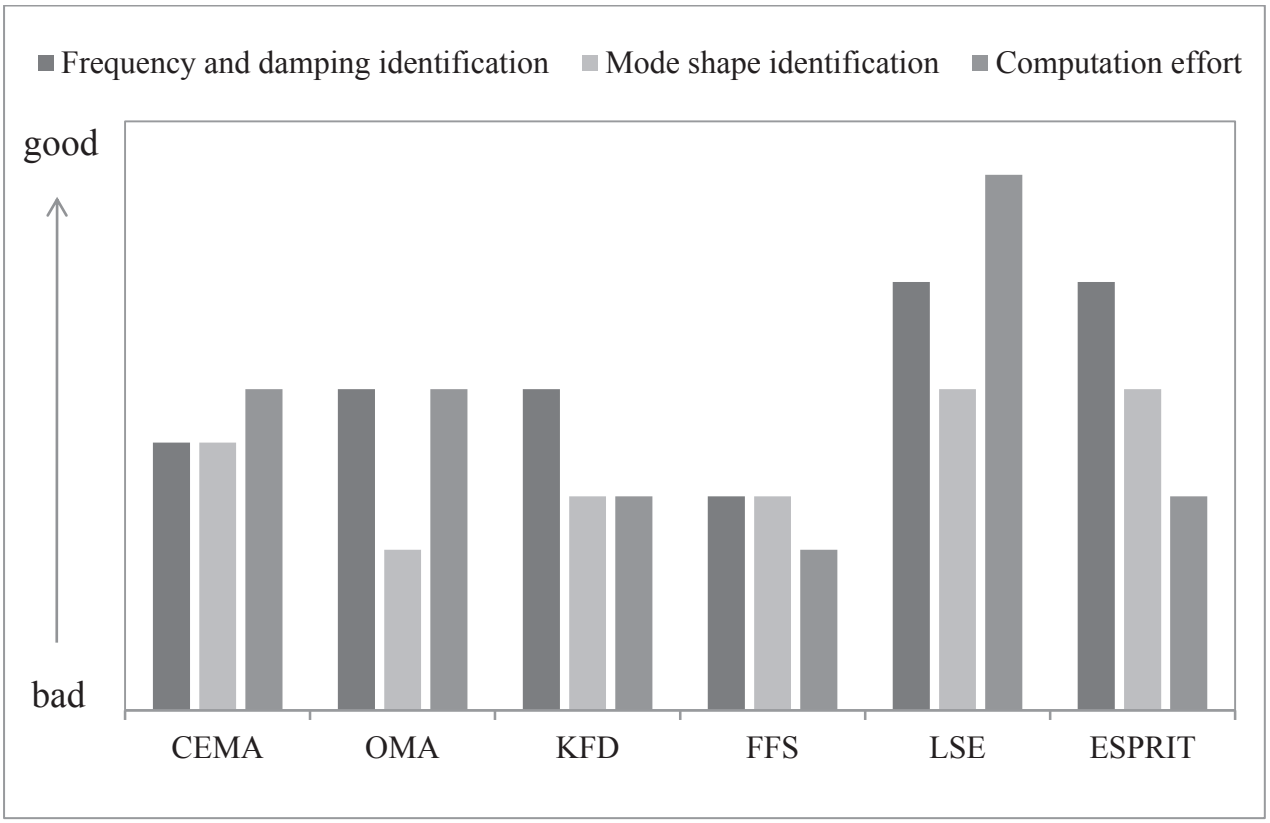

Figure 4: Performance comparison for short time identification. **CEMA**: classical experimental modal analysis, **OMA**: operational modal analysis, **KFD**: kernel function decomposition (short time Fourier transform, Wigner-Ville distribution, Wavelet transform), **FFS**: frequency family separation method (empirical mode decomposition, local mean decomposition, random decrement technique), **LSE**: least squares estimation technique, **ESPRIT**: estimation of signal parameters via rotational invariance technique. [BAD05, BEN06, EWI00, GRÖ00, KAN13, PAD04, PET01, POO07, SMI05, SPI09, THA09, YAN08, ZAG09, ZUB00].

Chapter 3

Sliding Window Least Squares Estimation

The main procedure of the sliding window least squares estimation (SWLSE) for transient modal parameters identification is described in this section. The Least Squares method has been widely adopted in many engineering applications. But there are no applications in short time modal analysis (analyzed signal in range of millisecond) for detection of the transient modal parameters of systems. In this work，the analyzed signal can be divided into time blocks. The proposed method is used for each block in order to reveal the actual dynamic properties of structures.

3.1 Mathematical Background

The modal parameters (natural frequency and damping ratio) can be obtained by fitting time window data with a damped oscillating function using least squares algorithm. Thus, the transient modal parameters of the dynamic system can be detected in a short time window. The shifting of modal parameters during the whole time history can be estimated easily by using the moving window across the signal. The mathematical background for least squares algorithm is introduced in following, which is successfully applied to low-frequency oscillation parameters estimation for power systems [YAN08].

Consider a mono-frequency signal $x(k)$ which can be defined as follows:

$$x(k) = Xe^{\alpha k\Delta t}\cos(2\pi fk\Delta t + \varphi) \tag{3.1}$$

where X is the amplitude, α is the decay constant, f is the oscillation frequency, φ is the phase, k is the number of samples and Δt is the time interval. According to Euler theorem, $\cos\theta$ can be written as:

$$\cos\theta = \frac{e^{j\varphi} + e^{-j\varphi}}{2} \tag{3.2}$$

then $x(k)$ can be expressed as:

$$x(k) = \frac{1}{2}e^{\alpha k\Delta t}(Xe^{j\varphi}e^{2\pi fk\Delta t} + Xe^{-j\varphi}e^{-2\pi fk\Delta t}) \tag{3.3}$$

Using the following definitions:

$$A = \frac{X}{2} e^{j\varphi}, a = e^{j2\pi f \Delta t}, b = e^{\alpha \Delta t}, z = \mathrm{Re}(a) \tag{3.4}$$

equation (3.3) can be rewritten as:

$$x(k) = b^k (Aa^k + \overline{A} a^{-k}) \tag{3.5}$$

after linearization process, it could be obtained:

$$-bx(k) + 2zx(k+1) - b^{-1}x(k+2) = 0 \tag{3.6}$$

Linearization process for SWLSE algorithm

The process of linearization for the equation (3.6) is given in following. Assume a^k can be expressed as a complex type:

$$a^k = a^k (1 + j \cdot 0) \tag{3.7}$$

and used some trigonometric function calculations:

$$a^k = a^k \left[1 + \cos 2\theta - \cos 2\theta + j(\sin 2\theta - \sin 2\theta)\right] \tag{3.8}$$

$$a^k = a^k \left[2 \cdot \frac{1 + \cos 2\theta}{2} - \cos 2\theta + j(2\cos\theta \sin\theta - \sin 2\theta)\right] \tag{3.9}$$

$$a^k = a^k (2 \cdot \cos^2 \theta - \cos 2\theta + j2\cos\theta \sin\theta - j\sin 2\theta) \tag{3.10}$$

$$a^k = a^k \left[2\cos\theta(\cos\theta + j\sin\theta) - (\cos 2\theta - j\sin 2\theta)\right] \tag{3.11}$$

$$a^k = a^k (2\cos\theta \cdot e^{j\theta} - e^{j2\theta}) \tag{3.12}$$

Using the definition in equation (3.4), the equation (3.12) can be simplified in:

$$a^k = a^k(2za - a^2) \tag{3.13}$$

$$a^k = 2za^{k+1} - a^{k+2} \tag{3.14}$$

Then, put the equation (3.14) into (3.5):

$$x(k) = Ab^k(2za^{k+1} - a^{k+2}) + \bar{A}b^k(2za^{-(k+1)} - a^{-(k+2)}) \tag{3.15}$$

$$x(k) = Ab^k 2za^{k+1} + \bar{A}b^k 2za^{-(k+1)} - Ab^k a^{k+2} - \bar{A}b^k a^{-(k+2)} \tag{3.16}$$

$$\begin{aligned} x(k) = {} & 2zb^{-1}(Ab^{k+1}a^{k+1} + \bar{A}b^{k+1}a^{-(k+1)}) \\ & -b^{-2}(Ab^{k+2}a^{k+2} + \bar{A}b^{k+2}a^{-(k+2)}) \end{aligned} \tag{3.17}$$

$$x(k) = 2zb^{-1}x(k+1) - b^{-2}x(k+2) \tag{3.18}$$

$$b \cdot x(k) = 2z \cdot x(k+1) - b^{-1} \cdot x(k+2) \tag{3.19}$$

$$-b \cdot x(k) + 2z \cdot x(k+1) - b^{-1} \cdot x(k+2) = 0 \tag{3.20}$$

Finally, equation (3.5) is reconstructed by equation (3.6), so that the linear Least Squares method can be used for this linear relationship.

Rearrange equation (3.6) as:

$$\begin{bmatrix} x(k) & x(k+1) \\ x(k+1) & x(k+2) \\ \vdots & \vdots \\ x(k+L-3) & x(k+L-2) \end{bmatrix} \begin{bmatrix} p_1 \\ p_2 \end{bmatrix} = \begin{bmatrix} x(k+2) \\ x(k+3) \\ \vdots \\ x(k+L-1) \end{bmatrix} \tag{3.21}$$

where L indicates the data window size and

$$p_1 = -b_1^2 \ , \ p_2 = 2z_1 \cdot b_1 \tag{3.22}$$

Equation (3.21) can be simplified as $AP = B$.Thus, the parameter identification with non-linear equation (3.3) has been translated to the linear equation (3.21). The solution P can be easily obtained using least squares algorithm:

$$P = (A^T A)^{-1} A^T B \tag{3.23}$$

Equation (3.22) can be rewritten as:

$$b_1 = \sqrt{-p_1}\ , z_1 = \frac{p_2}{2b_1} \tag{3.24}$$

then, the applied window is shifted on the whole signal to obtain the b_i and z_i.

Transient natural frequency

According to the definitions (3.4), the actual natural frequencies can be obtained as the following equation:

$$f_i = \cos^{-1}(\frac{z_i}{2\pi \cdot \Delta t}) \tag{3.25}$$

Transient damping ratio

Similarly, the actual damping ratio can be computed with the following equation:

$$\xi_i = -\frac{a_i}{\sqrt{a_i^2 + (2\pi f)^2}}\ , a = \frac{\ln(b_i)}{\Delta t} \tag{3.26}$$

Transient mode shape

In order to obtain the mode shapes of the system, the measured history data are necessary to construct an equivalent eigensystem matrix. The characteristic equation for eigensystem can be written as follows according to (3.21) (see Appendix A.1):

$$[A] \cdot \{P\} = \delta \cdot \{P\} \tag{3.27}$$

where δ is the eigenvalue of the system $[A]$, and $\{P\}$ is the eigenvector. Equation (3.27) can be rewritten as:

$$([A]-\delta[I])\{P\}=\{0\} \tag{3.28}$$

where $[I]$ is the identity matrix, which can be written as:

$$I=\begin{bmatrix}1 & 0 & \cdots & 0\\ 0 & 1 & \cdots & 0\\ \vdots & \vdots & \ddots & \vdots\\ 0 & 0 & \cdots & 1\end{bmatrix} \tag{3.29}$$

The characteristic equation of (3.28) can be expressed as follows:

$$\left|\,[A]-\delta[I]\,\right|=0 \tag{3.30}$$

The solution of the equation (3.30) is:

$$\delta=e^{2\pi j\Delta t} \tag{3.31}$$

Writing the solution δ in (3.28), the corresponding $\{P\}$ can be obtained:

$$\{P\}=\begin{Bmatrix}R\\ \overline{R}\end{Bmatrix} \tag{3.32}$$

where R is called residue. It can be computed as follows:

$$R_i=2\cdot\left|\frac{x(k+1)\cdot\delta_i-x(k)\cdot b_i}{b_i\cdot(\delta_i^2-1)}\right| \tag{3.33}$$

In order to obtain the mode shape of the system, more sensing locations are needed. For each sensing location the residue can be computed and reformed to the eigenvector.

$$\{\Phi_i\}=\begin{bmatrix}R_{i1} & R_{i2} & \cdots & R_{in}\end{bmatrix}^T \tag{3.34}$$

Due to the relative motion between measured points, it is necessary that the shapes are normalized according to the modal mass or modal stiffness [AU11]. A simple scaling can be done with maximum value of one of the calculated residues. For example, a

measurement has n sensing locations, where point m has max. value of residue, then the mode shapes can be expressed as:

$$\{\Phi_i\} = \begin{bmatrix} R_{i1} & R_{i2} & \cdots & R_{in} \end{bmatrix}^T / R_{im} \tag{3.35}$$

It is notice that the spatial resolution of mode shape can only be improved by increasing the number of sensing locations.

This proposed SWLSE method allows the identification only if the analyzed signal is a single degree damped data. For multi-degree of freedom systems, a band-pass filtering of the free response is necessary in order to separate each mode. In other words, a filter technique as pre-processing must be used with SWLSE method.

3.2 Pre-processing for SWLSE

Least squares estimation can be augmented with a sliding-window operation (SWLSE) to reveal the actual system dynamic behavior at every time instance. When the window is shifted in time, modal parameters of time-varying systems can be obtained in each analyzing window. As mentioned in the previous section, a filtering as pre-processing must be applied. In this work, an ideal frequency filter with Hanning window is applied for this pre-processing. The results of estimated parameters using SWLSE method are compared with the results of classical EMA method.

A sketch of the operation procedure is shown in Figure 5. Firstly, a time signal (acceleration) is sampled. For the SWLS method the signal is filtered by ideal digital frequency filter as the pre-processing to decompose the original signal into a narrow-band signal. Now the filtered narrow-band signal is identified using SWLSE method. The obtained modal parameters are compared with the results of the classical EMA, which is using FFT technique to construct the FRFs and coherence functions. To detect the modal parameters the curve fitting method is applied in frequency domain and the half power bandwidth method is used to calculate the damping ratios [MAI97].

By classical EMA method, the coherence function can be used to determine the linearity of the FRF measurement, and the length of the measurement determines the frequency resolution. However, it is assumed that the estimation accuracy of SWLSE algorithm depends on the window size, the sampling rate, noise level and filtering technique. The identification accuracy is investigated in next chapter.

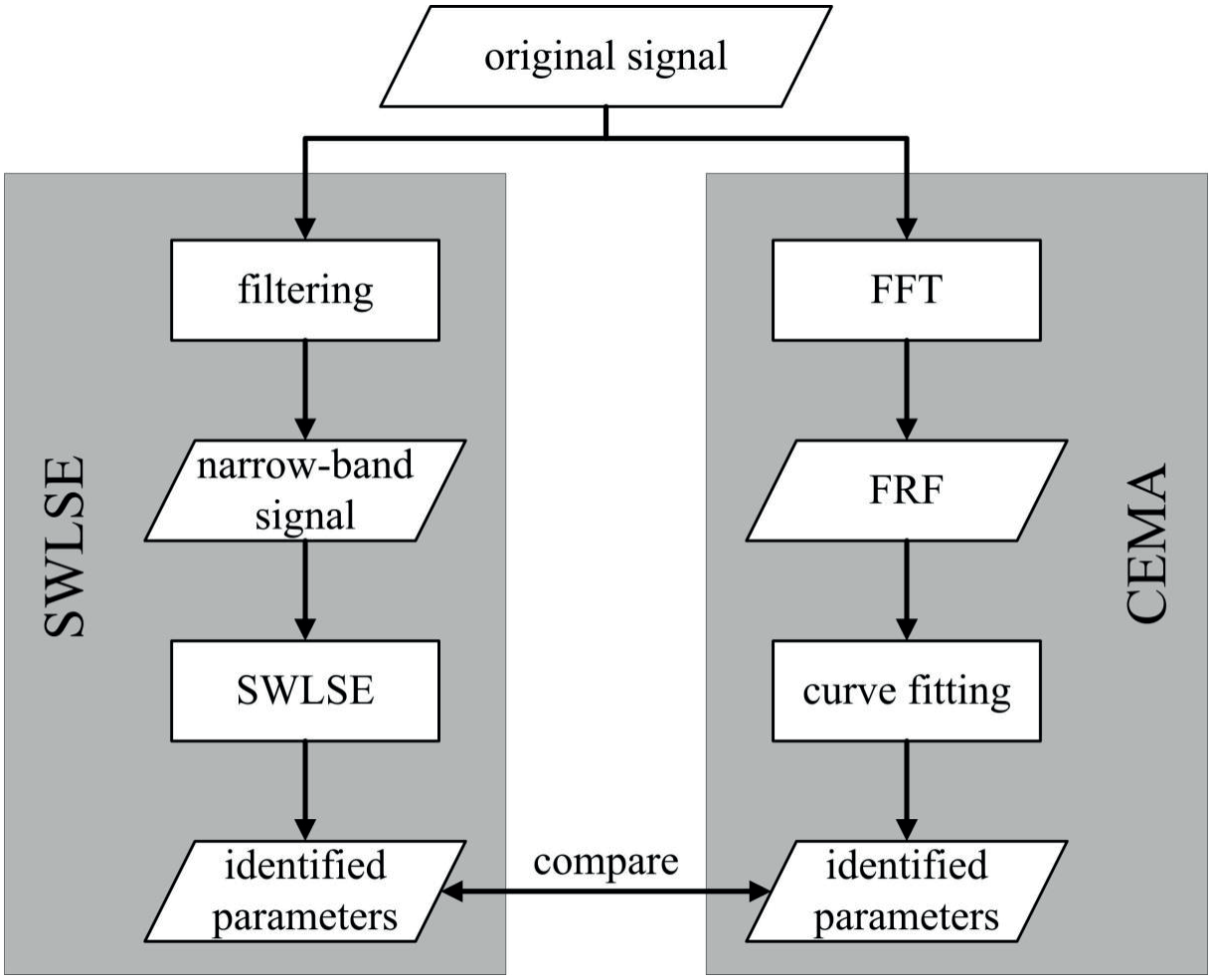

Figure 5: Flow Chart of the operation procedure

Chapter 4

Comparison and Validation using Numerical Simulations

This chapter addresses the performance of the sliding-window Least Squares estimation (SWLSE) algorithm using numerical examples. This method is compared in terms of computational reliability. The accuracy of modal parameters estimation is estimated by the comprehensive evaluation from several aspects. The identification accuracy of SWLSE algorithm is compared with classical experimental modal analysis method (Chapter 5.1) and ESPRIT method (Chapter 5.2) in this section.

4.1 Investigation of Identification Accuracy Comparing with Classical Experimental Modal Analysis

In practice the measured FRFs contain a certain amount of noise. The accuracy of identification results depends on the quality of data, especially on the level of the experimental noise. The simulation analysis is performed on the following single degree damped sinusoid with narrowband noise:

$$x(t) = A_{signal} \cdot e^{-\xi 2\pi f_n t} \sin(2\pi f_n t) + y_{noise} \tag{4.1}$$

where the magnitude $A_{signal} = 1$, time range $0 < t < 1$, f_n is the natural frequency of the simulated signal, ξ is the damping ratio and y_{noise} is a narrowband white Gaussian noise.

In this work, the proposed method is tested under the noise condition using a definition of signal to noise ratio (SNR). The SNR quantifies the relative magnitude of the harmonic and the random component in the output response [INM01]. It is defined as:

$$SNR_{dB} = 10 \cdot \log_{10}\left(\frac{A_{signal}^2}{\sigma_{noise}^2}\right) \tag{4.2}$$

where σ_{noise}^2 is the standard deviation of the noise. By impact testing for lightly damped systems, an exponential window is applied to force the signal to near zero by the end of the record. The noise in our case is also multiplied by an exponential function, which is the upper envelope of the simulation noise, before added to the signal.

Experimental procedure

Table 1 shows preset parameters of the artificial signal. The simulated signal is analyzed and compared using the proposed SWLSE algorithm and CEMA method. To examine the performance of the proposed algorithms three experiments are produced in this section:

Table 1: Preset values of the artifical signal for chapter 4.1.1 and 4.1.2

Parameter		**Set value**	
preset frequency	102 Hz	302 Hz	502 Hz
preset damping ratio	0.05 %	0.5 %	2 %
preset signal length	0.5s to 5s (increment 0.1s)		

In chapter 4.1.1, the artificial signals without noise are tested first. The signal length is one of the most important parameters, which directly influence the frequency estimation accuracy by CEMA method. The length of the artificial signal is varied from L=0.5 s to L=5 s to verify the performance of SWLSE method. The artificial signal less than 0.5 s is not investigated in this section due to the bad resolution of estimated parameters by CEMA method. For example for a signal with length L = 0.1 s, the resolution of the frequency estimated by CEMA method has just 10 Hz. However, for a signal with length less than 0.1 s the SWLSE method can even provide high resolution that will be mentioned in the following chapters.

In this test the proposed method uses the analyzing window, whereas the length of the window is same as the length of the whole signal. The estimated frequencies and damping ratios are computed for each signal. The experiment is repeated 5 times. The mean values are calculated and illustrated.

In chapter 4.1.2, the same experiment is carried out, just the artificial signal with 30dB noise level. An example signal with 30 dB is shown in Figure 6. The values of signal are set by 102 Hz frequency and 2 % damping ratio.

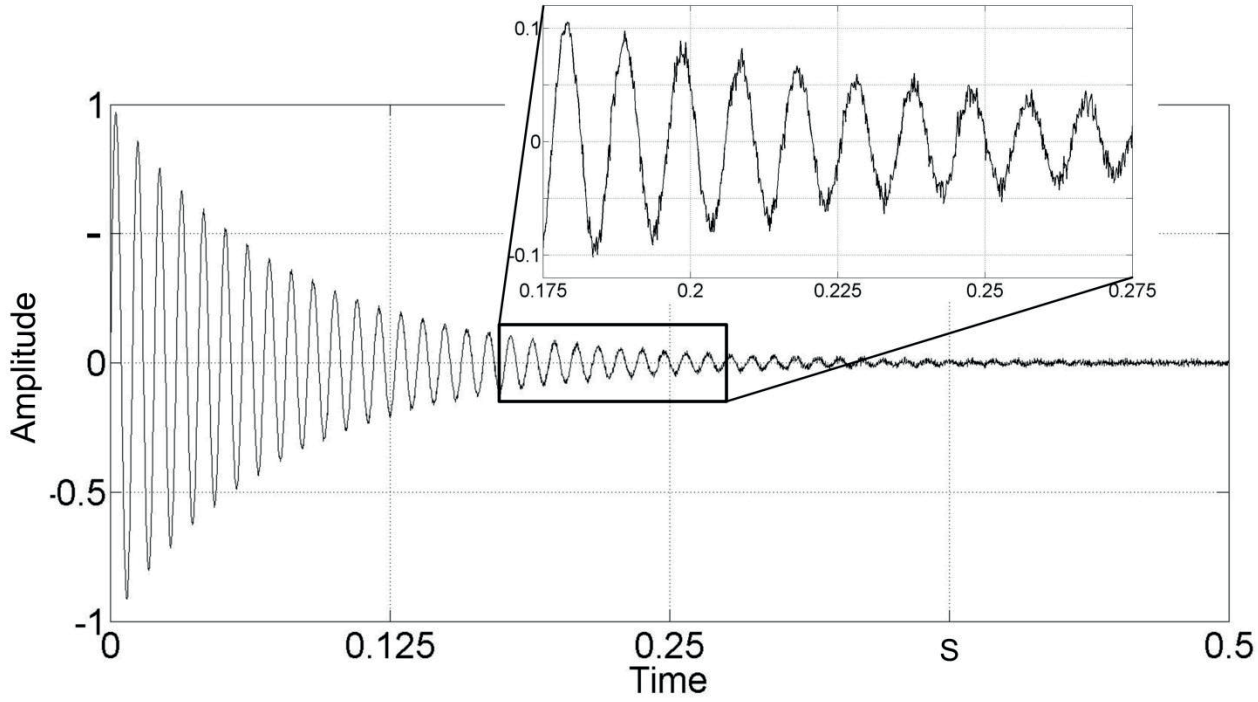

Figure 6: An artificial signal with 30 dB noise level. The preset values of signal are 102 Hz frequency and 2 % damping ratio.

In chapter 4.1.3, a system of closely spaced two degrees of freedom is considered. In the actual measurement especially on a symmetrical structure, the double mode is observed frequently. For example, a bending mode of the second order and a torsional mode of the first order have often a similar natural frequency within a symmetrical structure. The system equation has closely spaced poles, also the peaks of mode are located very close, that cause a low accuracy of the curve-fitting results. It is necessary to investigate the identification accuracy for the double peaks.

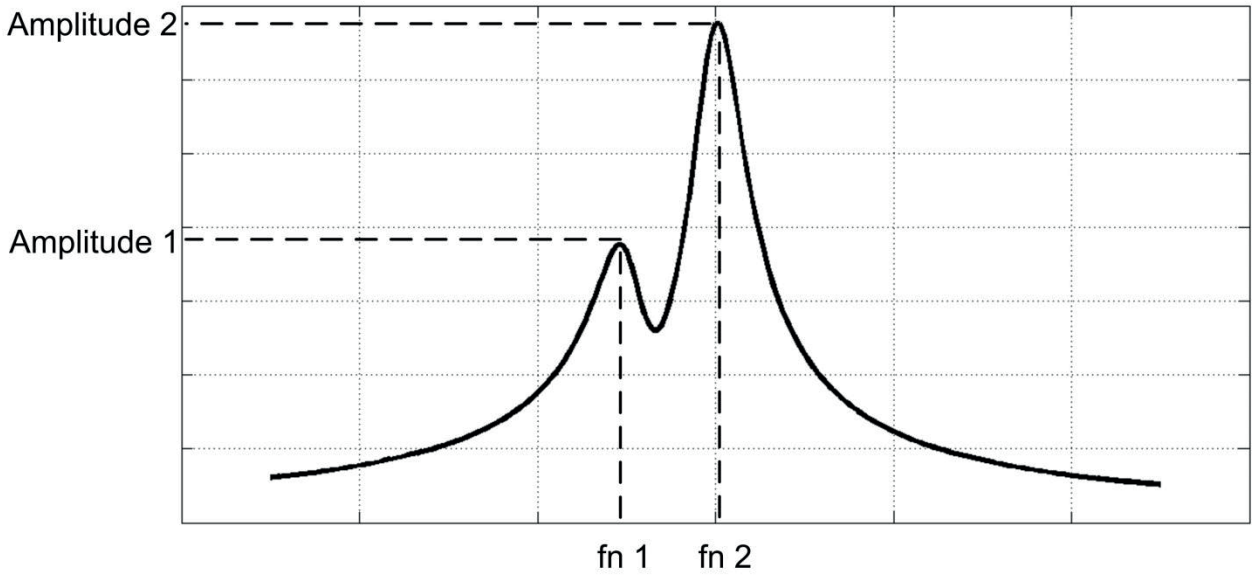

Figure 7:Spectrum for closely spaced modes

To describe the relationship between the both peaks two values are defined. One is the frequency difference (fn2-fn1), which is varied from 0.2 to 2 Hz. Other one is the amplitude ratio (Amp1/Amp2), which is varied from 0.1 to 10 in this work.

Table 2: Preset values of the artifical signal and computation parameters for chapter 4.1.3

Parameter	Set value
preset frequency	from 100 to 101.8 Hz
preset amplitudes ratio	from 0.1 to 10
analyzed signal length	5 second
sampling rate	10 kHz

To evaluate estimation performance for double peaks, the parameters of one of the peaks are fixed by frequency $f_n = 102Hz$, damping ratio $\xi = 0.3\%$. Another one is varied by the frequency difference parameter and amplitude ratio. The modal parameters by the frequency $f_n = 102Hz$ are identified using proposed method. The influences of another peak on this frequency (102 Hz) are discussed.

The modal parameters are estimated using both CEMA and SWLSE method. The preset values of the parameters of the double mode and computation parameters are given in Table 2. The results are illustrated with color-map diagram which results the deviation of identification accuracy as a function of the difference frequency and the amplitude ratio. The horizontal axis represents the frequency difference (fn2-fn1), and the vertical axis represents the amplitudes ratio (Amplitude1/Amplitude2).

4.1.1 Identification Accuracy without Noise

The deviation of the repeat simulation results is very small that it is not shown in the figures below. Figure 8 shows that the resulting estimations of different signals for CEMA and SWLSE are very close. Also the identification accuracy does not change much with varying of frequency. In the testing range, both methods provide high frequency identification accuracy.

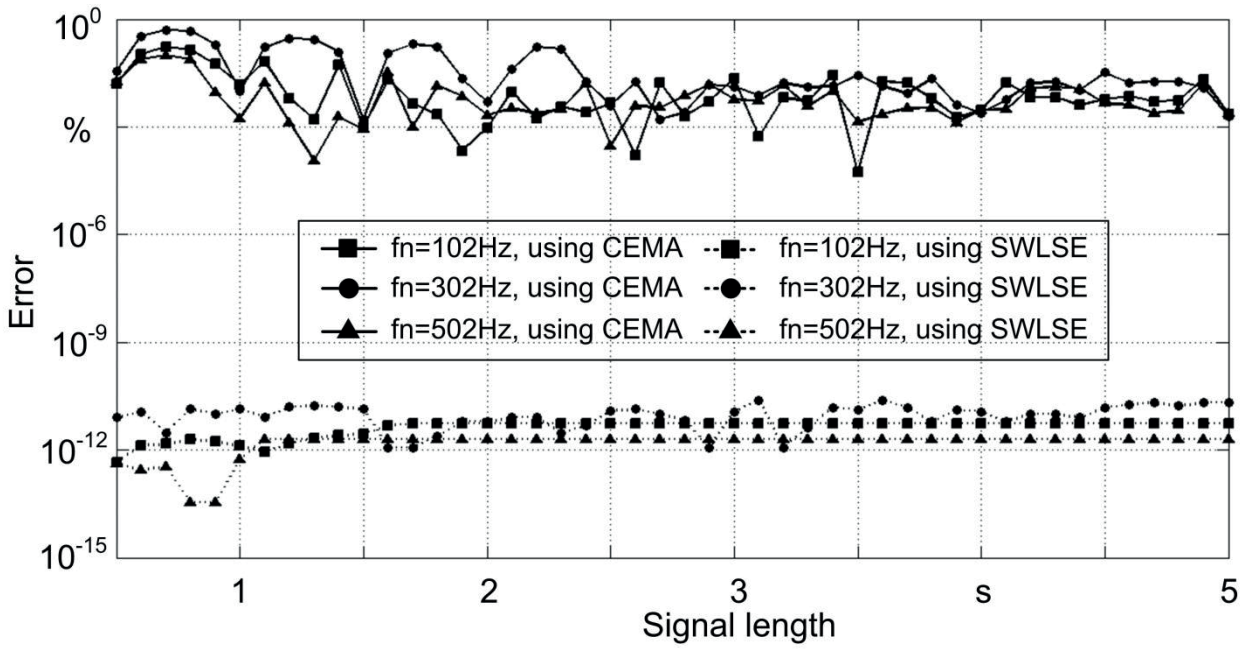

Figure 8: Frequency identification accuracy without noise using SWLSE and CEMA method, $\xi = 0.5\%$.

It is noticeable that the frequency resolution of the CEMA method depends on the sampled signal length. For a 0.5 s signal the frequency resolution is only to be 2 Hz. One of the significant advantages of SWLSE method is that it can provide also very high frequency resolution independ from the length of signal.

In the same testing, the damping ratio identification accuracy is shown in Figure 9. The SWLSE method provides a higher accuracy for damping identification than CEMA. The identification accuracy of high damping by CEMA is higher than of light damping, confirming the common assumption that CEMA is the preferred method in case of high damping. That is because a lightly damped structure in frequency domain yields a narrower peak or less acquired points, thus reduces the accuracy of the curve fitting processing. Whereas a highly damped structure in time domain yields a less acquired points, the quality of the fit decreased.

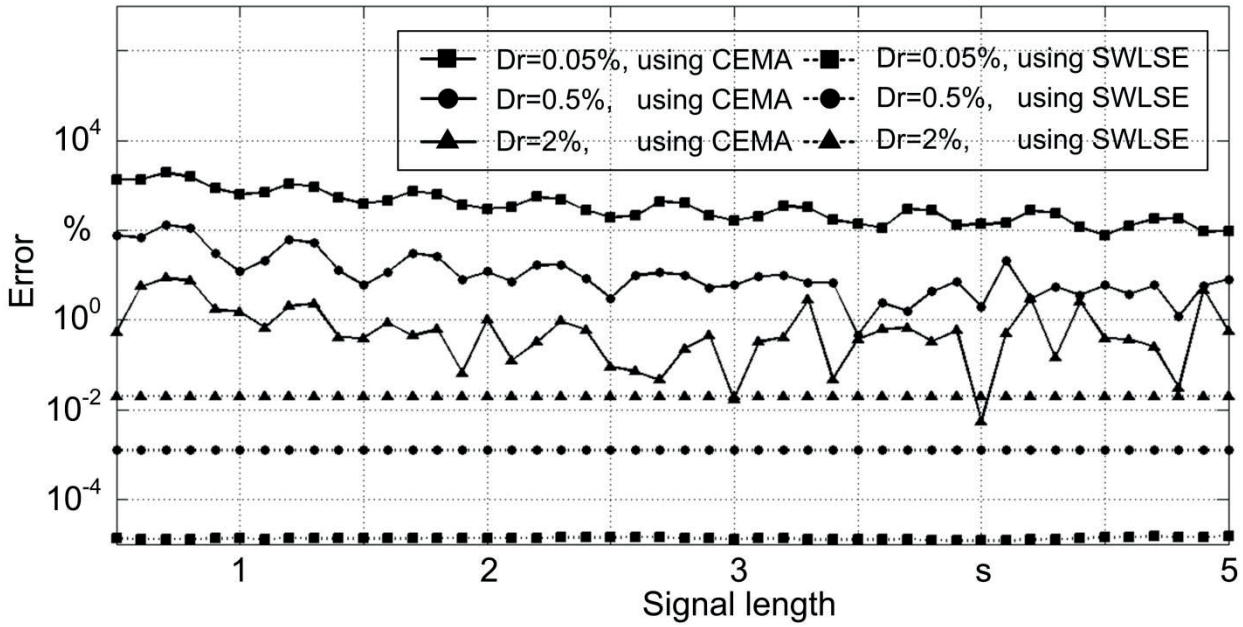

Figure 9: Damping ratio identification accuracy without noise using SWLSE and CEMA method, $f = 102Hz$

4.1.2 Identification Accuracy with Noise

Figure 10 and Figure 11 show the same test as in the previous subsection, but the artificial signals with noise level 30 dB.

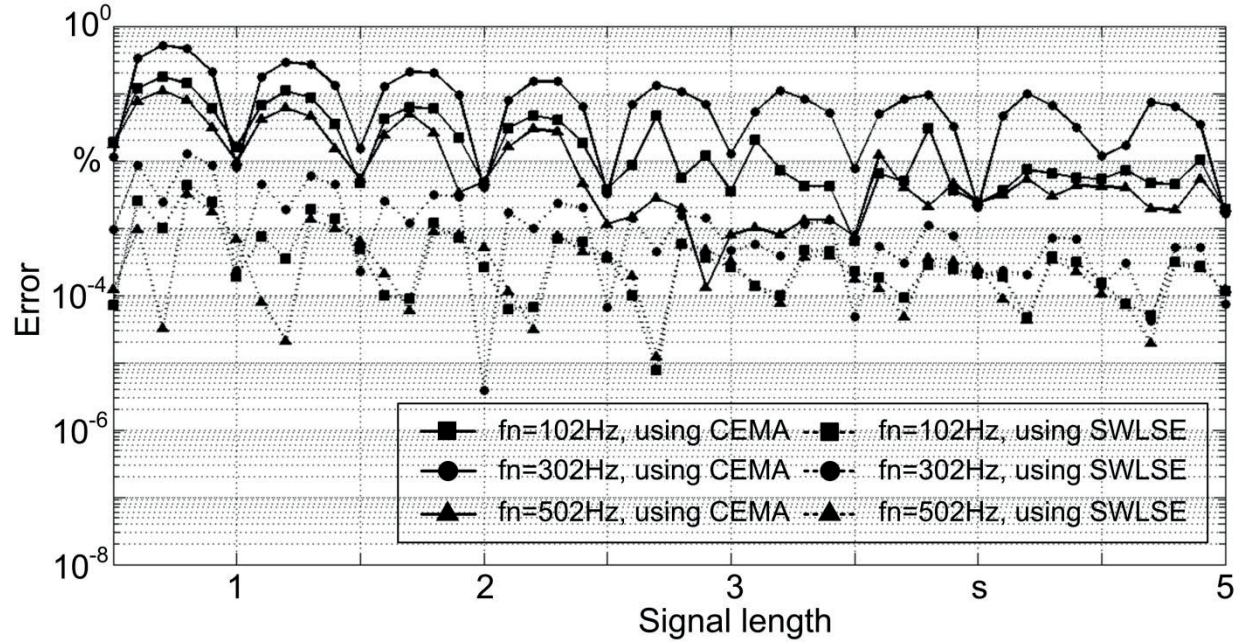

Figure 10: Frequency identification accuracy with 30dB noise level using SWLSE and CEMA method, $\xi = 0.5\%$.

By comparing Figure 10 and Figure 8, the identification accuracy of SWLSE method is reduced clearly. However, as shown in Figure 10, the performance of the SWLSE method is still better than CEMA. The frequency identification accuracy of the SWLSE method is demonstrated to be less than 0.01 % estimation errors for a mono-frequency signal with 30 dB SNR.

Another important aspect to be studied concerns the influence of the signal length. It can be seen that frequency identification accuracy by SWLSE method is also increased with increasing of the signal length. When the sampled time data becomes longer, the data with more sampled points, the quality of the curve fitting processing is also increased.

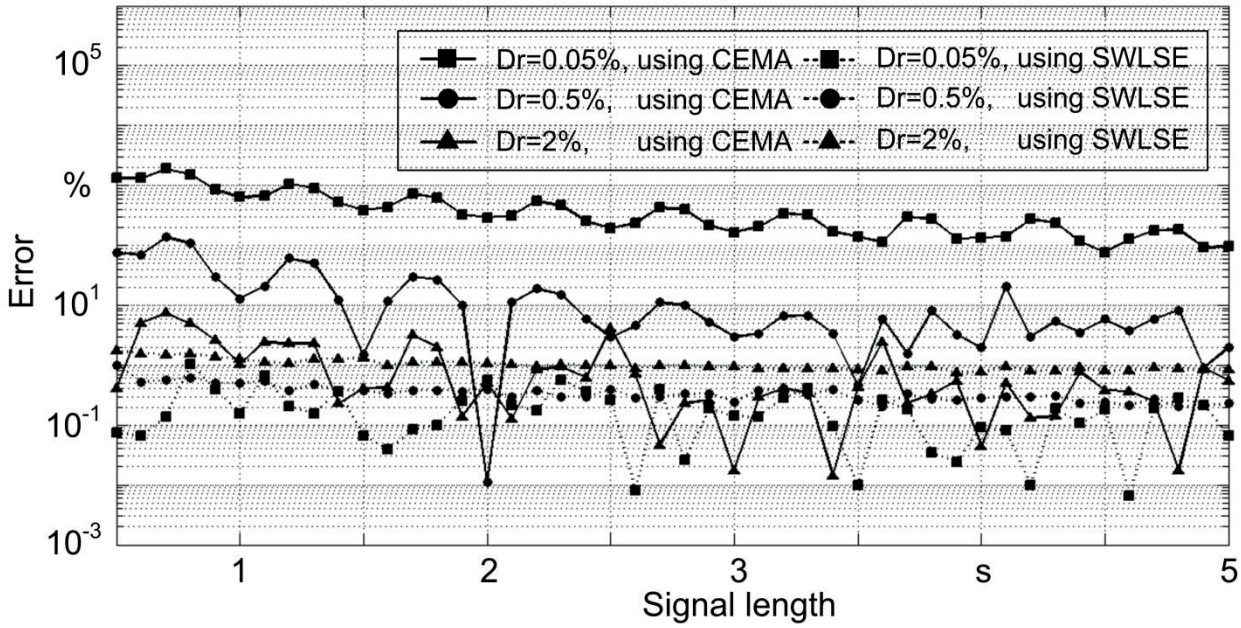

Figure 11: Damping ratio identification accuracy with 30dB noise level using SWLSE and CEMA method, $f = 102Hz$.

Figure 11 shows the damping ratio estimation with noisy signals. The accuracy is decreased by CEMA and is increased by SWLSE with reduced preset damping ratio. This also confirms as the expectation in the previous subsection, the CEMA is suitable for a highly damped structure and SWLSE is suitable for a lightly damped structure. Generally, the damping ratio accuracy by SWLSE method is better than by CEMA method. The maximum estimation error by SWLSE between the estimated value and preset value is less than 3% for a mono-frequency signal with 30dB SNR in this test.

4.1.3 Identification accuracy for double mode peaks

Figure 12 and Figure 13 show both color-map diagrams of frequency deviation. The identification accuracy for both methods is similar. By decreasing the frequency difference and by decreasing the amplitude ratio, the estimation accuracy is reduced.

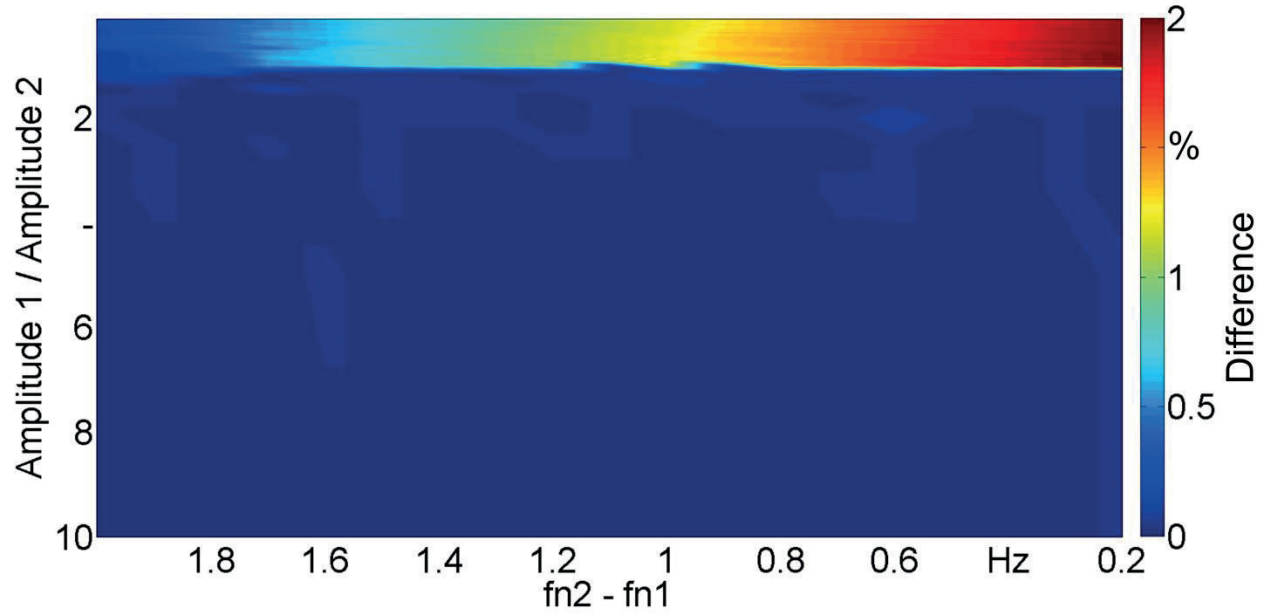

Figure 12: Freqeuncy identification accuracy for double modes using CEMA method

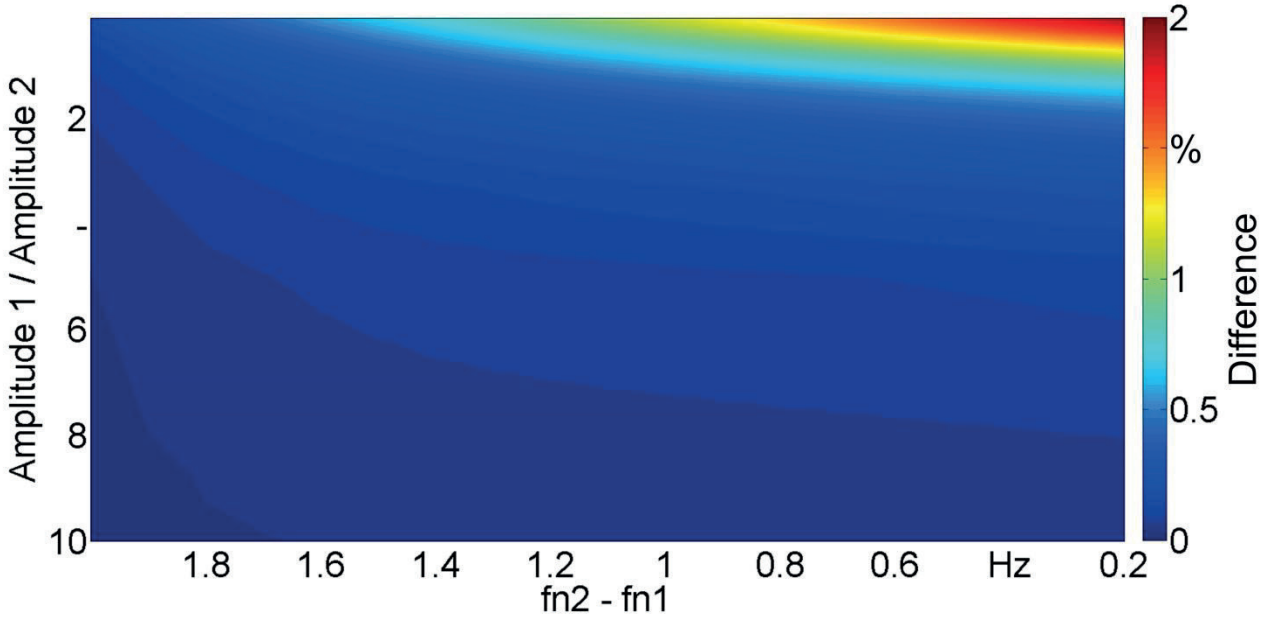

Figure 13: Freqeuncy identification accuracy for double modes using SWLSE method

Figure 14 and Figure 15 show both color-map diagrams of damping ratio deviation. In this example the SWLSE method is clearly better than the CEMA method, especially at lower amplitude ratio and higher frequency difference it provides much higher accuracy.

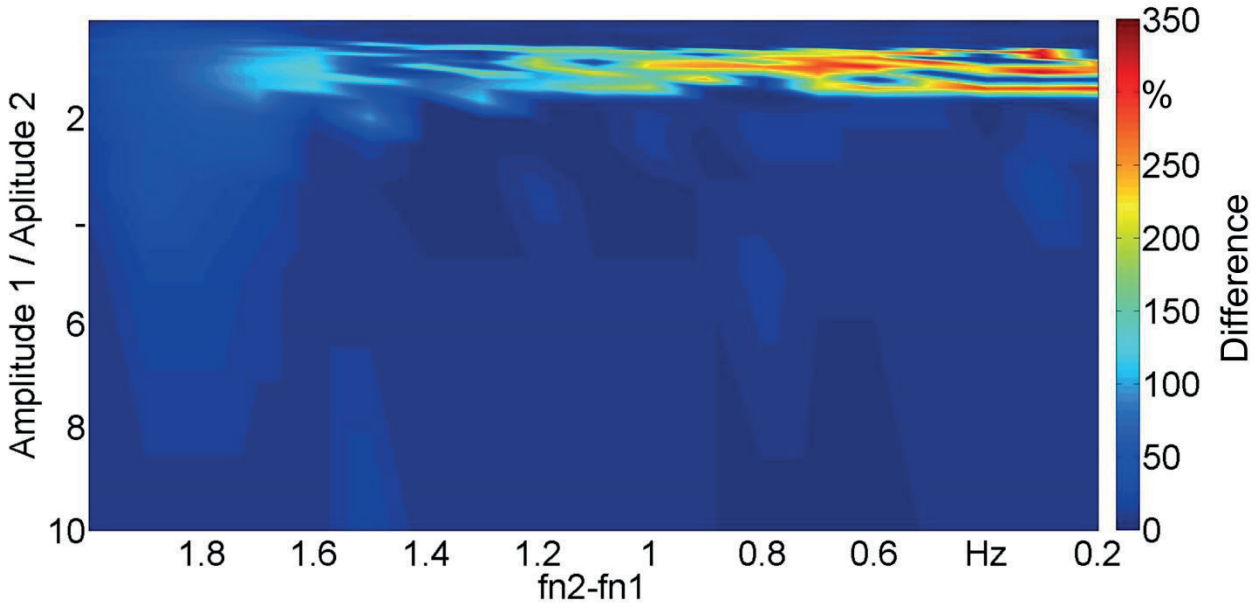

Figure 14: Damping ratio identification accuracy for double modes using CEMA method

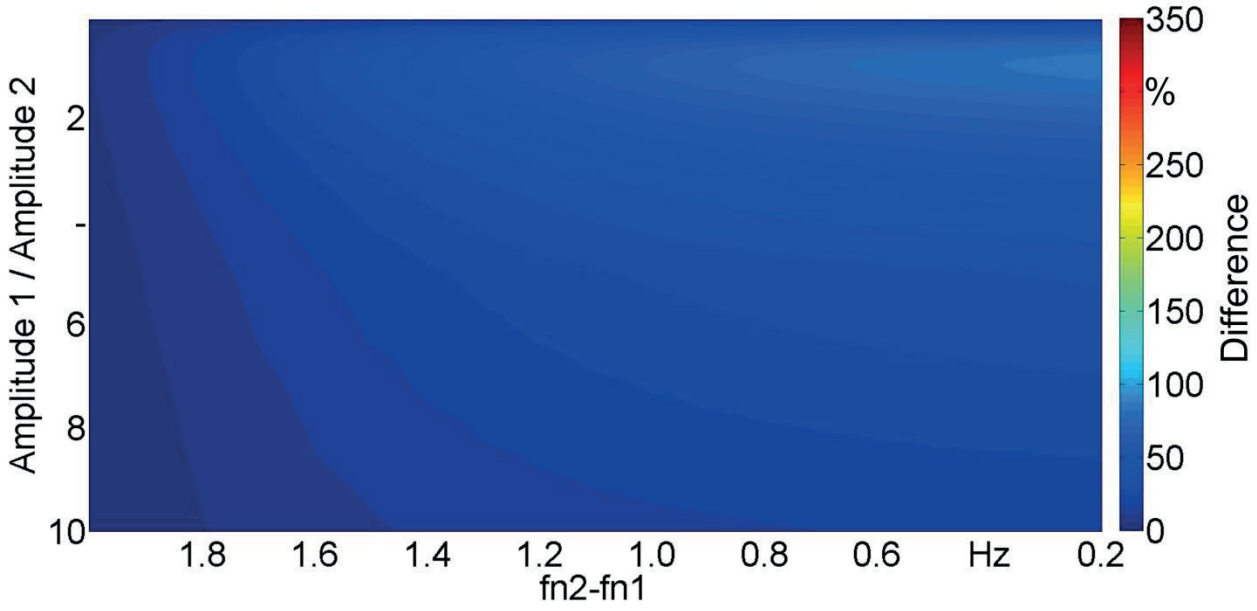

Figure 15: Damping ratio identification accuracy for double modes using SWLSE method

Comparing this result the proposed method can provide more identification accuracy for the damping ratio. When the amplitude ratio is pointed between the values from 0.2 to 2, the error for the CEMA method is increased clearly. The identification error for both method is increased, when the frequency difference value tends to be 0.2 Hz. Overall, the SWLSE method provides a result which is much better, more smooth and accurate than the CEMA method.

4.2 Testing with Various Criterions

For further testing the performance of the SWLSE method is examined by various window sizes and the noise levels etc. using numerical calculation. Because the CEMA method cannot provide enough frequency resolution for a signal length less than 500 ms, the proposed method is compared not with the CEMA method in this section, but with other parametric ESPRIT method which can be also applied as a short time identification technique [KUH11d].

Table 3: Preset values and computing parameters

Parameter	**Value**
preset frequency	260 Hz
preset damping ratio	0.2 %
filter pass band	210 Hz-310 Hz
shifting step of window	4 ms
sampling rate	5120 Hz
signal length	1 s

An artificial signal x(t) with 1 s signal length, 260 Hz preset frequency and 0.2% damping ratio is simulated. The signal is analyzed using the proposed algorithms augmented with a sliding window operation. The window size is varied from L=20 ms to L=80 ms. The window is shifted through the whole signal with a step 4 ms. The frequencies and damping ratios are estimated for each window using the proposed identification algorithms. The mean value is then computed. This measurement is repeated by 5 times, and the mean value of all measurements and standard deviation are computed. The results are compared with each other to examine the performance of the proposed algorithms. Detailed preset values are listed in Table 3.

Experimental procedure

The accuracy of this method depends on the window size, the noise ratio and the sampling rate. The influence of these parameters is discussed in this section, respectively:

In chapter 4.2.1, the modal parameters are estimated with different analyzing window length in order to evaluate the influence of the window size. The window size is varied from L=20 ms to L=80 ms. The SNR is set to 5 dB. The results by SWLSE and ESPRIT method are plotted in Figure 16 and Figure 17, respectively.

In chapter 4.2.2, the modal parameters are estimated for different noise levels in order to evaluate the influence of the noise level. The window size is constant and set to be L=20 ms.

In chapter 4.2.3, the estimation accuracy by the applied pass band filter is discussed. Due to time varying systems, in which the natural frequency shifts, the influence on the identification accuracy of the pass band filter value W, is investigated in this example. The value W is defined as the distance between the natural frequency fn of the simulated signal and the center frequency of the pass band, while the total width of the applied frequency filter remains constant at 100 Hz. The window size is set to 20 ms and the SNR is set to 20 dB.

In chapter 4.2.4, a single degree damped sinusoid with fn = 5Hz, ξ = 0.2% is simulated. The identification accuracy is examined, while the window length is set to less than a quarter of the frequency's period. The analyzing window size is set to 40 ms. The pass band is set from 1 Hz to 9 Hz.

In chapter 4.2.5, the computation efforts for the proposed algorithms are listed. Because the purpose of this work is to find an optimal algorithm for real-time control systems or online monitoring, the computational cost is also a very important parameter. The time, used for the required computations of each proposed algorithm is investigated for the simulated signal with preset values as seen in Tab.1 and a window size of 40 ms. It should be noted that the time of computation depends on the optimization of the programs and the CPU. The algorithms were implemented in MatLab 7.11.0 and run on an Intel Pentium Dual processor with a 2.20 GHz CPU and 2 GB RAM.

4.2.1 Variation of the window length

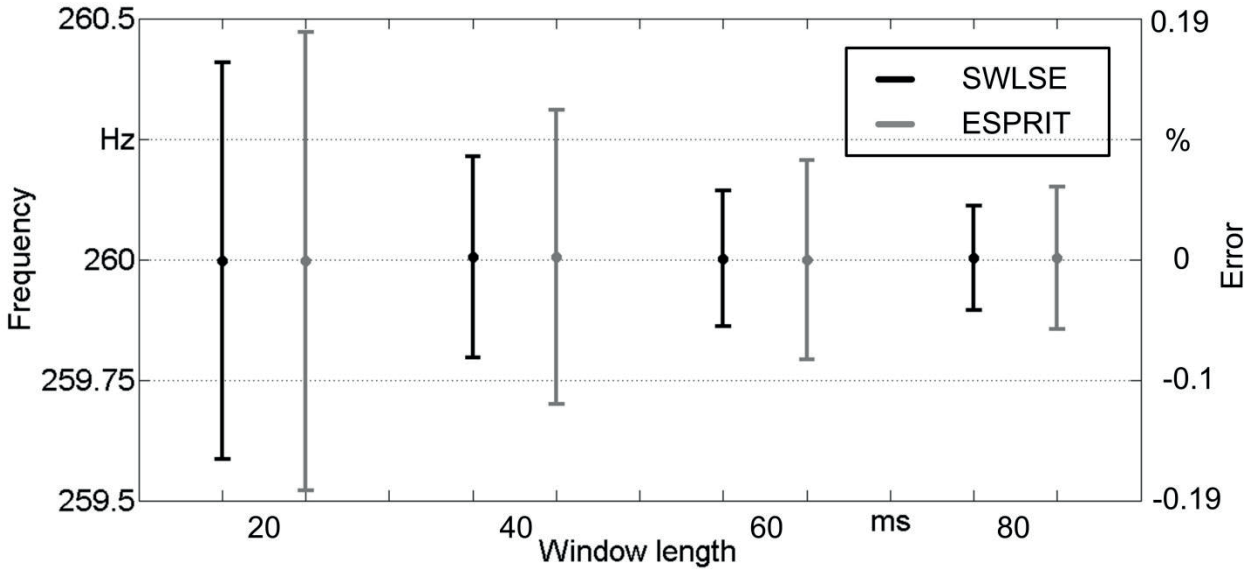

Figure 16: Frequency estimation with varying window length

It can be seen that the frequency estimation of the SWLSE and ESPRIT has a high accuracy (less than 0.19 % error). The increasing window size improves the identification accuracy. The result by SWLSE method provides slightly better accuracy than by ESPRIT method.

The estimation for damping ratio under various window sizes is shown in Figure 17. The estimation accuracy for SWLSE and ESPRIT is relative low. The maximum error between the estimated value and the preset value for 80ms window size is 25% for a signal with 5dB noise level. The accuracy increases with increasing window size. It can be seen that the accuracy of the SWLSE is also a little bit higher than of the ESPRIT method.

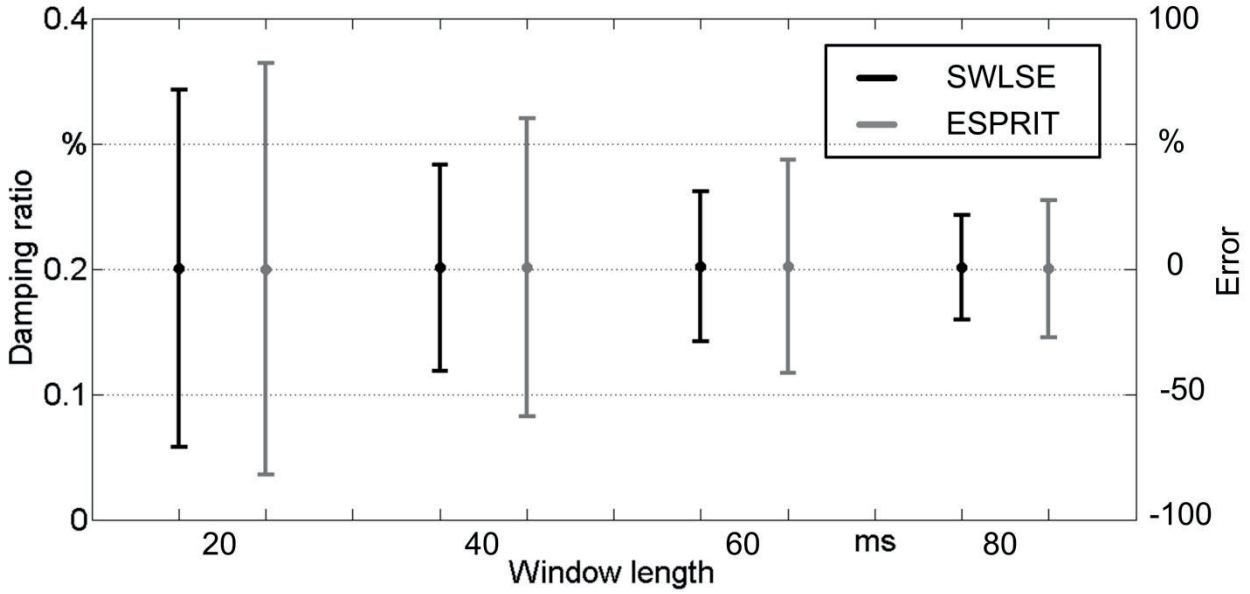

Figure 17: Damping ratio estimation with varying window length

4.2.2 Variation of the noise level

The identification results at different noise levels are given in Figure 18 and Figure 19. The accuracy is obviously improved, if the SNR is reduced from 5 dB to 20 dB. The estimation accuracy of both methods sensitively depends on the noise level.

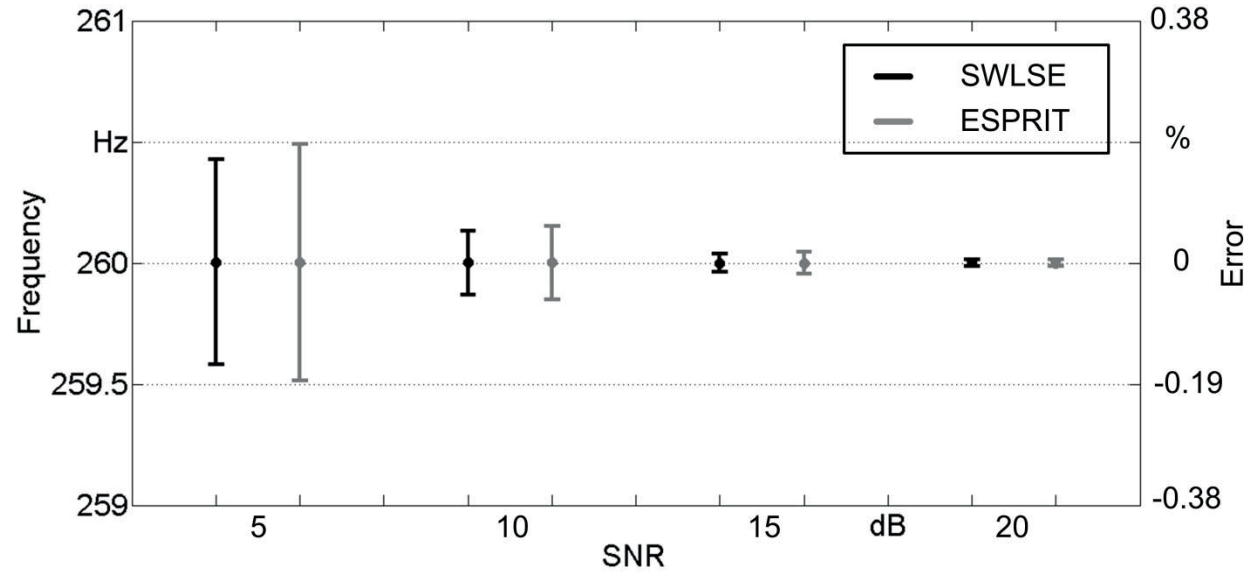

Figure 18: Frequency estimation with varying noise levels, L=20 ms

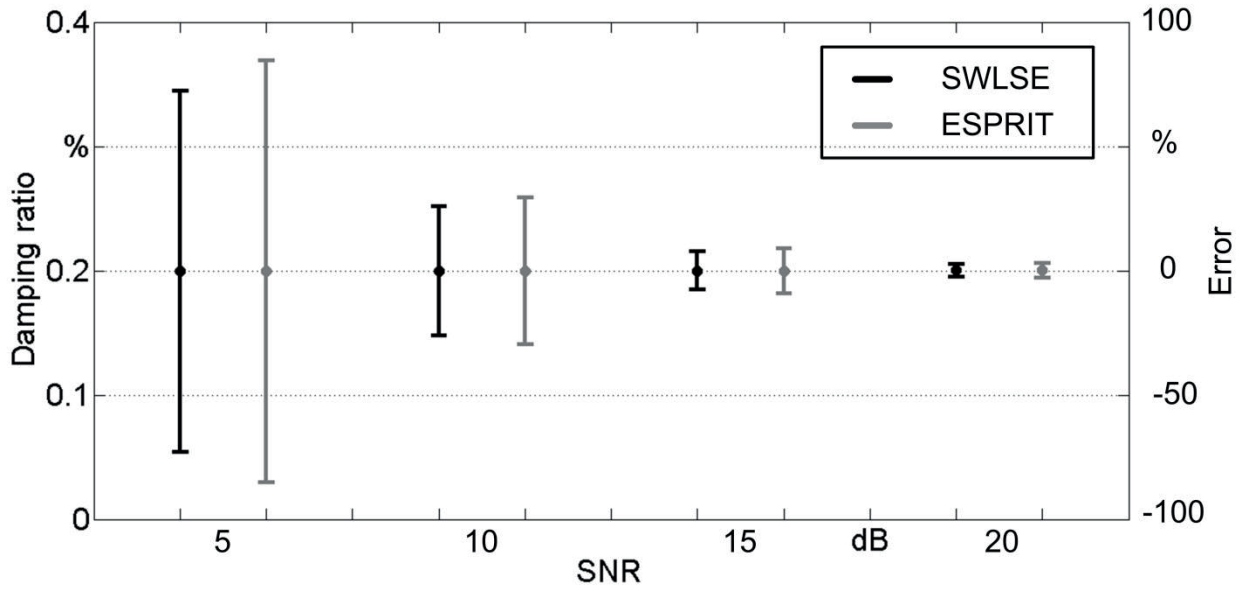

Figure 19: Damping ratio estimation with varying noise levels, L=20 ms

4.2.3 Variation of the pass band value W

The influence on the identification accuracy of the pass band filter value W, is investigated in this example. The value W is defined as the distance between the natural frequency f_n of the simulated signal and the center frequency of the pass band. As shown in Figure 20 and Figure 21, shifting the pass band does not have a large influence on the estimated values. In machining processes or engineering structures, the range in which modal parameters change is proved to be relatively small, as in a parallel kinematic machine the change in frequency stays within 2.1 Hz [ZHO07]. Therefore, the setting of the pass band has little influence on the accuracy of modal parameter estimation, even for time-varying systems.

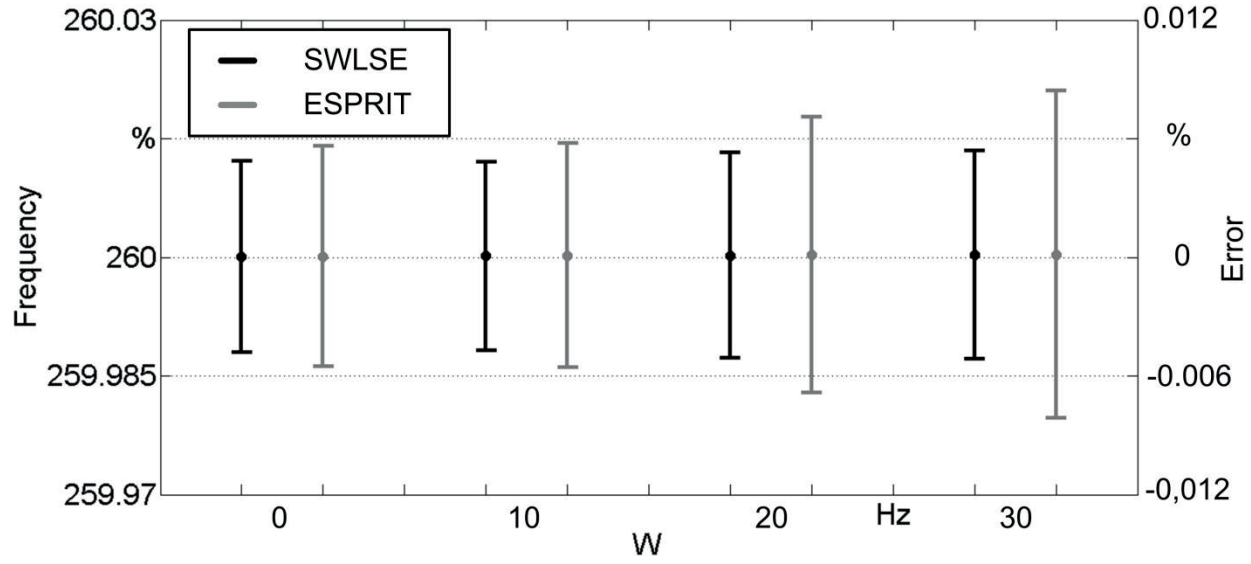

Figure 20: Frequency estimation with varying pass band value W

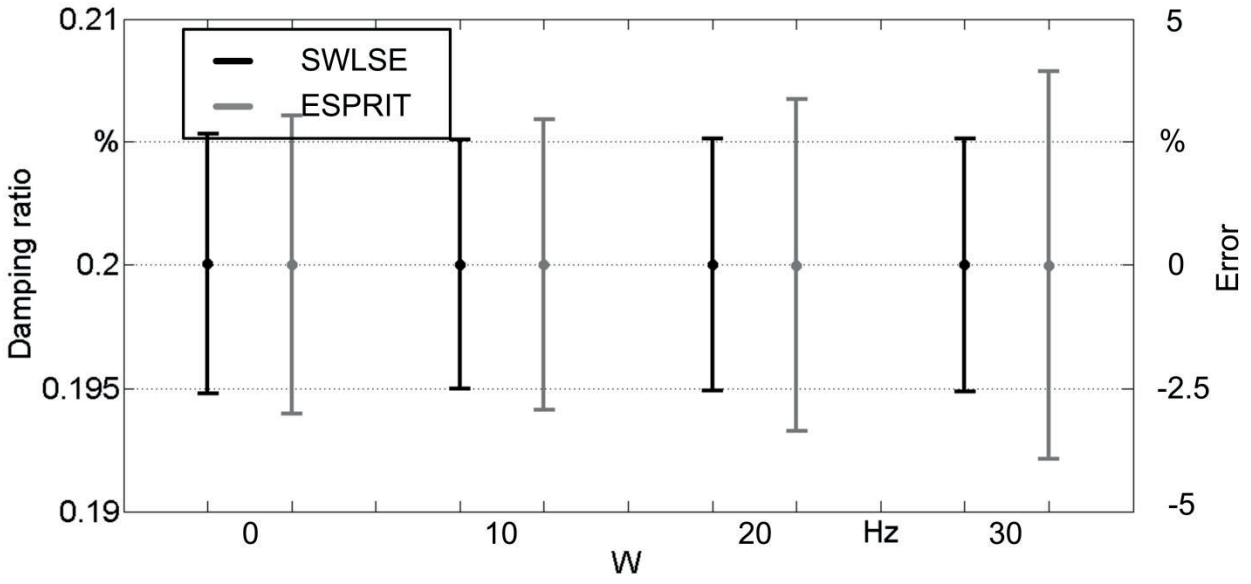

Figure 21: Damping ratio estimation with varying pass band value W

4.2.4 Testing at low frequency signal

As shown in Figure 22 and Figure 23, the frequency identification accuracy for low-frequent signals is also high and decreases with decreasing SNR. The damping ratio estimation exhibit large errors but approach the preset value with reducing the noise.

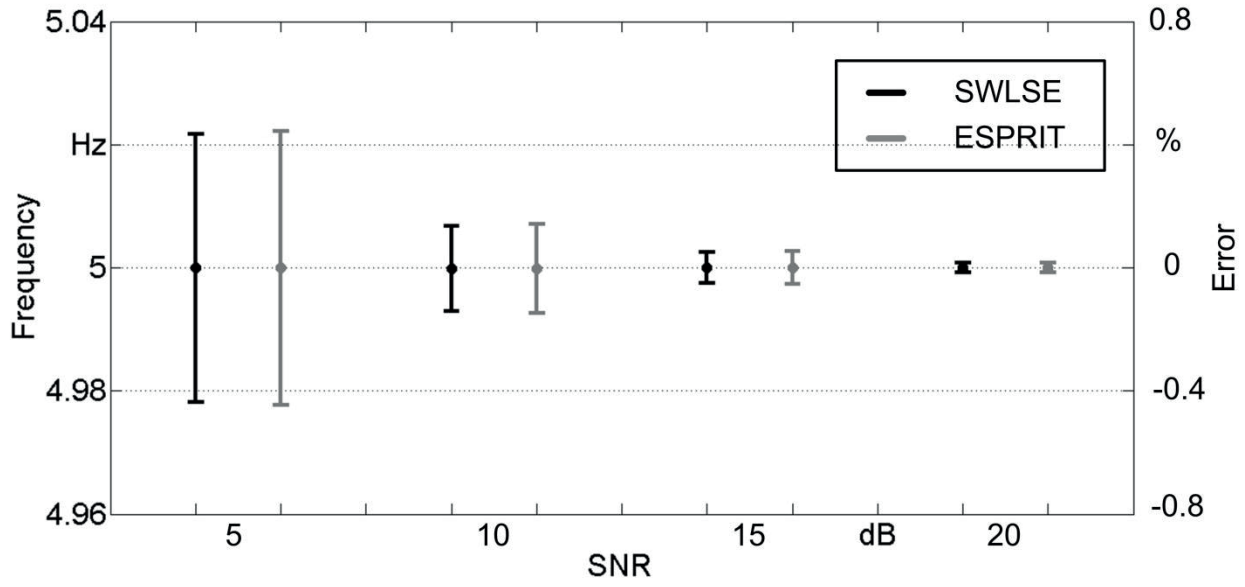

Figure 22: Frequency estimation for low frequency signal with varying noise level

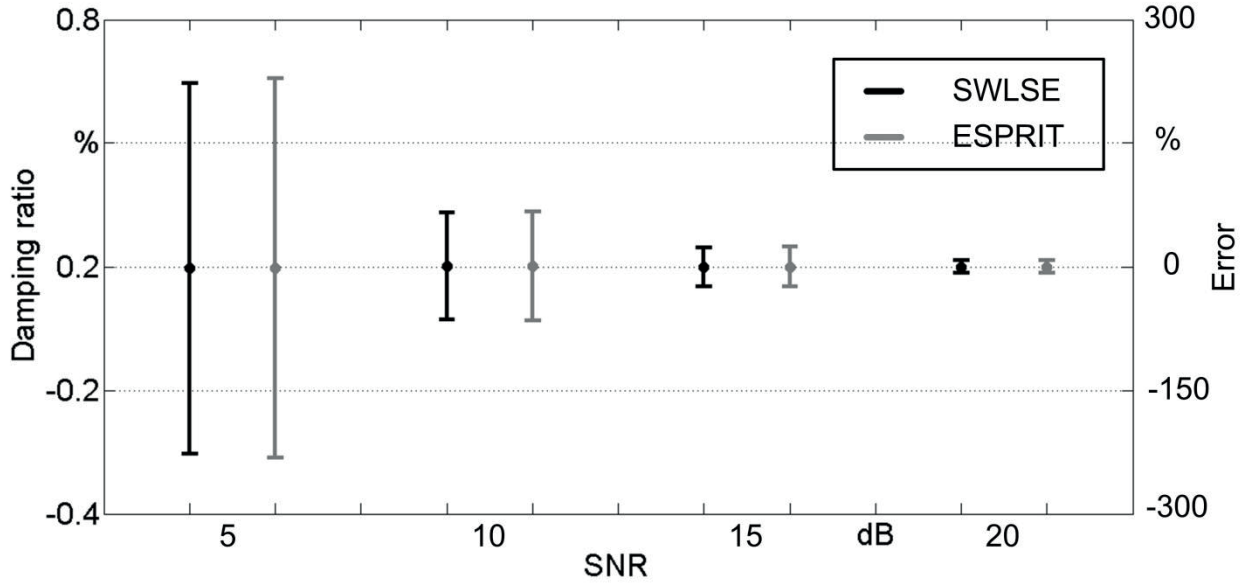

Figure 23: Damping ratio estimation for low frequency signal with varying noise level

4.2.5 Computation effort

The computing time, used for one analyzing window is presented in Tab.2 for each method. With 0.2 ms, the SWLSE has fastest computing time for one analyzing window. The ESPRIT algorithm requires more computational load than the SWLSE algorithm, since it requires computing eigenvectors and singular value using singular value decomposition method (SVD). It should be noted that the time of computation depends

on the hardware environment. The algorithms were implemented in MatLab 7.11.0 and run on an Intel Pentium Dual processor with a 2.20 GHz CPU and 2 GB RAM.

Table 4: Time required in proposed algorithms; Test environment: MatLab 7.11.0, Intel Pentium Dual processor with 2.20 GHz CPU and 2 GB RAM.

Algorithm	Used time
SWLSE	0.2 ms
ESPRIT	32 ms

4.3 Testing with an Artificial Signal

To validate the applicability of the proposed algorithms in engineering practice, a time-varying signal is provided to be considered. The natural frequency increases linearly from 255 Hz to 265 Hz with time. Similarly, the damping ratio changes linearly from 0.2 % to 0.3 %. The instantaneous frequency and damping ratio are obtained using a SWLSE method. As a result, the identification error is illustrated. The window size is set to 40 ms and the SNR is set to 10 dB.

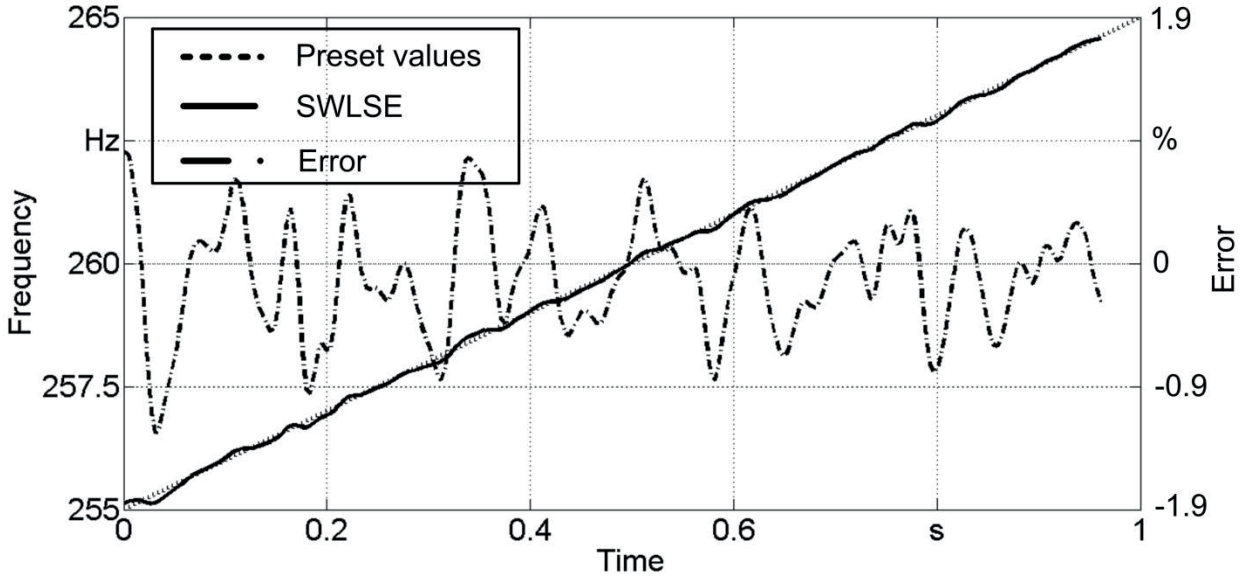

Figure 24: Frequency estimation using SWLSE

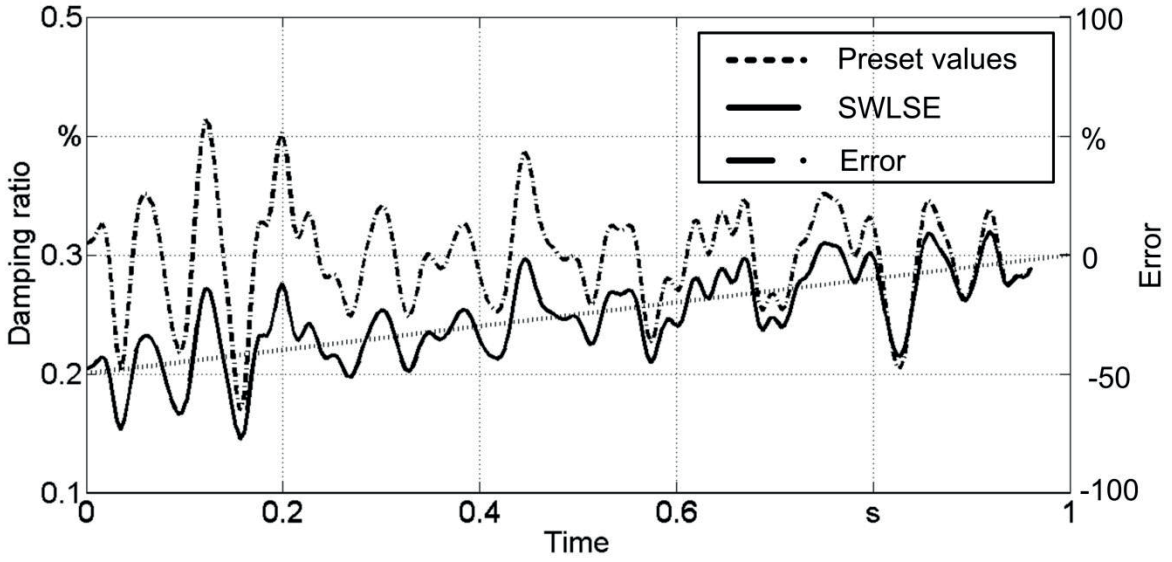

Figure 25: Damping ratio estimation using SWLSE

The instantaneous frequency and damping ratio are obtained and plotted in Figure 24 and Figure 25, respectively. The shifting of the natural frequency and damping ratio are recovered effectively. The estimation error for the frequency is bound by 1 % and by 50 % for the damping ratio.

4.4 Summary of SWLSE Method

The excellent identification results obtained with the SWLSE method are confirmed by comparing the CEMA and ESPRIT methods with several conditions.

Generally, the proposed method has clearly more accuracy than the CEMA method. It is very important that it can provide very high resolution in frequency domain. The frequency resolution is independent on the samplings rate. The SWLSE is therefore more suitable for the short time identification of modal parameters [KUH11a, KUH11e].

The SWLSE method and the ESPRIT method produced almost similar identification accuracy, but advantage of the SWLSE method is faster computing speed.

The error of the damping ratio estimation by SWLSE method is also clearly more than the frequency estimation. Other mainly shortcoming of this method is that the noise has a great influence on the identification accuracy. In the further work, a pass-band filter could be implemented as pre-processing, in order to filter out the noise.

Chapter5

Experimental test

5.1 Testing Environment

After numerical testing it is necessary that the proposed algorithm is carried out by a practical testing in order to evaluate this identification algorithm. A measured data from a real structure is not only contaminated by noise, but also includes many complex factors which may be not considered by the mathematical modeling. Therefore, the performance of the proposed algorithm on a physical structure plays an important role.

In this chapter the experiments performed to obtain modal parameters of the laboratory beam are discussed. The discussion is divided into two parts: the stationary and instationary measurements.

5.1.1 Laboratory beam system

The experimental tests are carried out on a laboratory beam system, which is made of aluminum material. The experimental device consists of two coupling assemblies (see Figure 26), with which the stiffness and damping can be independently adjusted thus changing the dynamic behavior of the beam system. A 3-D coupling assembly model is shown in Figure 26b. The coupling assembly is based on four friction dampers (see Figure 26d) and six stiffness adapters (see Figure 26c). As shown in Figure 26e and Figure 26f, these elements are mounted on a web element, which is connected to the beam, and fixed with a frame. The friction damper can change the damping characteristics of the experimental device by changing friction force between the damper and the web element. The stiffness adapter can be rotated, and its special structure is determined that it can be preloaded in different directions having different stiffness characteristics. The mechanical structure of the coupling assembly is shown in Figure 27.

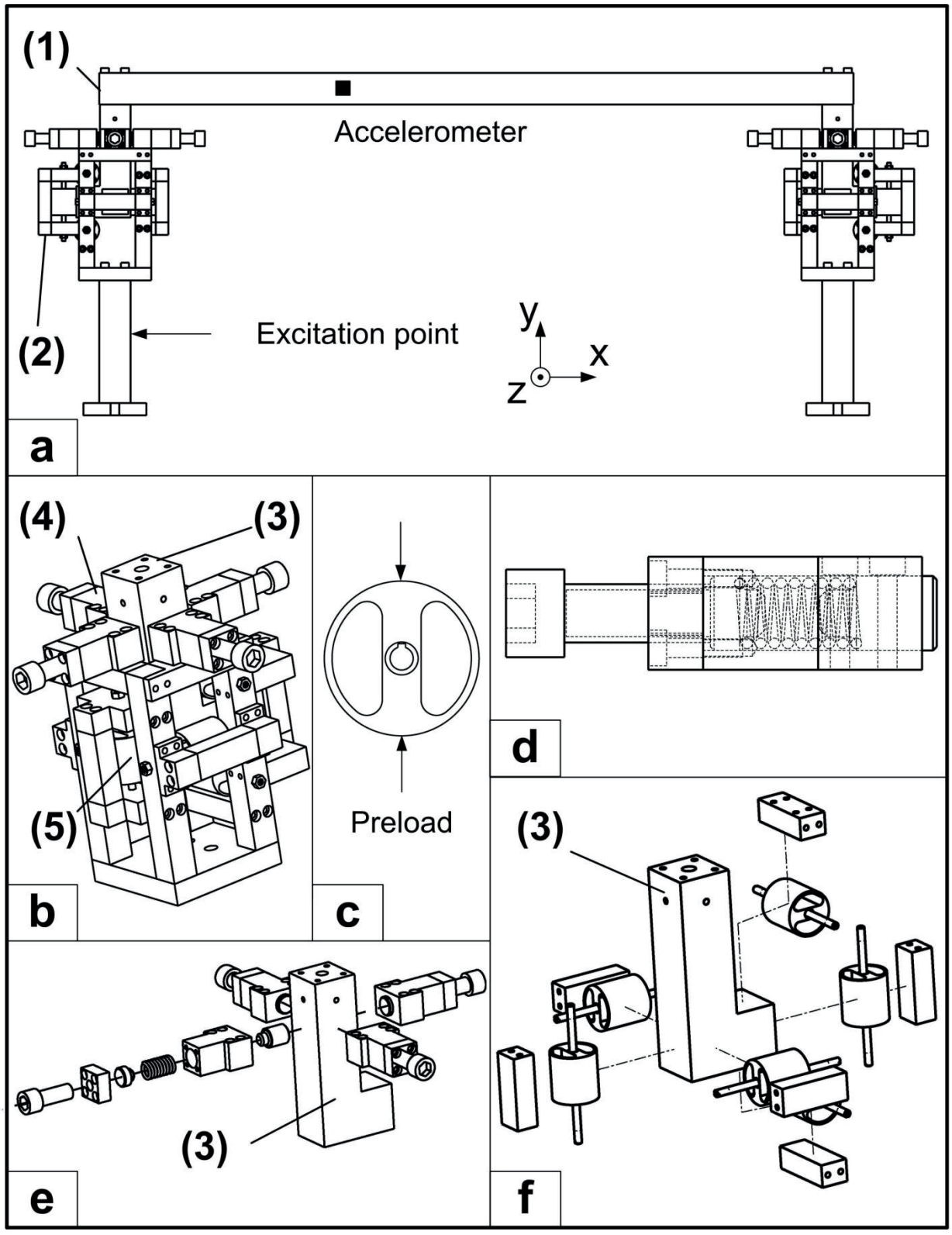

Figure 26: Principle of the laboratory beam system. a) experimental setup, b)coupling assembly, c)stiffness adapter, d) friction damper e) assembly drawing of friction dampers f) assembly drawing of stiffness adapters. (1) beam, (2) coupling assembly, (3) web element, (4) friction damper, (5) stiffness adapter.

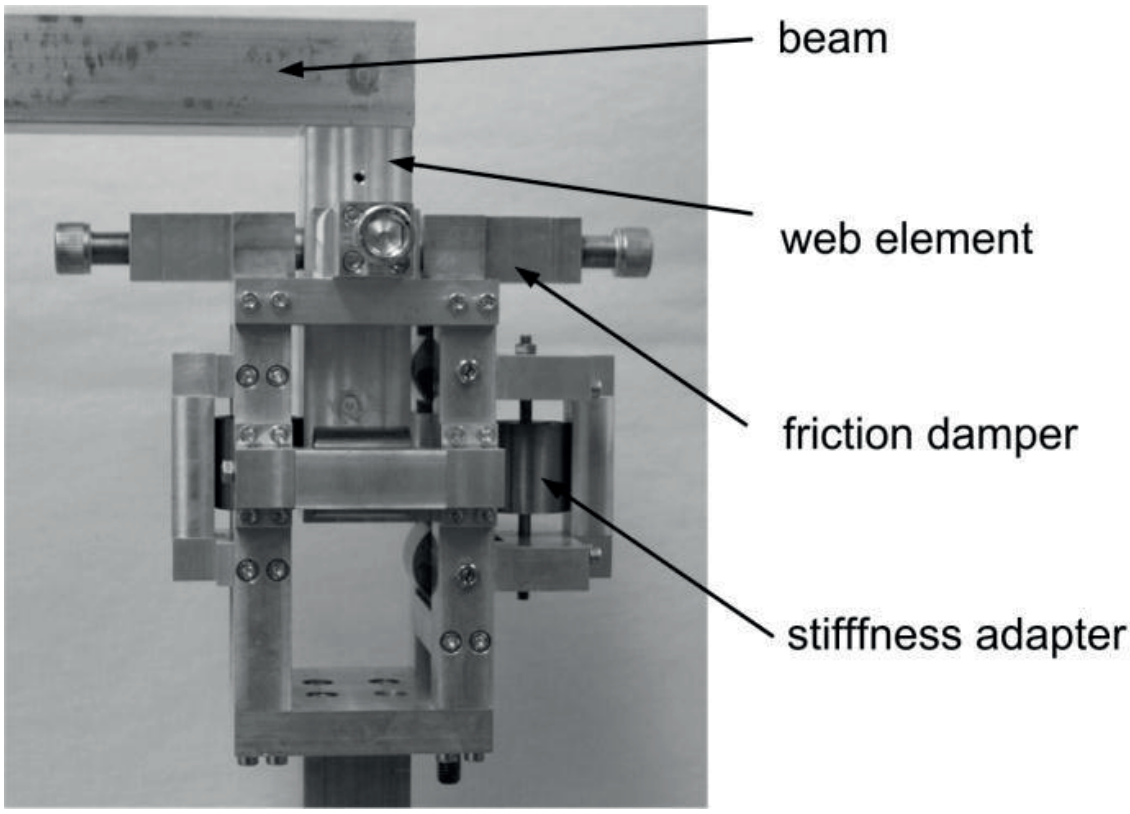

Figure 27: Mechanical structure

It should be noticed that friction dampers are used for this experimental work, while in SWLSE algorithm and in CEMA method, the applied differential equations are based on the viscous damping model. However, this difference in damping modeling will not significantly affect the results of this work, because emphasis of the work is based on the comparison between SWLSE algorithm and CEMA method to verify the feasibility of SWLSE algorithm. The both method focuses the change of damping ratio rather than absolute value.

In this paper, the main emphasis is based on the comparison between SWLSE algorithm and CEMA method to verify the feasibility of SWLSE algorithm.

5.1.2 Testing equipment

In the experimental testing, the mechanical excitation is provided by an impact hammer with a load cell or an electromagnetic shaker. As system response, the piezoelectric accelerometers are mounted on the beam.

The time series data of the force and acceleration are sampled using a USB-based data acquisition device and analyzed in a PC using software Structure Dynamics Tool, which specializes in providing open and extensible MatLab based solutions in experimental modal analysis and finite element modeling for vibration problems [SDT12].

5.2 Stationary Testing

To examine the efficiency of the SWLSE method the experimental tests are performed on a laboratory beam system, and the results are compared with those obtained by the classical EMA method. The assembled experimental device is adjustable for the stiffness and damping ratio in structure.

5.2.1 Experimental setup

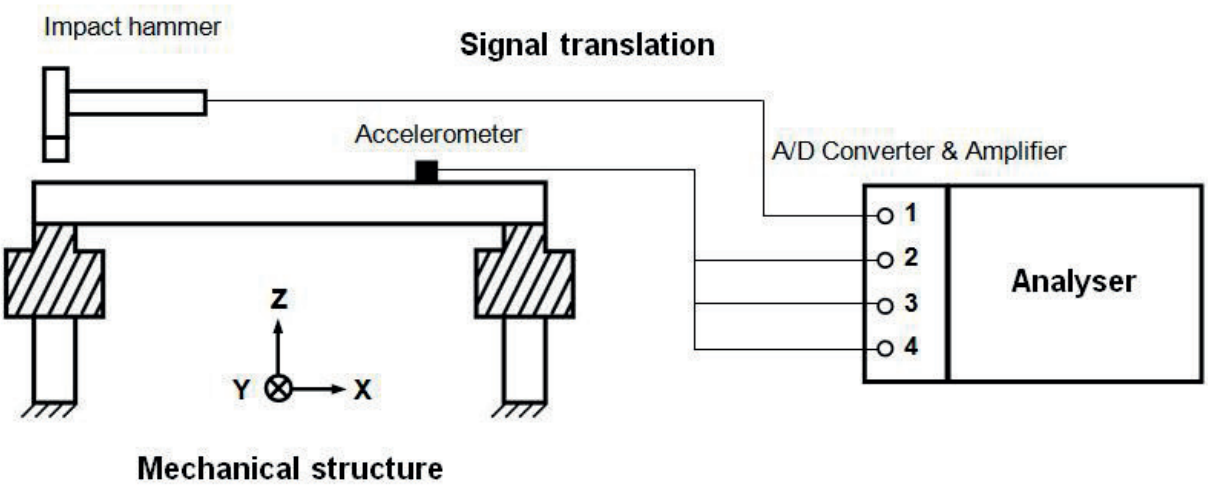

Figure 28: Sketch of experiment set up

The experimental setup used in this thesis is presented in [KUH11a]. A laboratory beam structure is excited by using an impact hammer. A low mass accelerometer is placed on the beam to measure the acceleration response in the x, y and z directions. The impact hammer excites on a fixed position and the accelerometer is moved on all of the measured positions. The hammer force and acceleration data are collected by a data acquisition unit. The signal is sampled at 10 kHz. The dynamic behavior of the experimental device is tested under three different stiffness of the stiffness adapter, and two situations (non-contact and in-contact) of the friction damper. In the following sections they are called stiffness 1, stiffness 2, stiffness 3, damping 1, damping 2, and their values have following relationship:

$$stiffness\ 1 > stiffness\ 2 > stiffness\ 3$$
$$damping\ 1\ (non\text{-}contact) < damping\ 2\ (in\text{-}contact)$$

5.2.2 Results and discussion

In this section, the proposed SWLS is applied to the laboratory beam system. Figure 29a shows a spectrum diagram of the structure response in z-direction in the case damping 1 and stiffness 1. According to the frequency spectrum, there are several natural frequencies in the range of 0-800 Hz to be found. As an example for the following signal process the mode about 280 Hz is discussed in detail, where the input and output signals are perfectly correlated as indicated by the coherence function.

As introduced above the ideal digital frequency filter is applied to the original time signal. Figure 29b shows the filtered signal with pass band of 220 Hz to 320 Hz. Now the SWLSE method is applied to this filtered signal to obtain the parameters for every window. The window size of the SWLSE method is set to 10 milliseconds with an overlap length of 8 milliseconds (i.e., the sliding window moves forward 2 ms in each step). The calculated natural frequencies and damping ratios are shown in Figure 29c and d. Since every window calculates an actual set of the parameters, these obtained values are averaged to be compared with the results by CEMA which is illustrated by a straight line. The identification of modal parameters by CEMA used the whole signal, because the frequency resolution is very low (just 20 Hz for a signal length of 50 ms).

As shown in Figure 29c and d, the estimated parameters before 20 ms by SWLSE are higher than the results by CEMA. It is clear that the oscillation period of low frequency component is longer than of high frequency component. That means the pass band signal (from 220 Hz to 320 Hz) has more high frequency component in range of first 20 ms. Therefore, the estimated natural frequencies have higher values. The actual modal parameters are more accuracy identified than CEMA method in this short time. The SWLSE method still has much better identification performance in short signal length, because the CEMA method has very low frequency resolution (just 100 Hz resolution by a signal length of 10 ms).

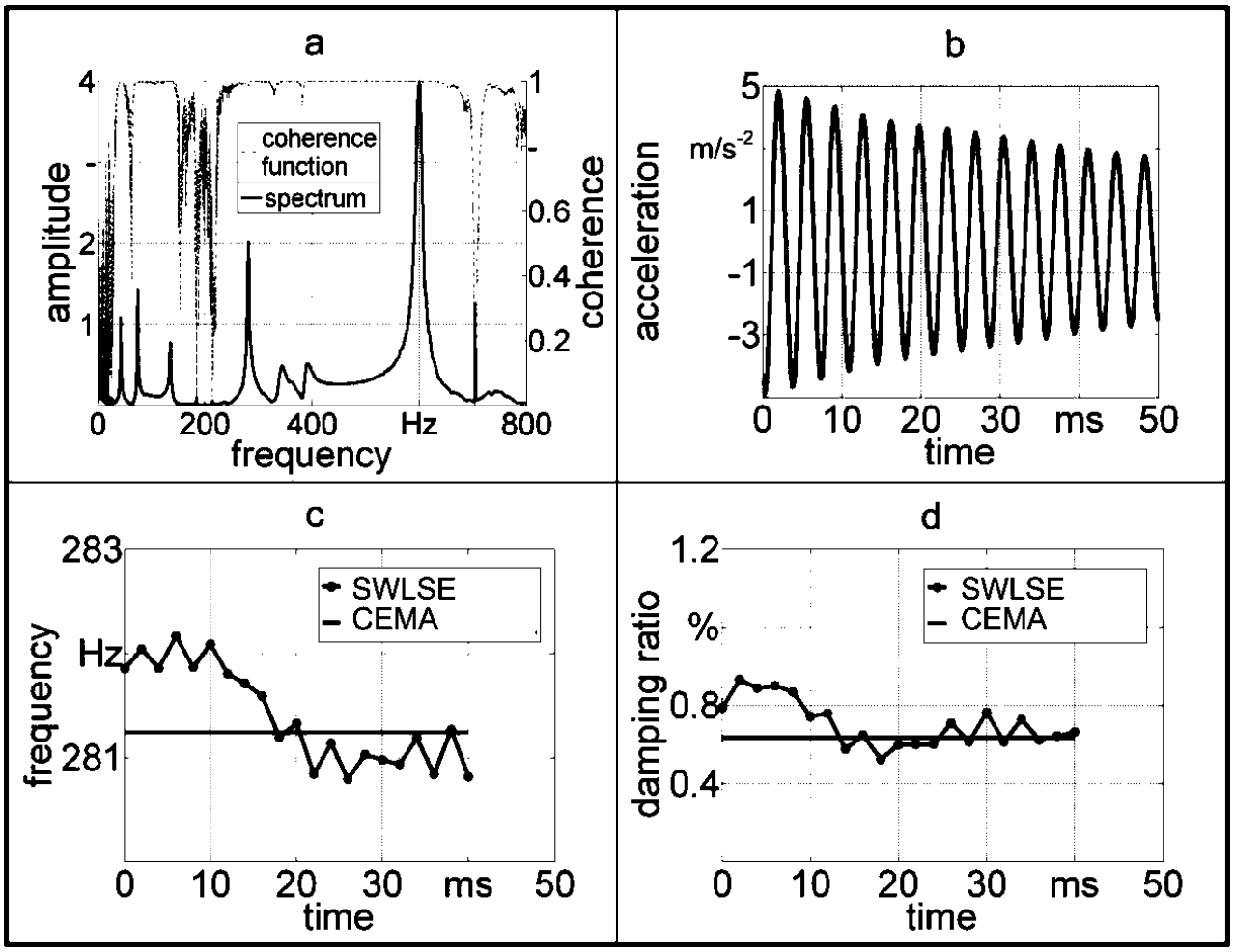

Figure 29: The calculated spectrum and SWLS results for non-contact friction dampers and stiffness adapters by stiffness 1: (a) spectrum and coherence function for response in z-direction (b) filtered signal (c) calculated natural frequencies by SWLS and classical EMA method (d) calculated damping ratios by SWLS and classical EMA method

Table 5 and Table 6 summarize the estimated natural frequency and damping ratio of the different tested conditions using both methods and list the percent deviation by SWLSE algorithm from the CEMA method.

Results show that if the stiffness adapters are adjusted from stiffness 1 to stiffness 3, the measured natural frequency decreases with the reduction of stiffness in the structure which is in agreement with theoretical analysis. On the other hand, when the friction dampers are located in damping 2 (in-contact) positions, the damping ratios increase sharply. This result proves that the stiffness and damping of the assembled experimental mechanism are adjustable in a range.

Table 5: Results of natural frequency (in Hz)

friction damper	stiffness adapter	CEMA	SWLSE	deviation (%)
damping 1	stiffness 1	281.24	281.24	0
	stiffness 2	276.52	276.22	-0.1
	stiffness 3	258.46	257.93	-0.2
damping 2	stiffness 1	285.37	285.49	0
	stiffness 2	284.83	282.93	-0.7
	stiffness 3	265.22	274.72	3.4

Table 6: Results of damping ratio (in %)

friction damper	stiffness adapter	CEMA	SWLSE	deviation (%)
damping 1	stiffness 1	0.63	0.71	12.7
	stiffness 2	0.71	0.75	5.6
	stiffness 3	0.93	0.84	-9.7
damping 2	stiffness 1	2.47	2.99	21.1
	stiffness 2	3.44	3.83	11.3
	stiffness 3	4.94	4.58	-7.3

The estimated natural frequencies with SWLS algorithm have a deviation less than 1 % in most measurements in comparison with the EMA method. However, there is always the large deviation by estimated damping ratios. The maximum deviation of damping ratios is 21.1 % between SWLS and EMA method. The differences could be explained by the estimated damping ratio by classical EMA method using half power bandwidth method in frequency domain which is also inaccurate. There are some different methods to identify damping ratio in time or frequency domain, however these methods have low identification accuracy in comparison with estimation of other parameters like natural frequency, especially when the sampled data is disturbed by noise. [HUA07, YIN08, NAG09] present the investigations of the half power bandwidth method.

5.3 Instationary Testing

5.3.1 Experimental setup

As illustrated in Figure 30, the experimental work of the transient mode estimation is performed on a laboratory beam system, in which mass distribution is varied with time. A toothed guide way is mounted on the laboratory beam system and a passing vehicle can be moved with a constant speed by a stepper motor driving a pinion. In practice, if the mass is added at a point and moving on the structure, it is inevitable to change the elements in the mass matrix. The varying mass distribution influences the structure's dynamic behavior. This means that it is practically impossible to identify the transient modal parameters using CEMA method. In the test an electromechanical shaker equipped with a stinger, excites the structure with zero-mean Gauss white noise force and piezoelectric accelerometers are used for the measurement of the resulting vertical random vibration. This response is analyzed using SWLSE to obtain the instantaneous frequencies and damping ratios.

To eliminate a retroactive effect of excitation some rubber springs haven been mounted between the table and the electromechanical shaker. The natural frequency of the rubber spring is 40 Hz. Moreover, the stepper motor has a stepping frequency by 98 Hz in the case of the moving speed equal to 40 mm/s. The estimated actual modal parameters using SWLSE method are compared with the results by stationary testing, in which the modal parameters are identified using CEMA method at the location of the moving mass by 1 to 5 (see Figure 30).

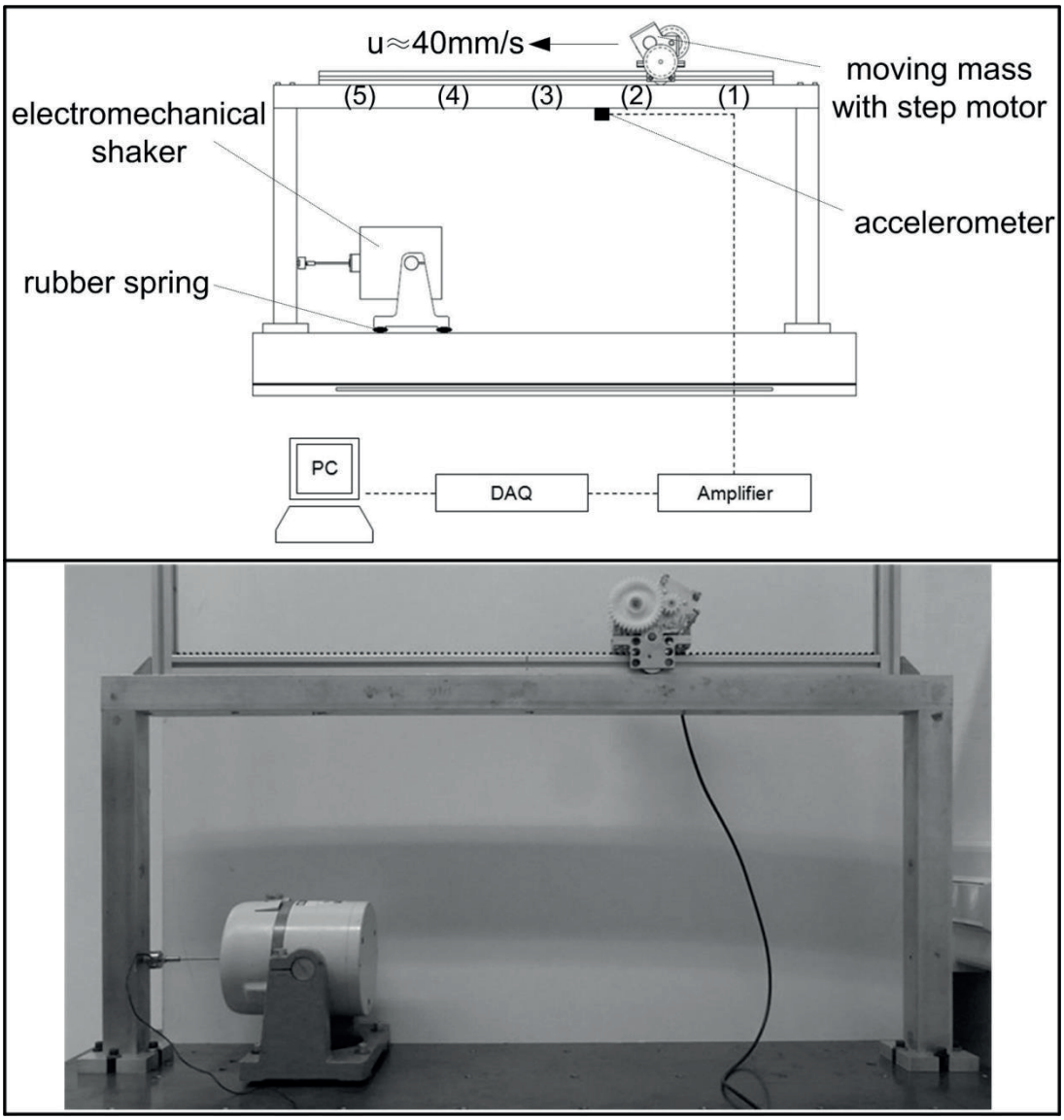

Figure 30: Schematic diagram and photo of the laboratory beam system

5.3.2 Results and discussion

The frequencies obtained by static measurement using classical modal analysis and the frequencies obtained by dynamic measurement using SWLSE algorithms are plotted in Figure 31. It can be seen that the both methods provide similar results and the shifting of the natural frequency is recovered effectively using SWLSE method.

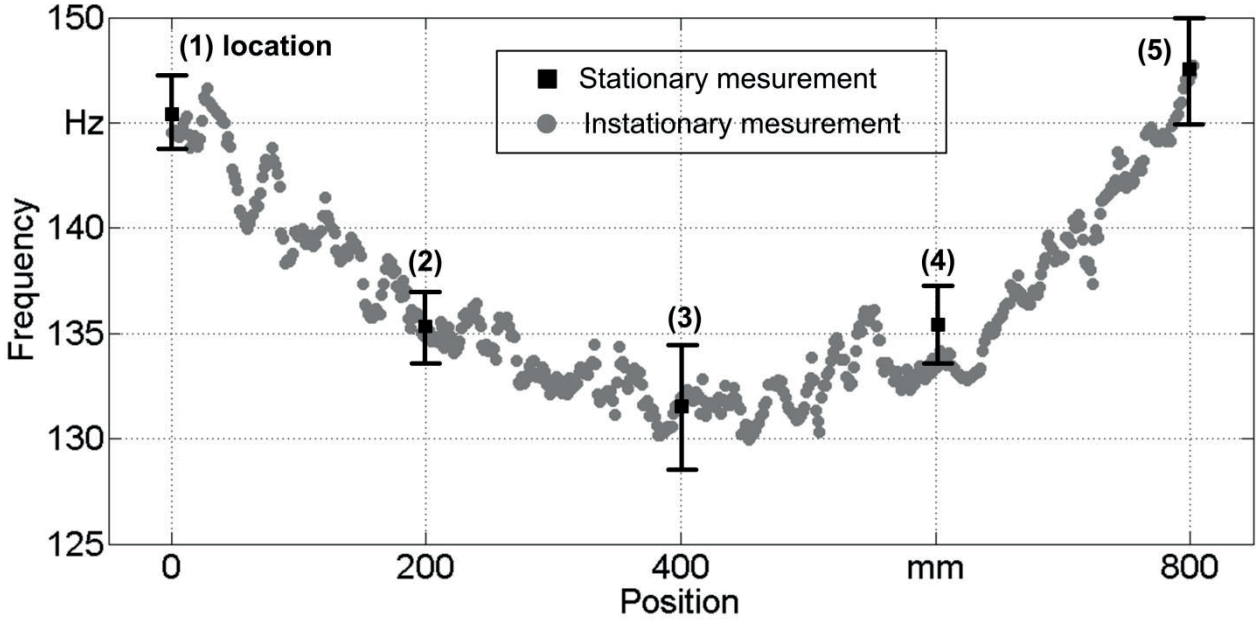

Figure 31: Comparing the results for frequency identification of static and dynamic measurements

Figure 32 shows the comparison of the results of the damping ratios identification using SWLSE and CEMA method. For the SWLSE method a smoothed curve is calculated using a simple model of Savitzky-Golay smoothing filter [SAV64]. There is a boundary value problem at the ends of the curve.

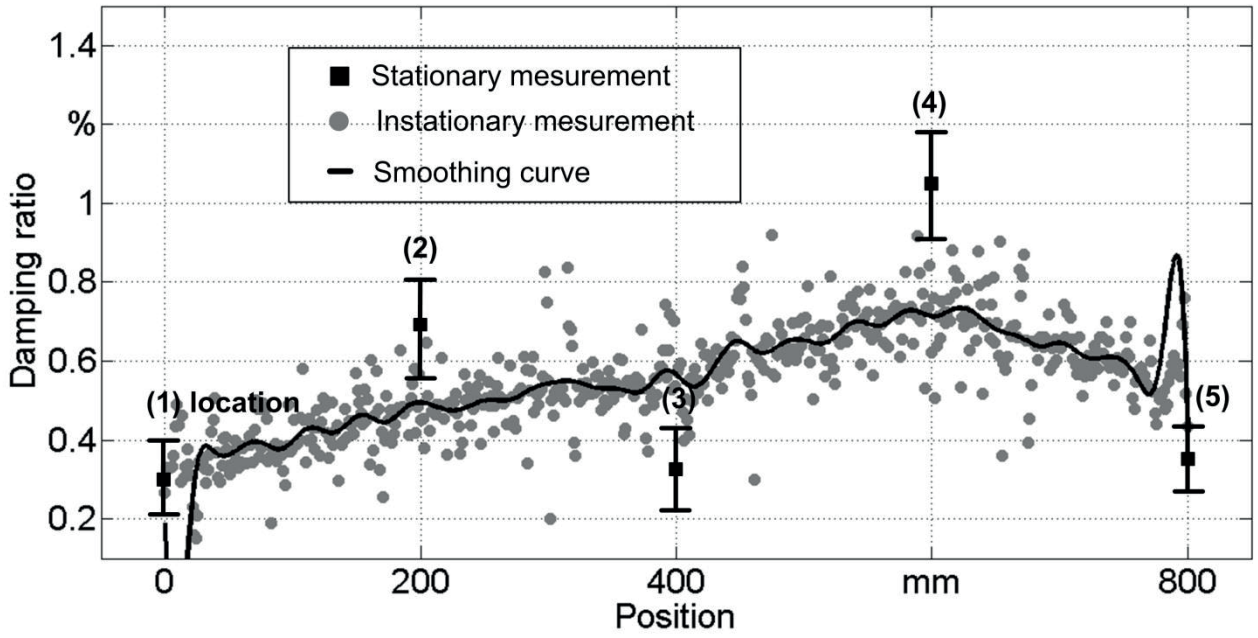

Figure 32: Comparing the results for damping ratio identification of static and dynamic measurements

It is observed in Figure 32 that the tendency of the instationary measurement does not exactly coincide with the stationary measurement. The maximum error between SWLSE and CEMA by the damping ratio identification is about 50%. The damping ratios at the points 3 and 4 have more error between the SWLSE and CEMA method. For this completely symmetrical structure the results at the points 2 and 4 usually should be the same. The different result in this case might be caused by the interaction between the structure and the shaker through stinger [ASH99]. It can be concluded that the SWLSE method demonstrates better capability of the frequency identification than the damping ratio identification.

Chapter 6

Engineering Applications

Machine tools are made up of several interconnected elements, such as machine structure, spindle and workpiece fixtures etc. The movement of spindle is bound to change the machine tool structure and mass distribution, resulting in varying of dynamic characteristics of the structure. The modal parameters of machine tool's structure are dependent of the mass distribution of the system that means the natural frequencies and damping ratios are changing during machining. In the section 6.1, it presents the estimated actual modal parameters using SWLSE method to reveal the transient information of the structure.

Besides of the actual modal parameters, the process parameter which depends on the machining conditions can also be estimated in order to monitor the machining process. Section 6.2 demonstrates estimation of process damping ratio during a machining process using SWLSE method.

Other application, predicting the system transfer function on a nonlinear feed drive system, is studied in section 6.3. In order to improve the real trajectory of the nonlinear feed drive system, the actual coefficients of system transfer function can be identified using proposed method.

6.1 Transient Modal Parameters Identification

Definition of stationary and instationary measurement

Table 7: Three kinds of analysis

Analysis group
Stationary measurement using CEMA
Stationary measurement using SWLSE
Instationary measurement using SWLSE

There are two estimation methods. One is stationary measurement: The spindle of tested machine holds a few locations in the range of guideway and the modal

parameters for each location are evaluated using SWLSE method. CEMA method is also performed to verify the SWLSE results.

Second is instationary measurement: The modal parameters of structures are estimated using SWLSE method during moving of machine spindle.

These measurements are performed on a four column press machine and a High-speed machining center. The measurements are compared using three kinds of analysis, which are listed in Table 7.

6.1.1 Identification of actual modal parameters by four column press

Measurement setup

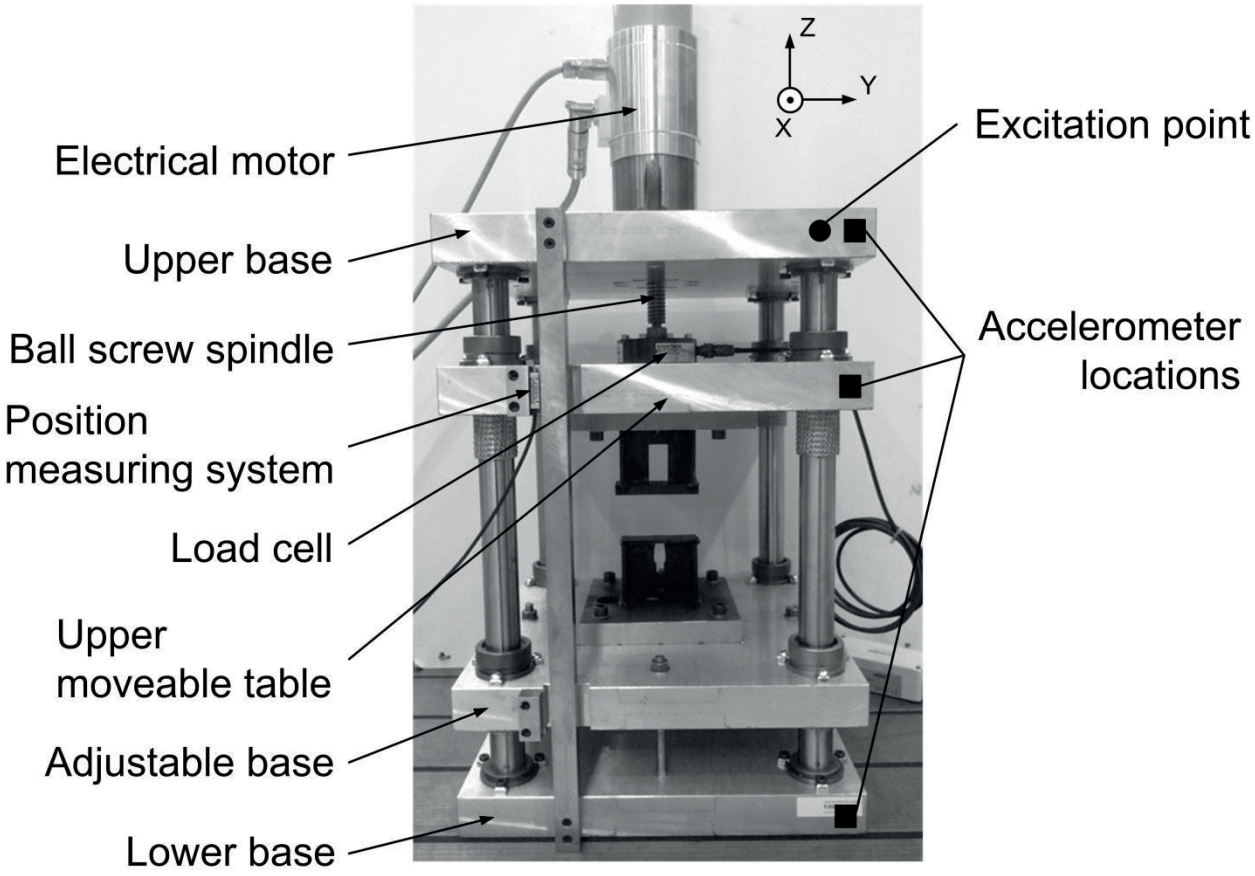

Figure 33: Mechanical structure of four column press

The transient modal parameters identification is performed on a four column press (FCP), which is a machine for micro forming, pressing and metallic joining processes. The mechanical structure is shown in Figure 33. In manufacturing, the movable table is

driven by an electrical motor, which is mounted on the upper stationary base. The structure is clearly time varying system by sliding of the movable table. The dynamic behavior of whole structure depends on the position of the movable table.

The machine is excited with an approximate period impact signal, which is generated using impact hammer manually. Because of the manual excitation, an interval between two excitations cannot be able to control accurately. The interval is approximately by 350 ms through trial and error. Figure 34 shows an example excitation force and its response of machine in time domain. The response signal for each excitation does not decay to near zero. This instationary condition does not meet the precondition of the CEMA method. The use of an exponential window can reduce the effects of leakage on this none completely damped response signal. However, the exponential window can also cause a significant stronger damping effect. Therefore this signal cannot be analyzed with CEMA method accurately. The benefit of SWLSE method is that it can identify the modal parameter within this short time (350 ms). The impact hammer is used instead of shaker, because the impact testing provides higher SNR than the random excitation by shaker testing.

Lightweight piezoelectric accelerometers are used for the measurement of the structure response. The measurements are acquired by a USB data acquisition module with 5 kHz sampling frequency. Each test was repeated by five times and the average taken in order to minimize the measure error.

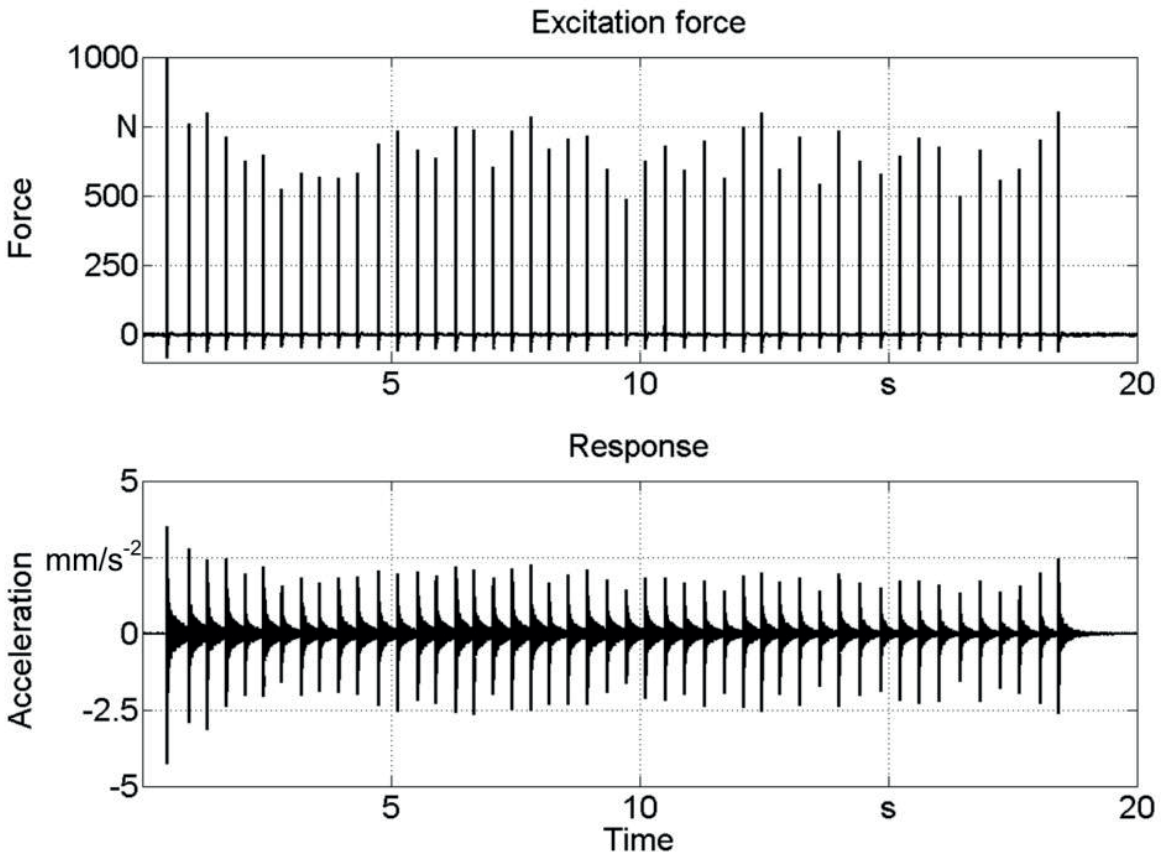

Figure 34: an example excitation force and its response of machine in time domain.

Experimental procedure

Due to the limitation of the number of sensors, just three sensing locations are used for measurement of the resulting vertical vibration response of the structure. The excitation point and sensing locations can be seen in Figure 33. For the stationary measurement the impact tests are performed on the locations of the movable table p = 0 mm, p = 58.5 mm and p = 117 mm, respectively. Modal parameters are identified using CMA and SWLSE method. For the instationary measurement the impact hammer excites manually to the structure with the approximate period impact signal which is mentioned in previous section. The table is risen from z = 0 mm to z = 117 mm with two different speeds of 75 mm/min and 150 mm/min. Transient modal parameters are also identified using SWLSE method and the results are compared with stationary measurement.

Results and discussion:

In Figure 35 and Figure 36 the identified frequency and damping ratio using three kinds of analysis are shown. It can be seen, that the main resonance frequency is decreased from 104 Hz to 80 Hz in total stroke of movable table. The three analyses provide similar results at tested positions of movable table. For the instationary measurement the SWLSE method provides also the further information of transient frequency, showing the

main resonance frequency is decreased exponentially. This is because the system's stiffness is decreased also exponentially with rising of the movable table.

Furthermore, the transient frequencies are varied in the form of waves. The length of waves is about 12 mm. It could be related to the effect of recirculating of a ball screw system. A period of recirculating has 12 mm of movement track. The axial ball bearing is preloaded. It has different stiffness depends on which position the nut is located in thread of the ball screw spindle. These varying of stiffness affect the changing of natural frequency.

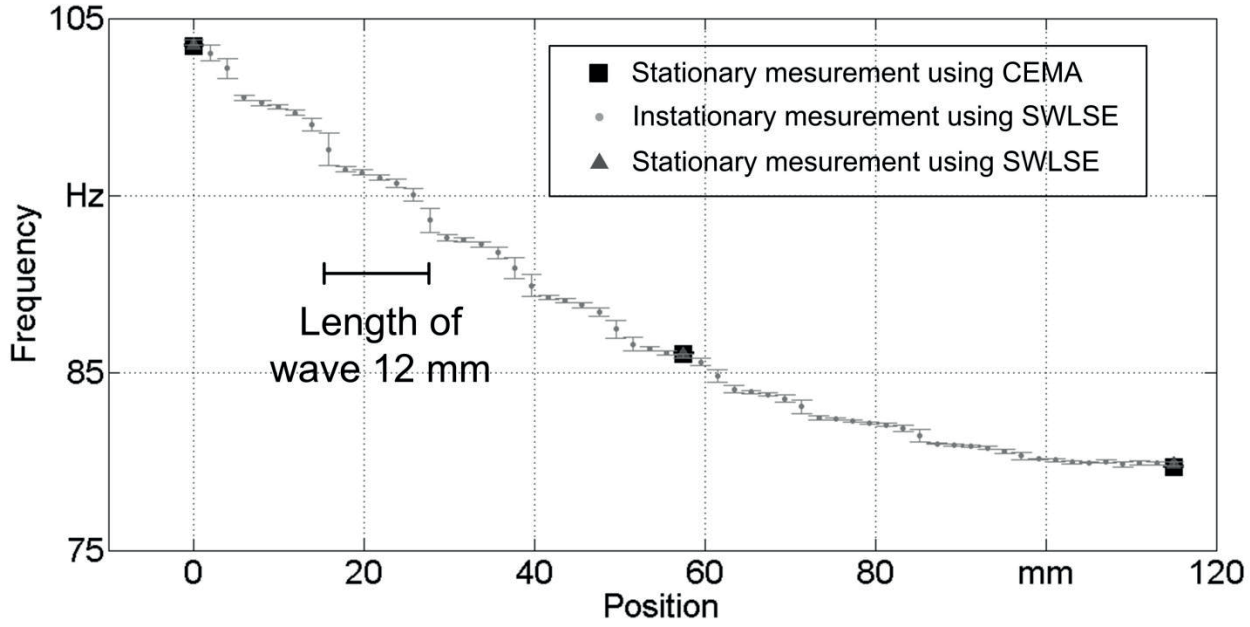

Figure 35: Comparison of the frequency estimation with the stationary and instationary measurement for the four column press machine

The result of damping ratio estimation is also similar. However, small deviations between each analysis method are also seen. Due to the manual period impact, the force and the position of excitations cannot be ensured constant. This could lead to increase the deviation. Therefore, it becomes necessary to achieve automotive excitation equipment with impact hammer to improve the measurement accuracy.

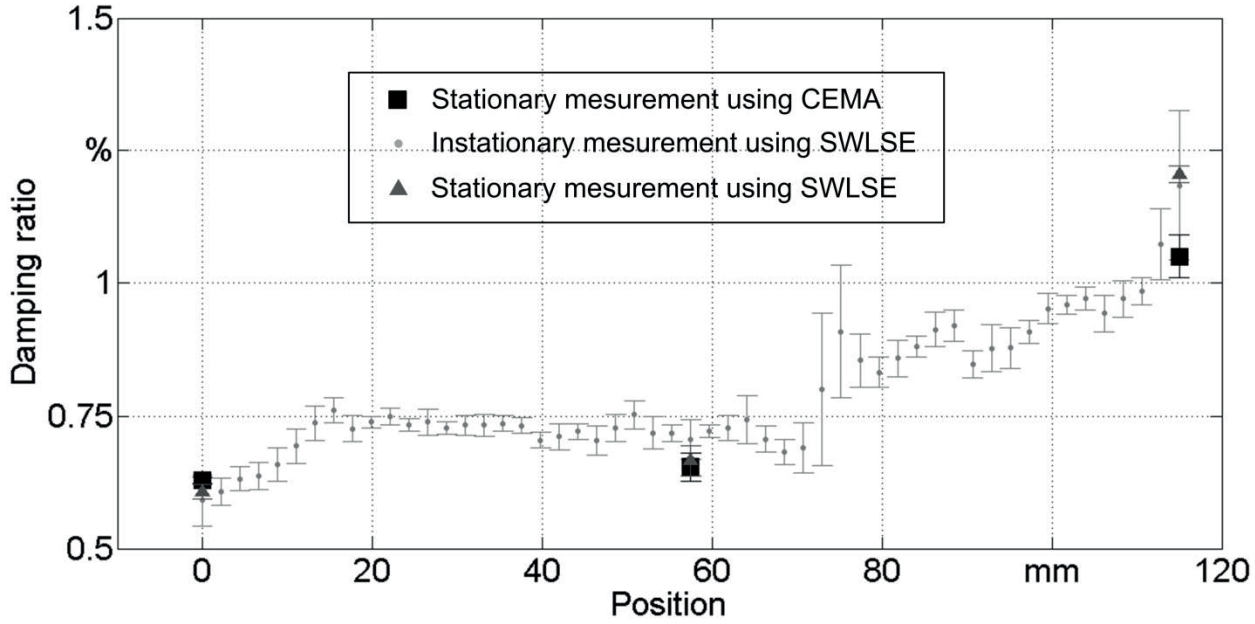

Figure 36: Comparison of the damping ratio estimation with the stationary and instationary measurement for the four column press machine

Figure 37 and Figure 38 show the estimation results at two different moving rates of movable table. It can be seen that the identified transient modal parameters are not changed significantly due to different feed rate.

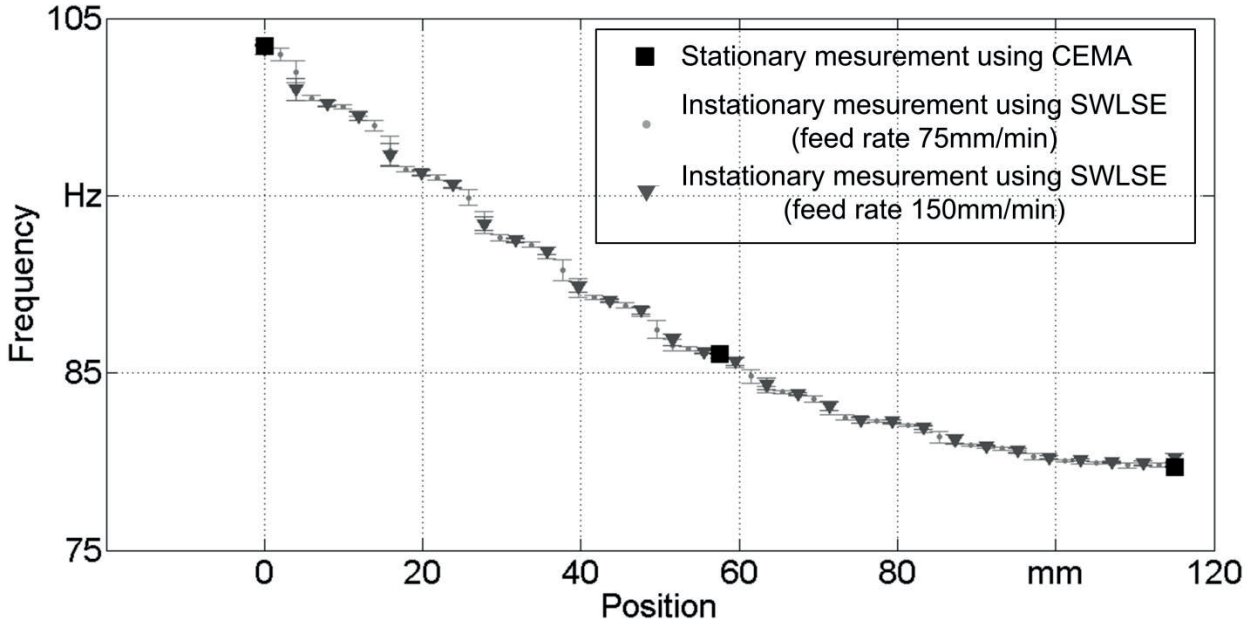

Figure 37: Comparison of the frequency estimation with different feed rate for the four column press machine

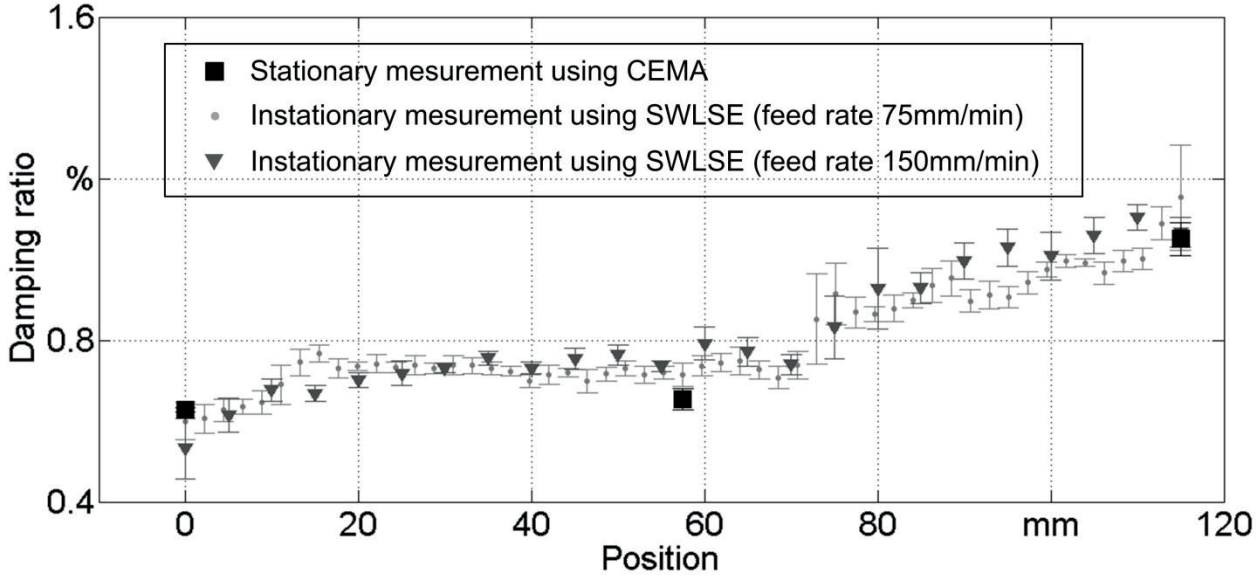

Figure 38: Comparison of the damping ratio estimation with different moving speed for the four column press machine

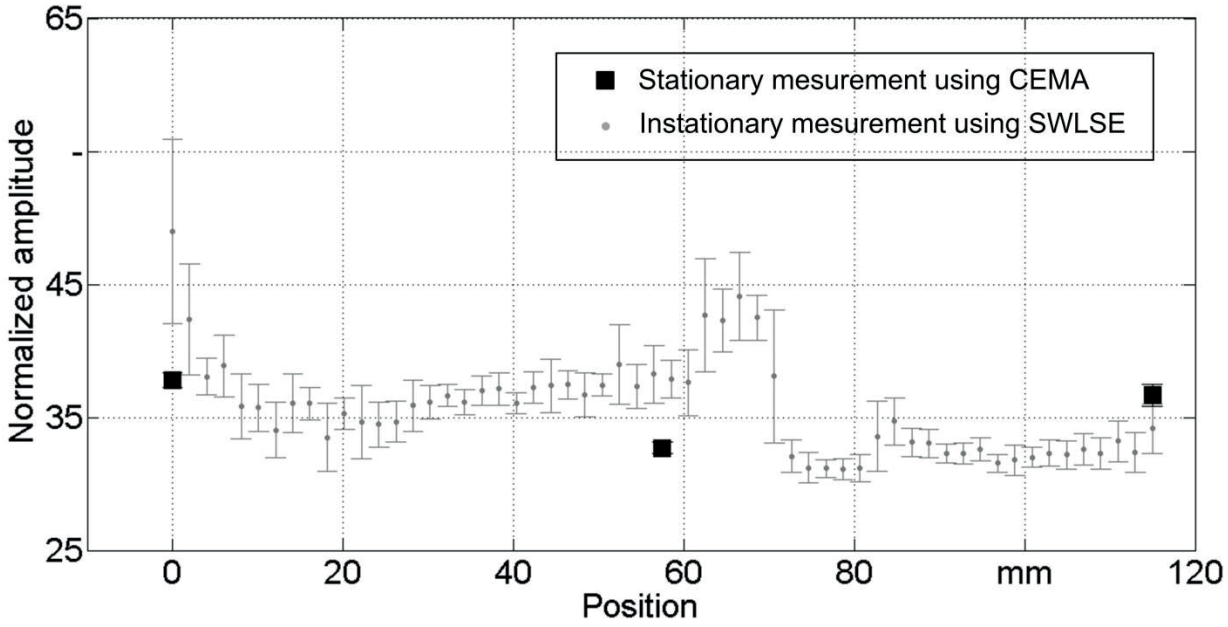

Figure 39: Normalized amplitude of the mode shape at measured point of upper table

It is noted that, the mode of structure's dynamic behavior is just shifted during moving of the table. The mode shapes are not changed, while the natural frequency is decreased from 104 Hz to 80 Hz. However, the amplitude at each measured point might be different. The normalized amplitudes of the mode shape for the upper table are plotted in Figure 39. According to the Eq. 4-19 the accuracy of the system residue depends on the computed eigenvalue. In other words, the accuracy of estimated frequency and damping

ratio can affect the accuracy of the mode shapes. This is one of possibilities of the deviation between CEMA and SWLSE method.

6.1.2 Identification of actual modal parameters on High-speed machining center

Measurement setup

In this chapter the same testing is performed on a high speed machining center (MIKROMAT 4V HSC). Due to more solid and heavier structure, this machining center has a high structural damping. A main spindle system with its vertical axis is mounted on a horizontal axis, so that it can move in horizontal and vertical ways. The Figure 40 and Figure 41 show the setup for this spindle system. The actual modal parameters are investigated in this section while the spindle is moving in vertical axis. As a pendulum system, the natural frequency of the spindle can be deceased when the spindle has a downward motion (in -Z direction).

All test equipment is the same as in the previous experiment. The spindle is excited also using impact hammer with the quasi-periodical impact signal. System responses are measured using three-axis accelerometers. The data acquisition unit is connected to PC with USB. The sampling rate is 16 kHz. The data are processed using MATLAB.

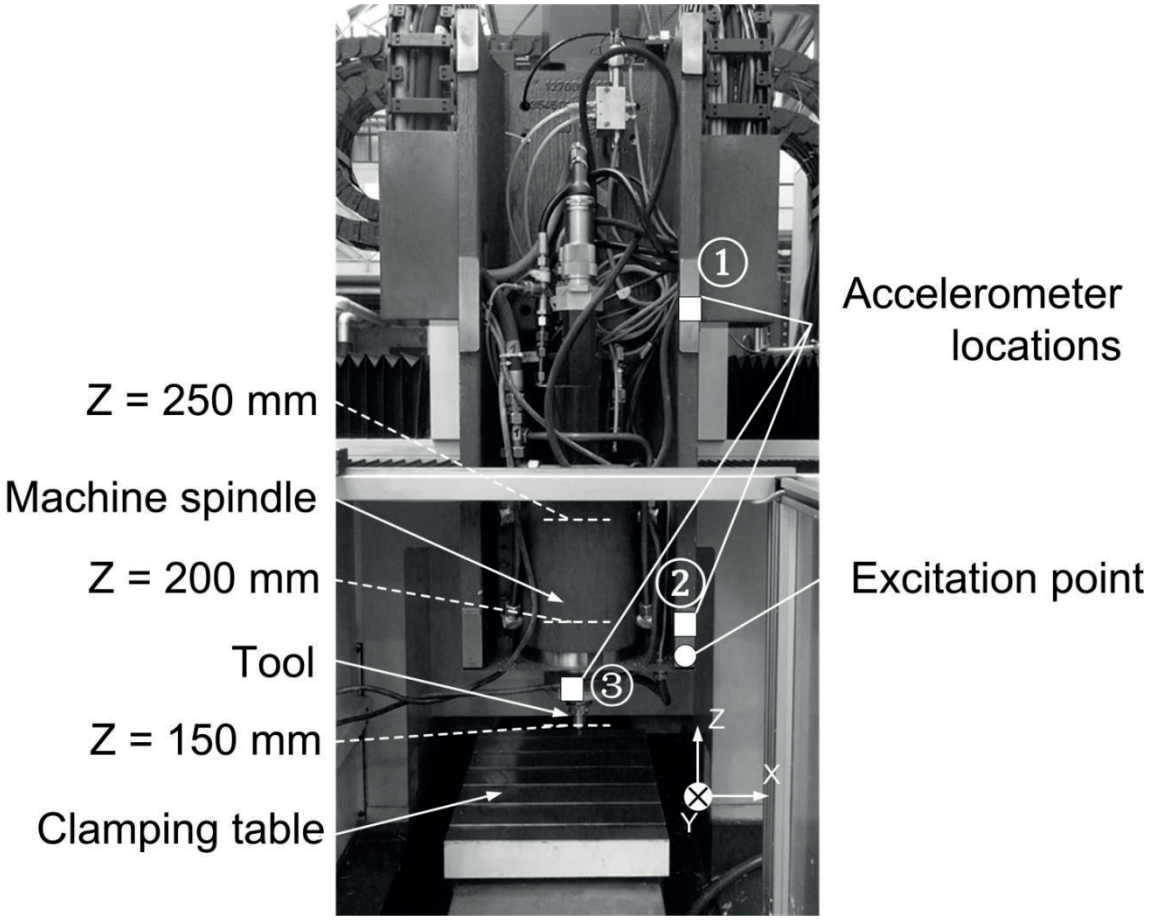

Figure 40: Main spindle of MIKROMAT 4V high speed machining center

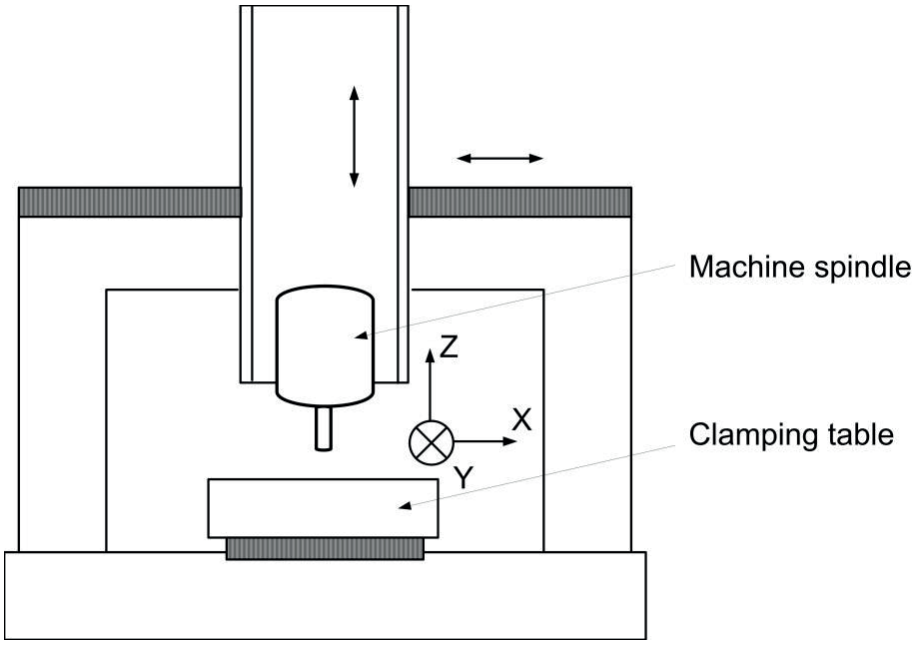

Figure 41: Sketch of MIKROMAT 4V high speed machining center

Experimental procedure

Due to the limitation of the number of sensors, just three sensing locations are used for measurement of the resulting vertical vibration response of the structure. The excitation point and sensing locations can be seen in Figure 40. For the stationary measurement the impact tests are performed on the locations of the spindle z = 150 mm, z = 200 mm and z = 250 mm, respectively. Modal parameters are identified using CEMA and SWLSE method. For the instationary measurement the impact hammer excites manually to the structure with the approximate period impact signal which is mentioned in pre-section. The table is risen from z = 150 mm to z = 250 mm with two different feed rates at 300 mm/min and 600 mm/min. Transient modal parameters are also identified using SWLSE method, that the results are compared with stationary measurement.

Results and discussion:

Figure 42 and Figure 44 show the frequency and damping ratio identification results by using CEMA and SWLSE methods, respectively. The frequency identification results show that the frequency of the measured structure is increased with rising of the spindle, which is in agreement with the expected behavior. It can be seen from Figure 42 that the results between CEMA and SWLSE are different. At position z = 200 mm the deviation is 2.8%.

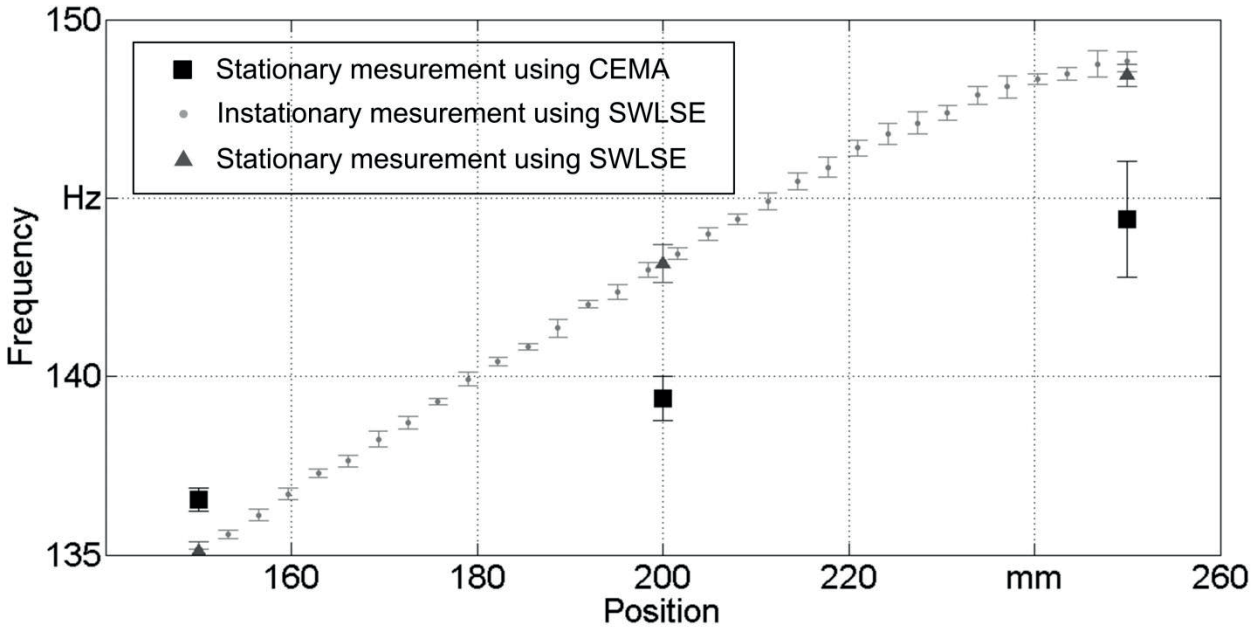

Figure 42: Comparison of the frequency estimation with the stationary and instationary measurement for the high speed machining center

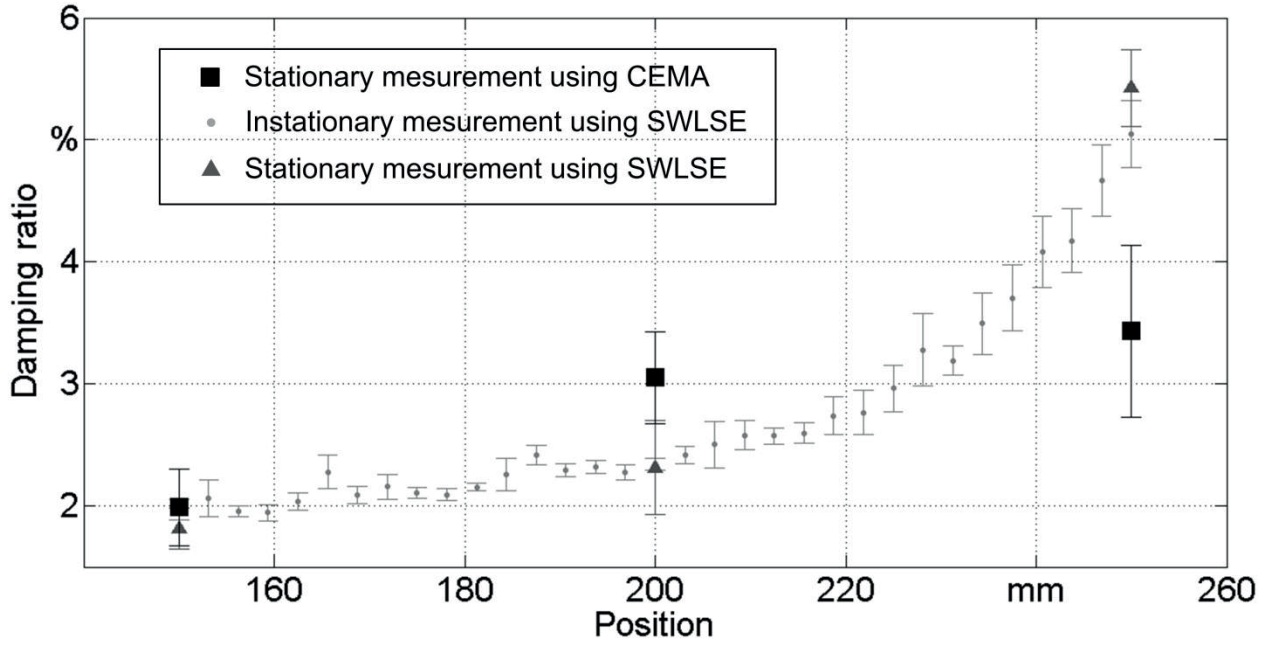

Figure 43: Comparison of the damping ratio estimation with the stationary and instationary measurement for the high speed machining center

Figure 43 represents that the identified damping ratios are also increased with rising of the spindle. Because of increasing of stiffness of the structure, this stronger structure can induce larger damping effect. It can be seen that the estimated damping ratios between CEMA and SWLSE are different. The main spindle is equipped with a pneumatic brake. For the stationary measurement with CEMA method, the position control unit is inactive, so that the brake has no effect to the spindle. For the instationary measurement with SWLES method, the brake system enhances the system damping effect, and increases the stiffness of the system. That is also why the estimated natural frequency with SWLSE method is higher than with CEMA method in Figure 42. The maximum deviation of the estimated frequency between SWLSE and CEMA method is about 3 %, and the error of damping ratio is about 35 %.

Next, the actual frequency and damping ratio depended on feed rate of the z-axis are plotted in Figure 44 and Figure 45, respectively. It can be seen that the identified modal parameters do not depend on the feed speed. The SWLSE uses very short time block to calculate the actual modal parameters, and the used accelerometers for system response are also very sensitive. So the changing of the feed speed from 300 mm/min to 600 mm/min cannot obviously affect the identification accuracy of the algorithm.

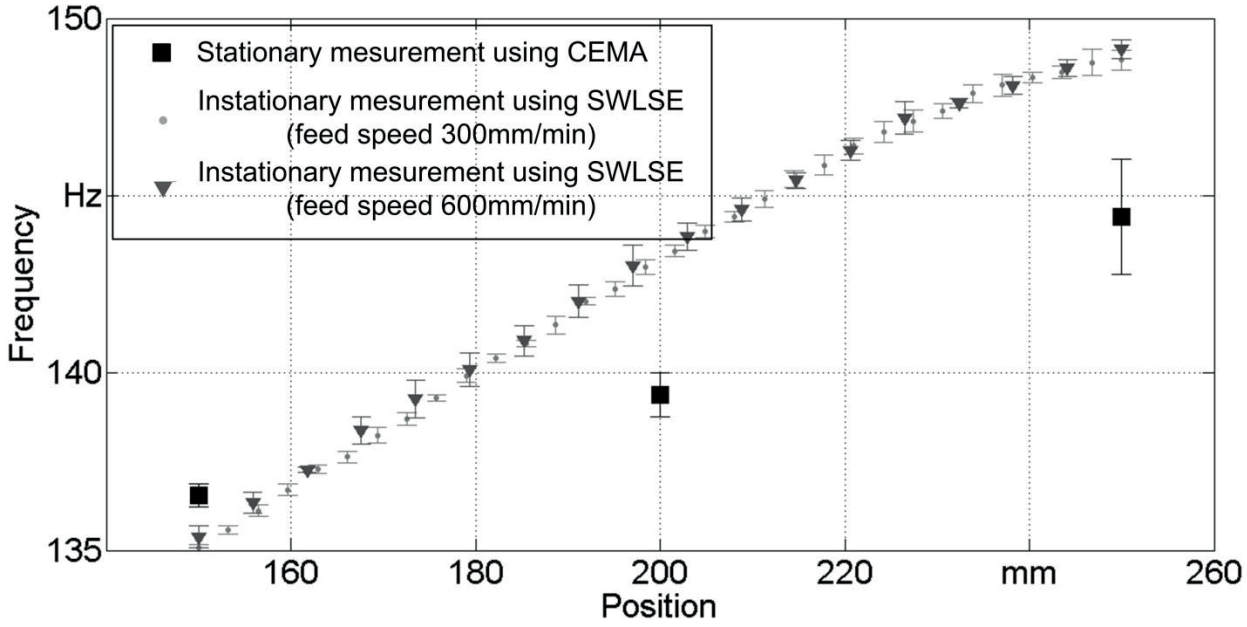

Figure 44: Comparison of the frequency estimation with different moving speed for the high speed machining center

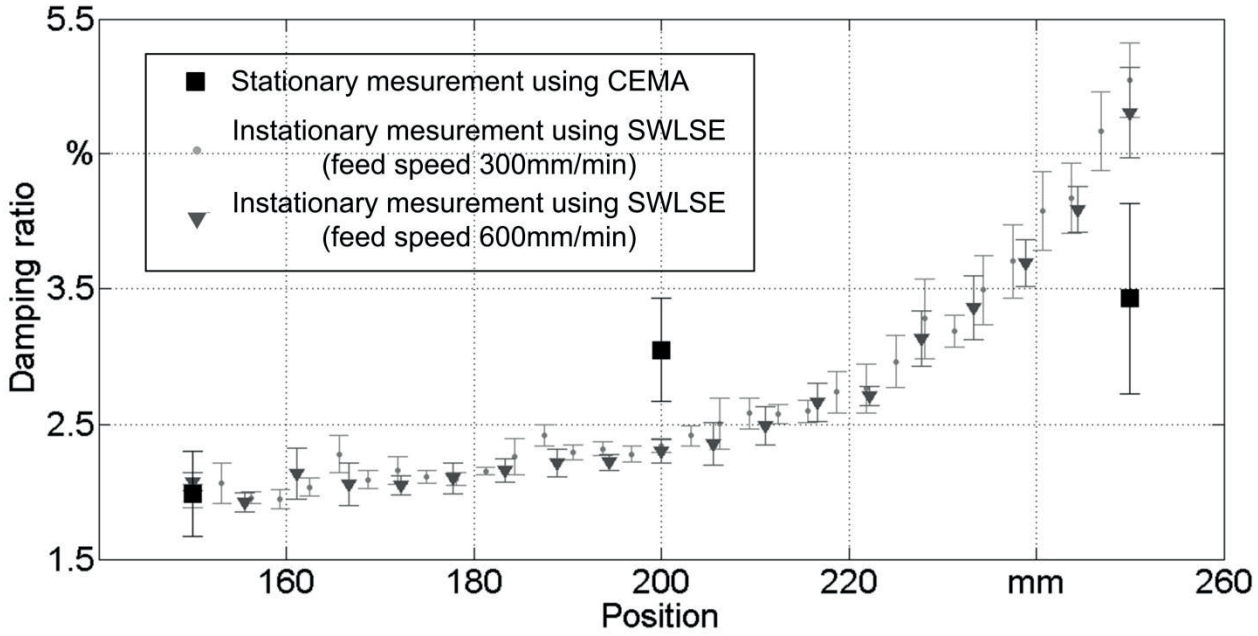

Figure 45: Comparison of the damping ratio estimation with different moving speed for the high speed machining center

Mode shapes are not changed during the shifting of frequency from 135 Hz to 148 Hz, but the vibrational amplitudes for each measured point are varied. Figure 46 shows the actual amplitude at the 3th measured position in comparison to with the results by CEMA method. According to the Eq. (3.34) the accuracy of the system residue depends on the computed eigenvalue. The accuracy of estimated frequency and damping ratio can

affect the accuracy of the vibrational amplitude. This is one of possibilities of the larger deviation between CEMA and SWLSE method by the location z = 250 mm. However, Figure 46 shows that the dispersions of amplitudes grow always by the both applied methods.

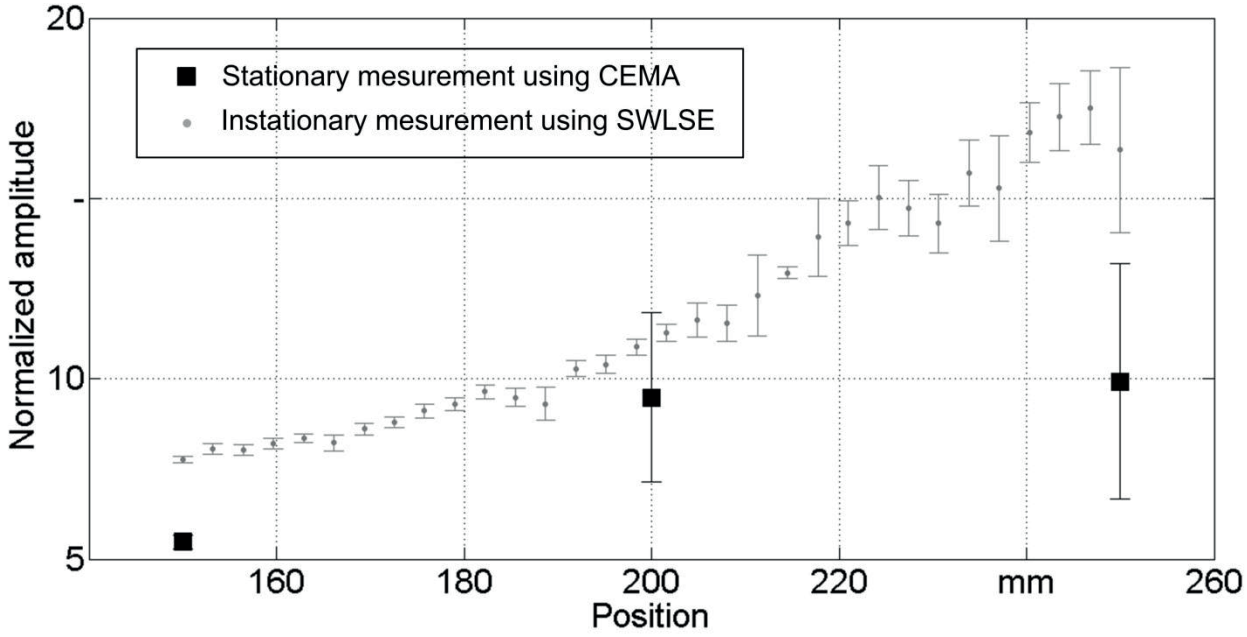

Figure 46 Normalized amplitude of the mode shape at the lower point

6.2 Identification of Process Damping

The SWLSE algorithm provides fast computation with high accuracy. It can identify system parameters within even less than one periodical signal component. Based on this advantage the theory of SWLSE algorithm is not only for modal analysis, but also can be used for developing real-time machining monitoring.

In the section the SWLSE analysis is carried out for process damping identification in a machining process. The process damping is defined as the damping effect of the vibration caused by cutting tool and workpiece interaction [TLU00]. It is well known that a dynamic force or shock results in vibrations.The tool-workpiece contact may lead to regenerative chatter in machining process especially at low cutting speeds [SIS69, ALT04, TLU78]. The process damping can alleviate this problem and enhance the stability in metal cutting operations, to improve the machining efficiency [TUN12]. Many researchers have developed a mathematical model to describe the dynamic machining process and extract the system dynamic parameters from tool points FRF [SCH01, BUD96, AHM12, SEL12].

In this section, a set of milling experiments is firstly performed to obtain the workpiece frequency response (WPFR) based on the sensor signals. The cutting frequency related

to tool-workpiece contact and its harmonic components are identified, and translated into the time domain with frequency pass-band filter using inverse fast Fourier transformation (IFFT). The process damping can be obtained from the translated time series data by fitting with a damped oscillating function using the SWLSE method. Chapter 6.2.1 proposes a new influence factor (the cooling lubricant) on the process damping and examined experimentally the changing of the process damping under different flow rate of the cooling lubricant. In the Chapter 6.2.2, the influence of the spindle speed on the process damping is reported.

6.2.1 Process damping identification in lubricant milling

In general, the exact cooling lubricant quantity and its relative efficiency are not considered, namely in flood cooling to the workpiece in order to reduce the temperature in the cutting zone. However, the cooling lubricant has some shortcomings as well, which seriously pollute the environment and can damage the employee health caused by generating oil mist, smoke chemical particles and bacteria [ZHO10, SOK01]. Another significant disadvantage is that the cost of using cooling lubricant in machining is very high. The cost related to cooling lubricant is even higher than the cost related to tool wear [DHA07, KLO97].

This chapter aims at the influence of the cooling lubricant on the process damping. By applying the SWLSE method the changing of the process damping is estimated in real-time machining process. The process damping ratios are examined experimentally under different flow rates of the cooling lubricant.

Measurement setup

The goal of this test is to experimentally determine whether the flow rate of cooling lubricant can affect the process damping in milling operation. The experimental tests are performed on Hermle U630T universal machining centre which is illustrated in Figure 47. For every test group (see Table 9), a new flat end mill cutter (Garant 20-2640) with 16 mm diameter and 4-flute is used. In the early stage the tools have a more serious wear. In order to reduce the effect caused by tool wear, every new mill cutter is performed a pre-cutting process without data acquisition. The workpiece material is a chromium alloy bearing steel (100Cr6) in the form of a 160 x 119 x 30 mm block. Cooling lubricants are listed in Table 9, which is sprayed to the cutting area with a single nozzle. Experimental cutting conditions are shown in Table 8.

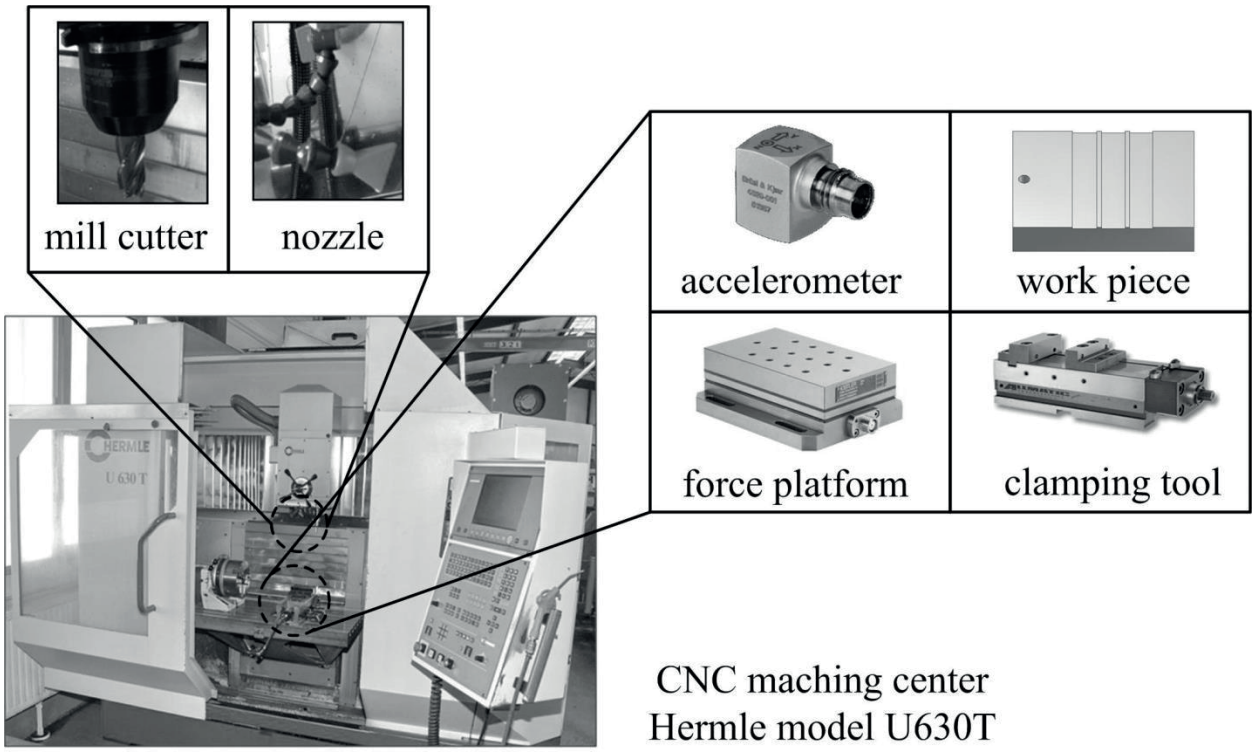

Figure 47: Experimental set up

Table 8: Experimental cutting parameters

Cutting speed (m/min)	Cut depth (mm)	Rotational speed (rpm)	Feed speed (mm/min)
50.27	1	1000	200

In order to strengthen the persuasiveness of the conclusions，two kinds of the data acquisition systems have been used. The first is a Kistler three-component dynamometer (type 9257B) which is mounted under a clamping element for workpiece to measure the cutting force (F_c), feed force (F_f) and tangential force (F_t). The second is a piezoelectric triaxial accelerometer (Brüel&Kjael DeltaTron type 4520-001) which is screwed on the workpiece to sample the vibration signal of the milling process. The sensor signals are amplified and sampled by data acquisition card (MC DaqBoard/3001USB), the sampling frequency is 16 kHz.

Experimental procedure

The experimental program consists of 60 tests, which are divided into four groups and performed on four workpieces. The only difference of these test groups is that the test

adopted different cooling lubricant conditions, namely dry milling (DRY), minimum quantity of lubrication (MQL), little quantity of lubrication (LQL) and wet quantity of lubrication (WQL).The cooling lubricant conditions in detail are summarized in Table 9.

Table 9: Cooling lubricant conditions

Group No.	Test No.	Name of condition	Flow rate	Material
1	1-15	DRY	-	-
2	16-30	MQL	20 (ml/h)	oil mist[a]
3	30-45	LQL	0.1 (l/s)	chemical lubricant[b]
4	46-60	WQL	0.2 (l/s)	chemical lubricant[b]

a: „r.meta TS 42“, RhenusLub GmbH & Co KG b: „ACMOSIT 67-2 Gleitmittel“, lubricant oil

There are 15 tests in each test group in order to evaluate the reproducibility of measurements. The workpiece is milled on three linear paths in each layer, with five layers altogether. A sketch of the experimental program for one test group is shown in Figure 48.

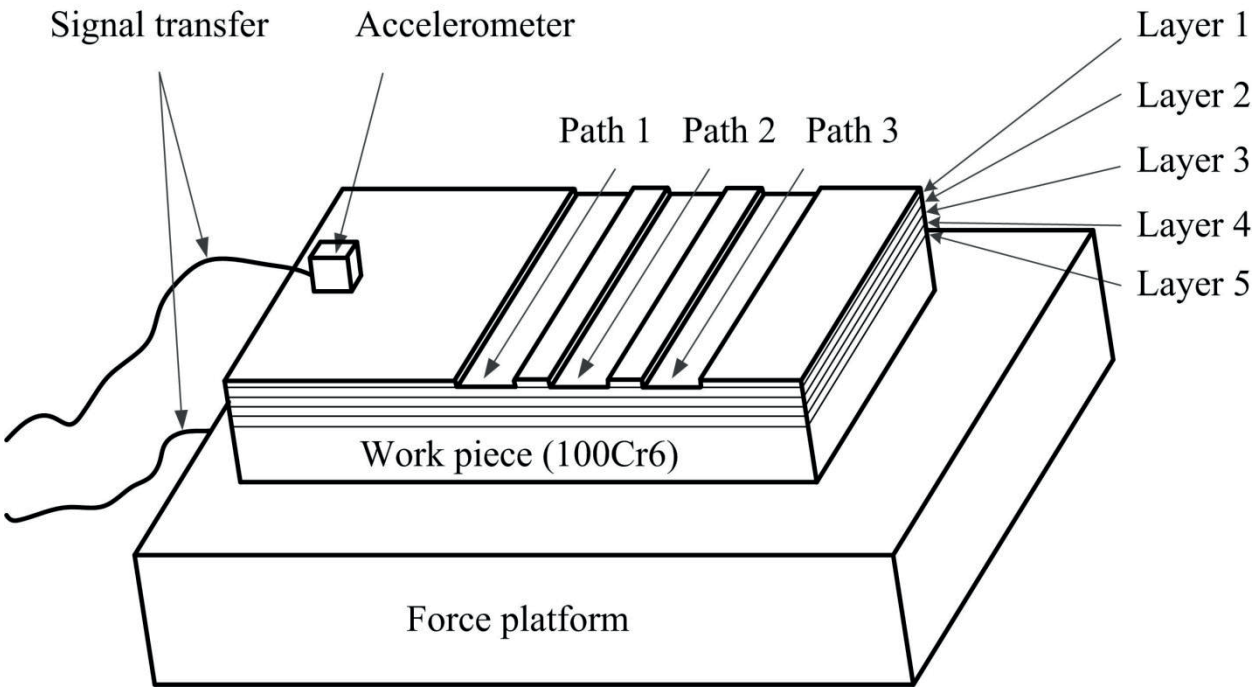

Figure 48: Sketch of experimental programm

The first and the last 16 mm of milling trajectory for every test are unstable processes, in which the cutting tool is turned into the workpiece and deviated from the workpiece. These unstable processes are removed from the measured signal in analysis. The

calculated process damping ratio in our case is based on the magnitude of the cutting force and acceleration signals. Due to the periodic feature of the milling process, the analysed signal can be divided into several signal blocks. The calculated damping ratio for one path is the mean value of the identified damping ratios in each signal blocks. The final damping ratio in next section can be therefore illustrated with statistical means for 15 paths and standard deviation.

As shown in Figure 49 many peak values can be observed apparently in the spectrum. The cutting frequency which is located at 66.31 Hz and its harmonics are significant and analysed.

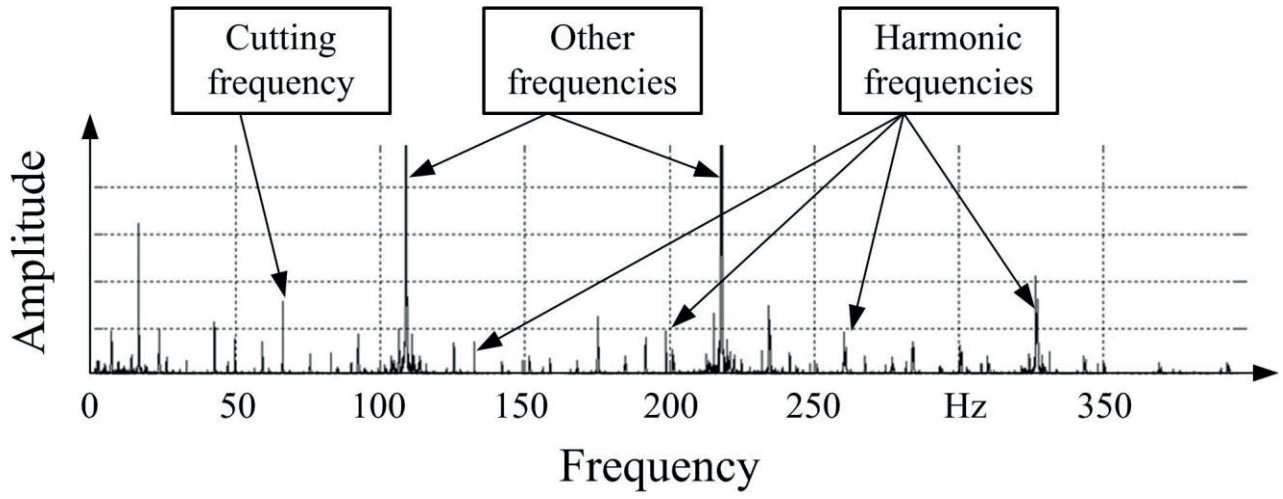

Figure 49: Spectrum of force magnitude

Results and discussion:

Figure 50 and Figure 51 present the estimated process damping ratio of the 5th harmonic for four different flow rates of cooling lubricant based on force signals and acceleration signals, respectively. It can be seen that the damping ratio has a rising trend with an increased spraying in cooling lubricant. The damping ratio is obviously increased by LQL in comparison with the value by MQL, because there is a large interval between MQL and LQL conditions (20 ml/h – 0.1 l/s).

For each test in one test group, the value of damping ratio keeps however not constant. The standard deviations of LQL and WQL are overlapped. The mean value of WQL based on acceleration signal is even smaller than the mean values of LQL. These can be explained that the changing of milling plane, tool wear or inhomogeneous features of material lead to the changes of dynamic behaviour of tool point. Another possibility is that the jet flux of cooling lubricant is not constant due to the simple pump equipment and spray nozzle.

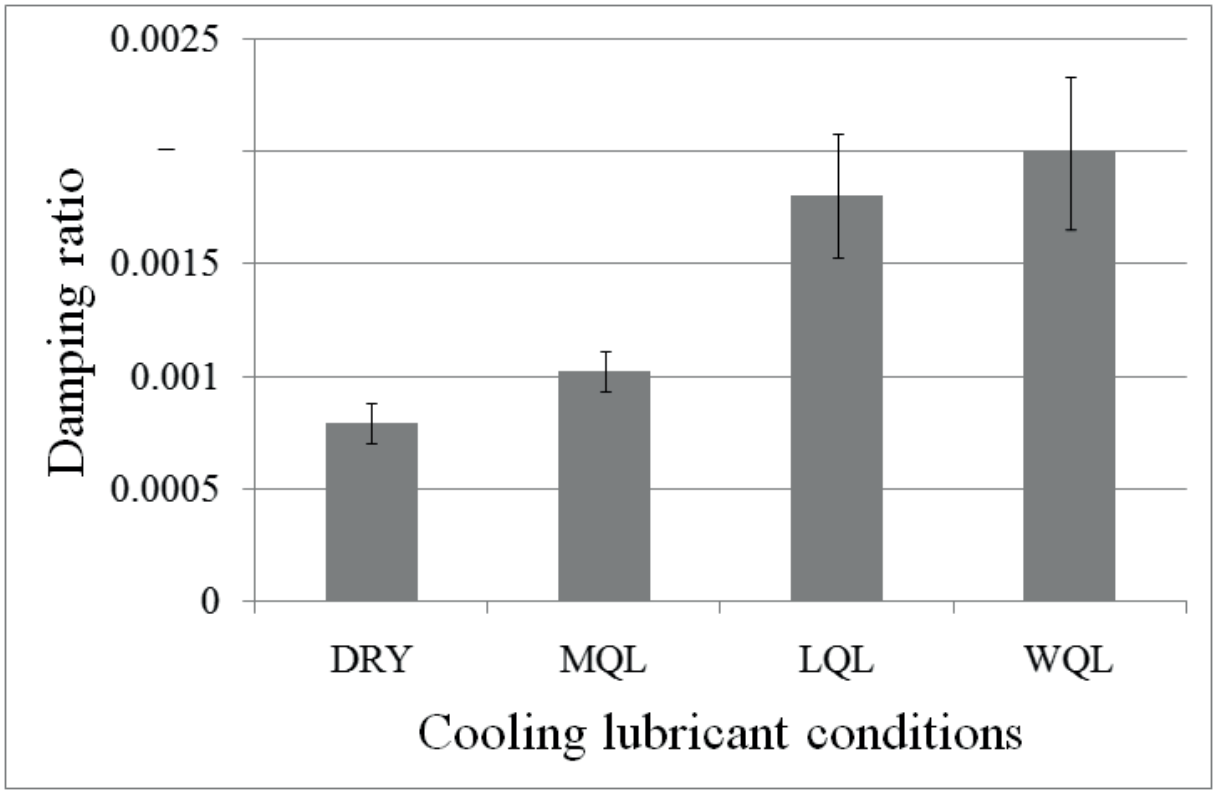

Figure 50: Computed process damping ratios based on force signals

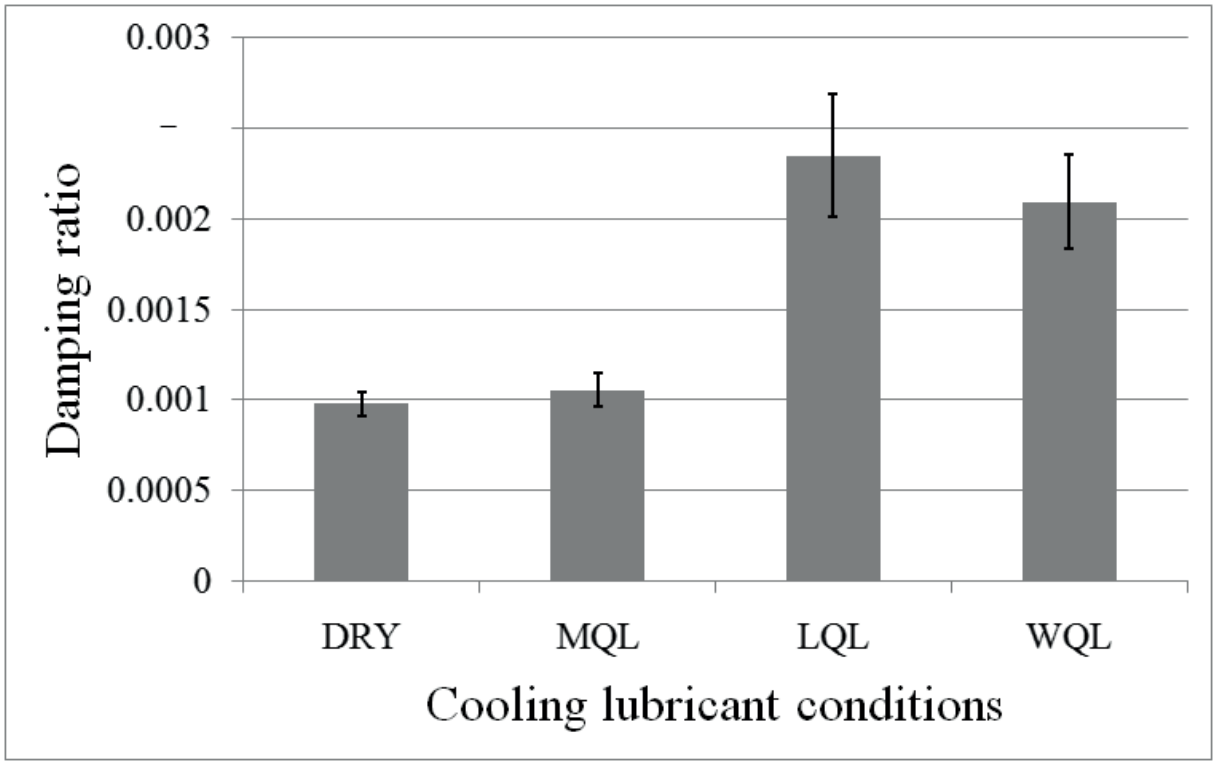

Figure 51: Computed process damping ratios based on acceleration signals

The flow rate of cooling lubricant might lead to change the characteristics of friction and adhesion between cutting tool and chip or between cutting tool and workpiece [ZHO10,

YON11]. These changes can affect not only the dynamic cutting force but also the dynamic behaviour of the tool point. Correspondingly, the process damping might be also varied caused by the lubricant quantity.

6.2.2 Process damping identification in swaging process

Process damping as a significant system parameter is identified using SWLSE method in real-time process by a swaging operation. Through a series of experiments it concludes the relationship between the process damping and other swaging parameters such as the deformation degree and spindle revolution speed. It is interesting to evaluate the process damping during machining operations to see how they change, this should help to control the swaging operation more effectively.

Measurement setup

The same analysed procedure like previous subsection is used for this experiment. The process damping ratios are estimated on a micro rotary swaging machine in this section under different revolution speed and different incremental deformation degree. In swaging process a workpiece (metal rod) is fed to swaging unit through a feeding device. The cross section of the metal rod is reduced. A principle of operation of the swaging unit is shown in Figure 52(b). Three groups of die segment and base jaw are arranged on a motorized spindle and rotated on its axis. Meanwhile, the roller cage with rollers is rotated on the same axis and in the same direction, but relative motion between the spindle and the roller cage due to the different speed. In this process, when the base jaws are crossing the rollers, an impact is implied to base jaws and forming dies respectively. The dies apply press forces in rapid sequence in the radial direction towards the workpiece, so that the cross section of the workpiece is reduced with simultaneous lengthening.

The system response is measured using a piezoelectric accelerometer (Brüel&Kjael DeltaTron type 4520-001) which is glued on the head of the rotary swaging machine (see Figure 52(a). The sensor signals are amplified and sampled by data acquisition card (MC DaqBoard/3001USB), the sampling frequency is 16 kHz.

The peak of swaging frequencies are analysed and the process damping ratios are estimated using SWLSE method under the different swaging conditions.

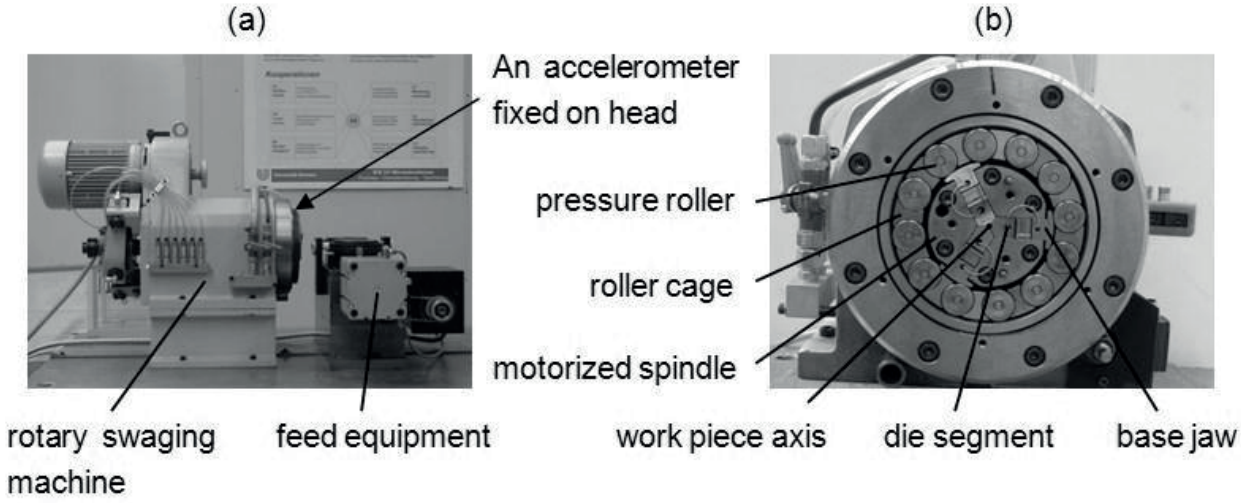

Figure 52: (a) Side view of rotary swaging machine (b) Cross section of swaging unit

In order to observe the influence of damping ratio on machined surfaces, the actual swaging tests are carried out with a 1.5 mm steel rod. Machined surfaces are observed by a digital microscope. Swaging conditions adopted in the tests are listed in Table 10.

Experimental procedure

Experiments are carried out by swaging a rod of 16MnCr5 steel with 1 mm diameter. In order to investigate the relationship between the revolution speed or deformation degree at each stroke and the process damping, the following measurements are tested on the rotary swaging machine. The details experimental conditions are given in Table 10.

The axial feed rate can be computed using the parameters revolution speed and deformation degree at each stroke. The deformation degree at each stroke can be defined as [KUH11b]:

$$\varphi_{st} = \ln\left(\frac{D_A - 2Z_H}{D_A}\right)^2 \tag{6.1}$$

where D_A is initial part diameter, Z_H is the effective stroke:

$$Z_H = \frac{v_f}{HZ}\tan\alpha \tag{6.2}$$

where v_f axial feed rate; α is one of the geometric angle of die segment, here $\alpha = 10^\circ$. HZ is stroke frequency.

Table 10: Swaging conditions

Test-number	Revolution speed (1/min)	Axial feed rate (mm/s)	Deformation degree at each stroke (-)
01	2800	1.00	-0.007
02	2500	0.89	-0.007
03	2200	0.79	-0.007
04	1900	0.68	-0.007
05	1600	0.57	-0.007
06	2800	2.00	-0.014
07	2500	1.79	-0.014
08	2200	1.57	-0.014
09	1900	1.36	-0.014
10	1600	1.14	-0.014
11	2800	4.00	-0.028
12	2500	3.57	-0.028
13	2200	3.14	-0.028
14	1900	2.71	-0.028
15	1600	2.29	-0.028
16	2800	6.00	-0.042
17	2500	5.36	-0.042
18	2200	4.71	-0.042
19	1900	4.07	-0.042
20	1600	3.43	-0.042
21	2800	8.00	-0.056
22	2500	7.14	-0.056
23	2200	6.29	-0.056
24	1900	5.43	-0.056
25	1600	4.57	-0.056

Results and discussion:

Figure 53 shows the identified process damping ratios based on different incremental deformation degree at each stroke and revolution speed. It can be seen that the process damping ratios are increased with increasing of the incremental deformation degree. This is because more material for each stroke is taken into the swaging process, while the incremental deformation degree increased. Figure 53 demonstrates also the damping ratios have obviously increased with decrease the revolution speed. While the revolution speed is decreased, the swaging forces are decreased. This decreasing of swaging forces leads to more damping effect, like a soft head of hammer be used in impact testing, the damping ratio of impact force can also increase.

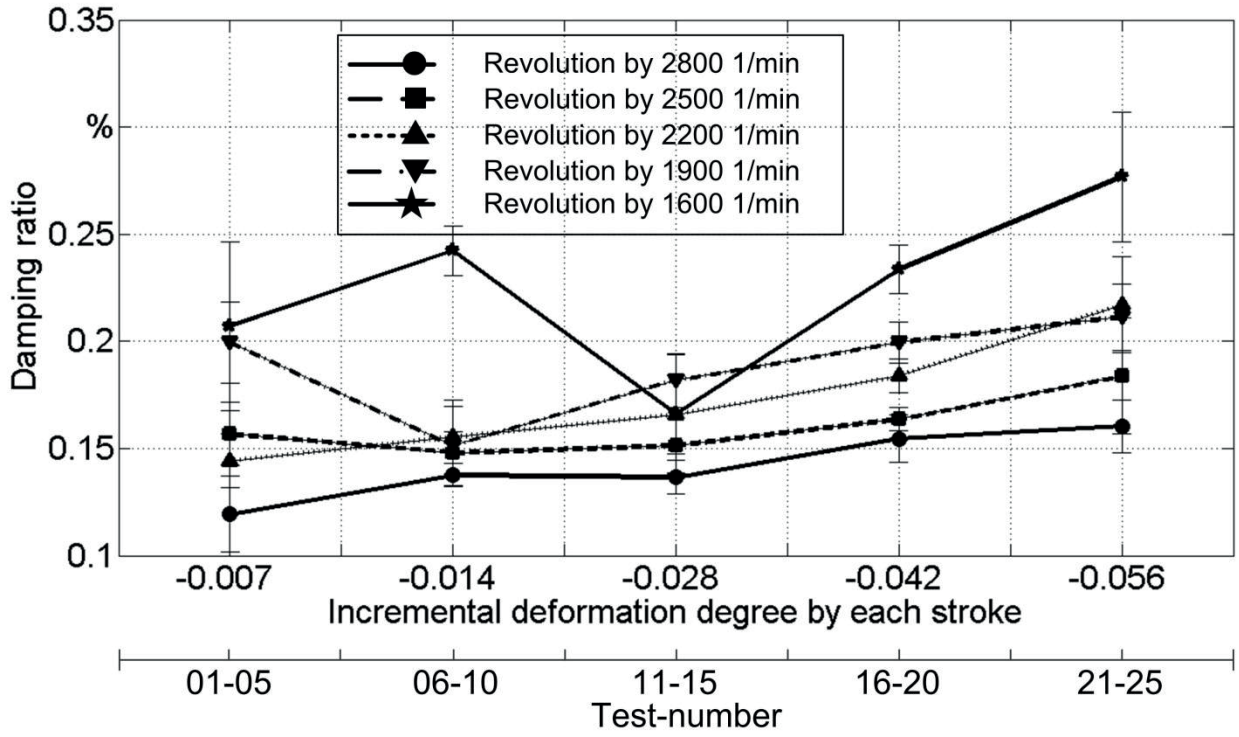

Figure 53: identified process damping based on different revolution speed and incremental deformation degree of swaging process

6.3 Predicting Transfer Function of Feed Drive Systems

A feed drive system is one of the most common types of machine components. The dynamic tracking error of feed drive systems influences the machined surface directly. Due to effects such as position dependant stiffness, mechanical friction and variable preloading, the systems transfer function which is identified from input and output data

as a black box model is time-varying during motion. In order to improve the tracking accuracy the coefficients of the system transfer function should be detected and verified in real-time. This chapter uses the SWLSE method which is proposed in this work but based on mathematical model of a system transfer function of feed drive systems to identify feed drive system coefficients in short time and predict the transfer function for next displacement segment in order to reduce the tracking error [KUH11c, KAK96, KIM05, CHE05].

Measurement setup

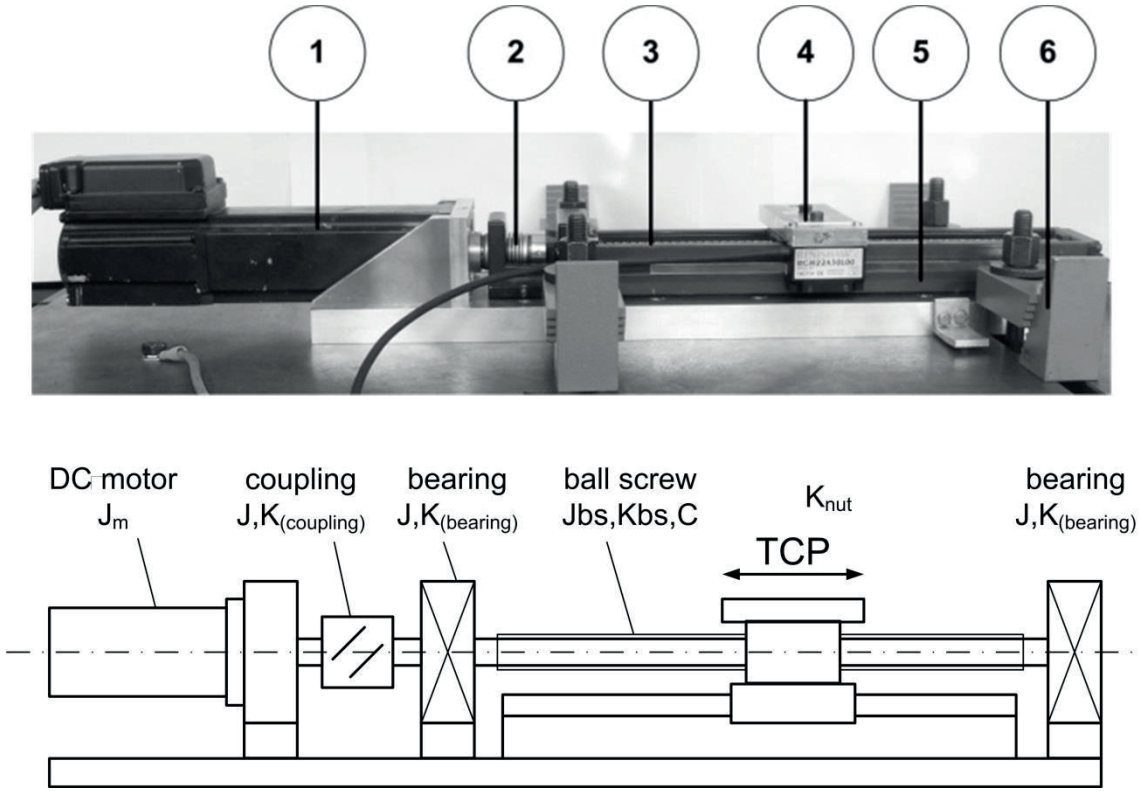

Figure 54: A ball screw feed drive system and its physical model: 1) DC motor, 2) flexible coupling. 3) ball screw, 4) tool center point and linear encoders, 5) linear bearing guideways, 6) fixation jig. $J_m, J_{bearing}, J_{coupling}$ and J_{bs} are the servo motor rotor, bearing, coupling and ball screw inertias. C is the viscous damping coefficient. $K_{bs}, K_{nut}, K_{coupling}$ and $K_{bearing}$ are the ball screw, nut, coupling and bearing stiffness [KUH11c].

The experiment is executed by a feed drive system which consists of a ball screw, a flexible coupling, nut and thrust bearings as shown in Figure 54. The ball screw has a 10 mm pitch, 10 mm diameter and 320 mm length. The nut supports the tool center point during feed motion. A closed loop servo system consisting of DC permanent magnet motor and a servo drive is used to drive the assembly and perform the tracking commands. The motion trajectories are measured by a dual position measuring system using rotary encoders (built in the servo motor) and linear encoders (mounted on the

table) which can measure relative motion trajectory of spindle and table of tool center. The linear encoder signals are interpreted and stored by a digital signal processing and acquisition device. The sampling frequency is same to $f_s = 5kHz$.

Experimental procedure

The transfer function (Tf) of the control system in the s-domain between the command position (input trajectory) and actual position (output trajectory) is expressed as in the following equation [KUH11c]:

$$Tf = X_a(S)/X_s(S) = \sum_{i=2}^{0} N_i S^i \Big/ \sum_{i=7}^{0} D_i S^i \tag{6.3}$$

where X_a and X_s are output and input trajectory. The work aims at determining the numerator and denominator coefficients N_i and D_i in descending powers of S. In this work, a rough but accepted simplification is made by assuming that the input and output signals from system are equal to the state description of numerator and denominator. And by applying the inverse Laplace transform the equation (6.3) can be reformed in time domain in (6.4).

$$\begin{cases} X_a(t) = \sum_{i=7}^{5} P_i t^i \\ X_s(t) = \sum_{i=7}^{0} Q_i t^i \end{cases} \tag{6.4}$$

where
$P_7 = N_0/5040,\quad P_6 = N_1/720,\quad P_5 = N_2/120,\quad Q_7 = D_0/5040,\quad Q_6 = D_1/720,\quad Q_5 = D_2/120,$
$Q_4 = D_3/24,\quad Q_3 = D_4/6,\quad Q_2 = D_5/2,\quad Q_1 = D_6,\quad Q_0 = D_7.$

Proposed predicting method consists of two steps. The first step is computation of actual coefficients values. The input and output signals within a observe window size 4 ms (20 samples) are acquired. The actual coefficients values (N_i and D_i) are then estimated using curve fitting technique and least squares estimator. Second step of proposed method is predicting process. The estimated coefficients in step one are substituted in the transfer function in equation (6.3) to predict the next 2 ms (10 samples) of trajectory.

The step one and step two are run in a reciprocating cycle. The observe window is shifted over the whole signal with an overlap of 50 % to obtain the predicted system

command response function. The work is executed experimentally and analytically by commanding the feed drive system to run with a ramp function and a step function. The ramp function has amplitude of 30 mm and set velocity of 50 mm/s. The step function has amplitude of 1 mm in 0.2 ms.

As results the command trajectory, the measured response, estimated response and simulated response are compared to each other. The measured data is from the axis motion, the simulated response is from the simulation model using MatLab [AMI08], the estimated response is identified model using least squares method (LSM) and curve fitting technique. The used simulation model for the feed drive system is explained in [KUH11c]. In addition, a calculated error is defined as the difference between estimated response and measured response, or between simulated response and measured response.

$$\begin{aligned} \text{LSM model error} &= \text{measured response} - \text{estimated response} \\ \text{simulation model error} &= \text{measured response} - \text{simulated response} \end{aligned} \tag{6.5}$$

Results and discussion:

Figure 55 and Figure 56 show the results in a zoomed view of the applied ramp function in first 60 ms. As compared to the simulation model, LSM response has more accuracy in tracking the measurements than the simulation model. As shown in Figure 56, the difference between LSM response and measurements is in range of 40 µm and measurement is equal to 80 µm. However, due to the high order of curve fitting functions the periodic ripples are presented in the LSM model response. To optimize this overfitting the problem has to be studied in future work.

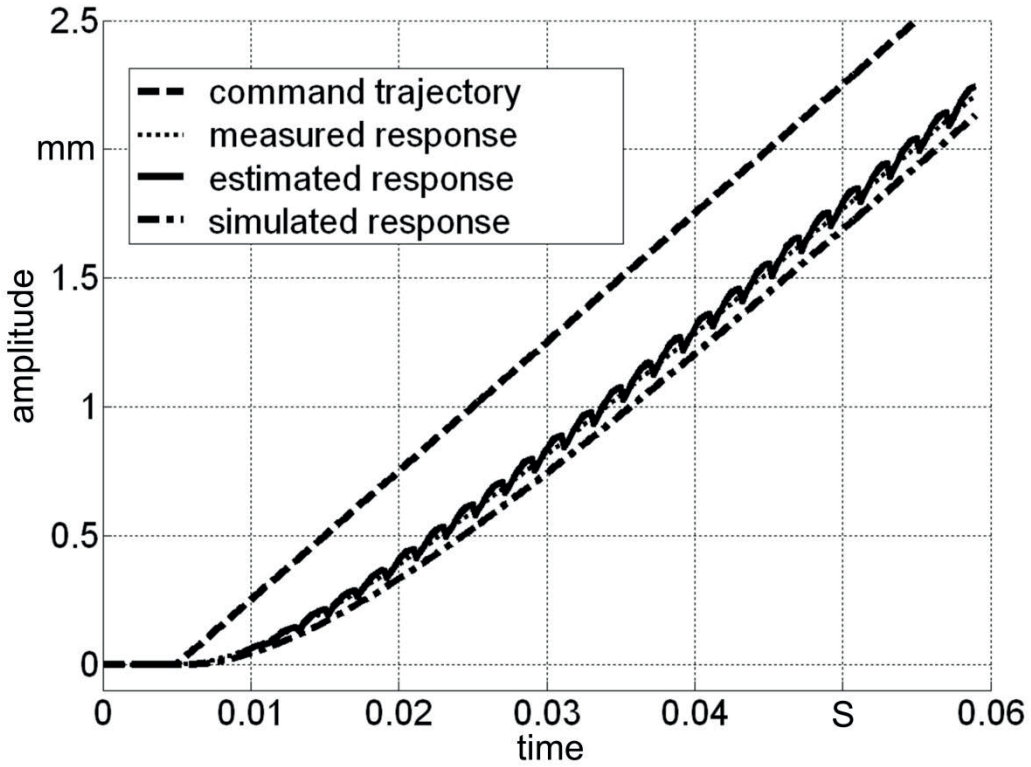

Figure 55: Identified model results against measured and simulated response results in the first 60 ms for a ramp function

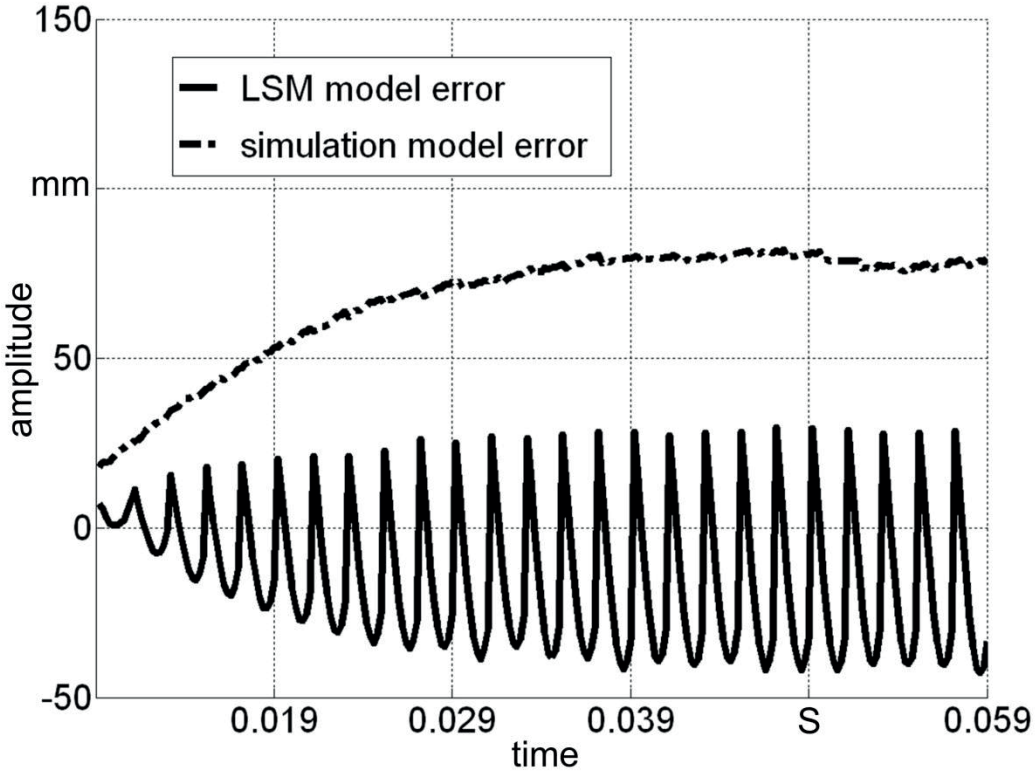

Figure 56: LSM model error and simulation model error as compared to real system measurements for a ramp function

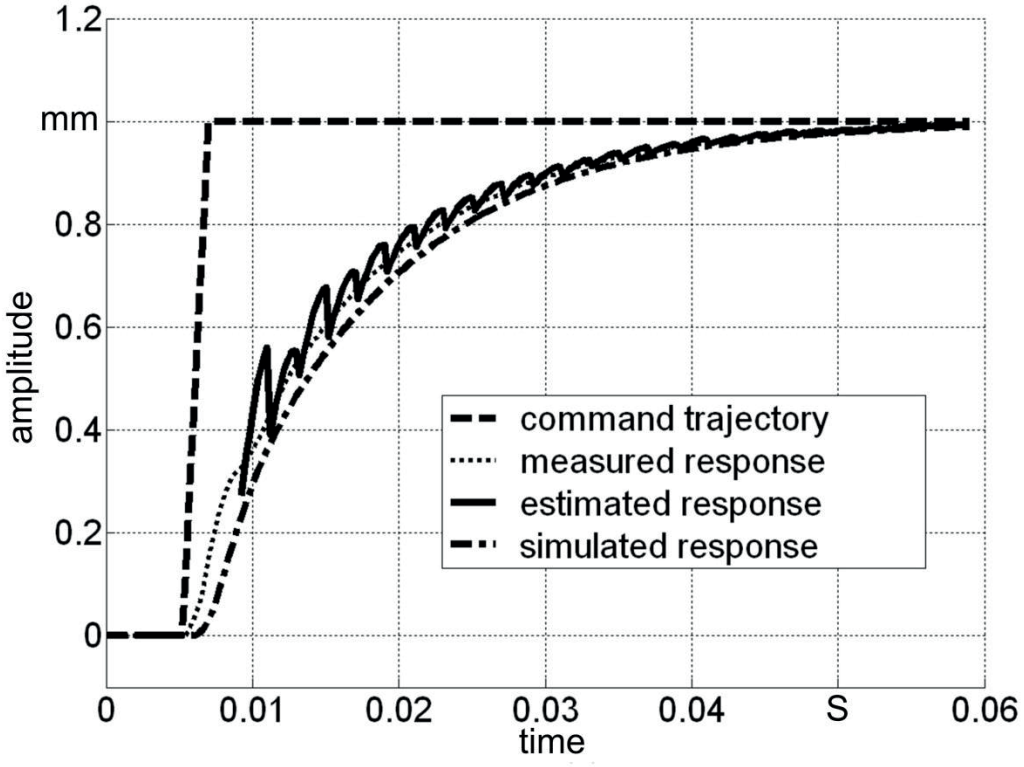

Figure 57: Identified model results against measured and simulated response results in the first 60 ms for a step function

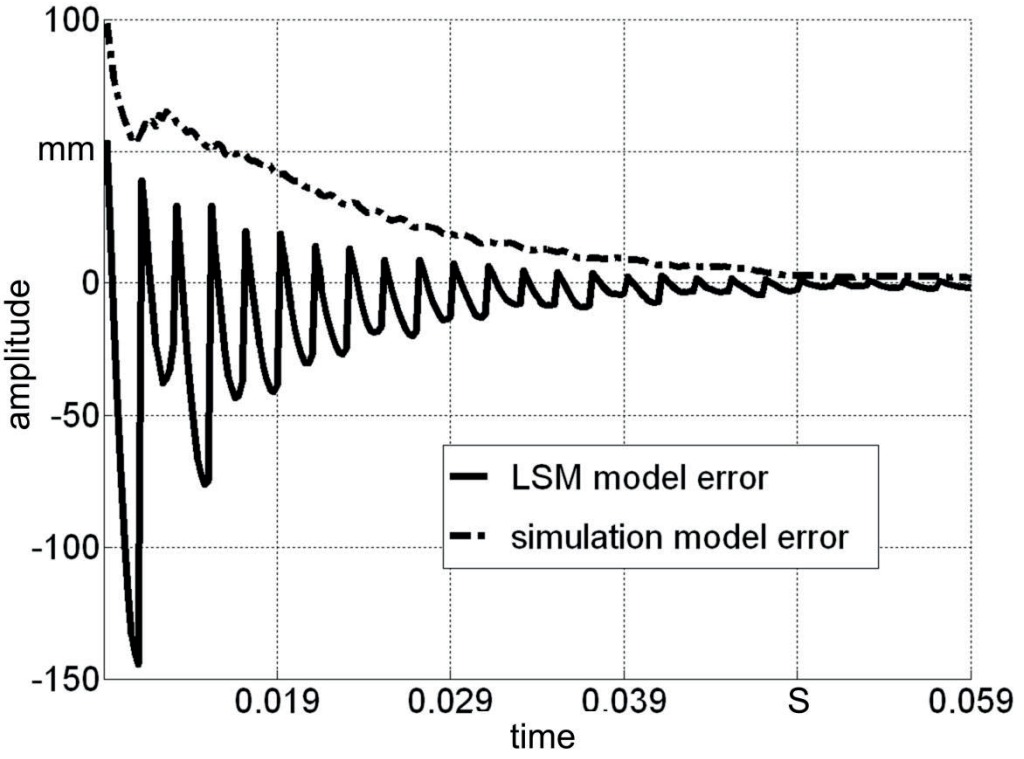

Figure 58: LSM model error and simulation model error as compared to real system measurements for a step function

The results of the step function in the zoomed view of 60 ms are presented in Figure 57 and Figure 58. The estimated model response in step function generates similar results that the same periodic ripples are present. The calculated error at the start of motion in the step function is higher than the error in the ramp function. The maximum error of LSM model is found around 0.15 mm. This is due to higher slope of the trajectory in the acceleration phase. The experimental results show that the proposed least squares model can identify the dynamic behavior in the short time window. The accuracy is reduced with increasing of the severity of curve slope.

6.4 Summary of Engineering Applications

In chapter 6.1, the proposed SWLSE method and CEMA method are applied on a four column press machine and a high-speed machining center. The stationary and instationary measurements are carried out and their results are compared. By instationary measurement using SWLSE method the system transient modal parameters are successfully identified in each 350 ms with high resolution. By CEMA method the frequency resolution can only reach 2.8 Hz with 350 ms window size. The SWLSE method in this case can more accurate reveal the varying of modal parameter while the machine table is moving.

In chapter 6.2, the proposed SWLSE method is further applied to estimate the process damping ratio of real machining process. Due to extreme low damping value the process damping ratio cannot be identified accurately using CEMA method. However, the proposed SWLSE method is more suitable for this short time block data and it can reveal the transient process damping ratio. Because of this, the proposed method can be applied in the field of machining monitoring or real-time control system. For example, the relationship between the flow rate of cooling lubricant and the process damping ratio is identified in chapter 6.2.1. Therefore, the flow rate of cooling lubricant can be monitored in real-time while measuring the signal of the process damping. In chapter 6.2.2, the relationship between the deformation degree at each stroke and the process damping ratio has been detected. It assumes that this deformation degree influences directly the surface roughness of workpiece, so the SLWSE method can also monitor the surface roughness through identifying the process damping in real-time. These hypotheses need certainly much more works to be verified in future.

In chapter 6.3, the proposed SWLSE algorithm can be also extended to identify the transient dynamic behavior of a nonlinear feed drive system in short time. The transfer function of the system based on windowed input/output inverse modeling is built first. Using inverse Laplace transform, the transfer function of the system is converted into a set of system equations in time domain and SWLSE is then conducted on the windowed signals to get information about the system coefficients. These transient identified coefficients can be used to predict the system output for next motion block. With shifting forward the time window, the dynamic response of the system is estimated accurately online.

Chapter 7

Limitation of Proposed Algorithm

In this work, through a series of tests for the proposed SWLSE algorithm, it can be detected that there are some shortcomings needing attention and more investigation in future work. Obvious shortcomings to this technique include:

First, due to the mathematical model the Least Squares estimation for identification of modal parameters is suitable in the current just for a single degree of freedom system. Rouguette and Najim have presented the ESPRIT Estimation method in two-dimensional type [ROU01]. An evaluation SWLSE method for a multi-degree of freedom system could be studied in further work.

Second, since the first limitation of SWLSE method, it is therefore necessary to have prior knowledge of the shifted frequency range, thus applying a pass-band filter to the analyzed signal. The choice and settings of the filter could have a major impact on the identification accuracy. In this work, a frequency filter with Hanning window is used for the pre-processing of the proposed algorithm. Other self-adapting filter technique like the Kalman filtering technique [KOR03] or the empirical mode decomposition [FLA04] could be considered for this process. It is due to self-adapting properties that these filter types could better suit for real control machining process.

Third, the identification accuracy of the proposed algorithm depends not only on the used pass-band filter type but also on the computed time block size, the SNR of the analyzed signal and the sampling rate of the analyzed signal, etc. Among them the noise has a great influence on the identification accuracy. This requires the used pre-processing filter having better denoising performance.

Fourth, the proposed algorithm is based on curve-fitting technique with a single-degree of freedom system. Therefore, when the spacing between two eigenmodes is not sufficient and these two modes cannot effectively be decomposed in time domain, accurate modal parameter estimation is not available using proposed method.

Fifth, as mentioned in chapter 6.1.2 a time-domain curve fitting technique cannot very accurately estimate for heavily damping structure. According to the Eq. 4-19 the accuracy of the system residue depends on the computing system eigenvalue. So the accuracy of estimated mode shapes might also have low precision.

Sixth, the SWLSE is one of the time-domain identification methods that bases on parametric identification to establish mathematical model, rather than one of the modal analysis methods. It cannot estimate all system modes at once, but is aimed at one system mode to detecting its time-varying behavior.

Chapter 8

Conclusions

Motivation

In machining processes, the modal parameters which characterize the dynamic behaviour may vary rapidly due to variations in the cutting parameters and changes in boundary conditions. The stationary machine condition cannot be achieved, what makes it difficult to analyze this transient feature of the signal due to insufficient frequency resolution of FFT determined by a short time analyzed window. The classical modal analysis based on the FFT cannot identify the transient modal parameters accurately. In this work, a short time identification method is developed to reveal the transient dynamic behavior of system with high resolution. Two hypotheses circumventing the analysis of non-stationary transient data are proposed in this work:

- The classical modal analysis based on the FFT cannot identify transient modal parameters accurately.
- The actual modal parameters for transient or non-stationary data that occur in a short time can be identified efficiently using a sliding-window least squares estimation method.

Procedure of the work

In this work, a time domain sliding-window Least Squares estimation (SWLSE) method has been presented for the identification of actual modal parameters in short time-window block. The SWLSE method is based on the least squares algorithm by fitting time window data with a damped oscillating function to identify the parameters. Using the moving window across the analyzed signal the actual modal parameters can be estimated with high resolution.

Through comparison of other classical identification methods, the proposed SWLSE method is more suitable especially for the transient modal parameters to detect the varying of the modal parameters during machining process. The identification accuracy of the proposed method depends on many parameters, such as applied window size, applied filter type, sampling rate, signal to noise ratio etc. The performance or applicability of the method is examined under these mentioned criteria using several numerical examples. In this study, the method is demonstrated not only numerically but also experimentally through a laboratory beam model and real machining conditions in order to verify actual modal parameters identification.

The theory of SWLSE method has also be combined with real-time operation for monitoring the machining process and predicting the system transfer function

Results and benefits

Numerical and verified results show that the proposed method can provide very high accuracy of frequency identification independently of analyzed mono-frequency component for a signal without noise. For a predefined damped oscillating signal with 30dB SNR, the estimated frequency error is less than 0.01%. Similarly, the estimated damping ratio identification accuracy is demonstrated to be less than 3%. Moreover, the identification accuracy for the lightly damping is better than the heavily damping. Overall, in comparison with classical modal analysis method the identification accuracy of the SWLSE method is higher.

The proposed algorithm is based on curve-fitting technique with a single-degree of freedom system. A closely spaced double mode can affect the identification accuracy depending on the applied pre-processing filter type. In this work, an ideal pass-band filter in frequency domain is used for pre-processing. For the artificial signal in this work the proposed method can provide more accuracy by the lower amplitude ratio and higher frequency difference between the double modes. From the illustrated results, it has been found that the SWLSE method can obtain much clearer, smooth and precise results than the CMEA method.

The identification accuracy of the proposed algorithm increases with increasing applied window size. The SWSLE method was set to be 80ms window size and executed on a damped oscillating signal with 5dB noise level. The estimated frequency and damping ratio have maximum 0.05% and 25% error comparing with the preset value, respectively. A main advantage of this method is that the frequency resolution is also very high by a short time window. For example, the natural frequency of the laboratory beam system has been even identified within the time window length of 10 ms, where the frequency resolution has just 100 Hz by CEMA method.

It is observed that the identification accuracies are abruptly reduced, when the SNR is increased form 20dB to 5dB, not only for frequency but also for damping ratio The estimation accuracy of the proposed algorithm sensitively depends on the noise level of the analyzed signal.

If the estimated frequency and the center frequency of the applied pass-band filter are different, the numerical result shows no significant influence on the identification accuracy (in chapter 4.1.3).

A highlight benefit of this method is that, the identification accuracy does not depend on the frequency range of analyzed signal. Added to it, the frequency can be more precisely

estimated even for a signal that is less than one time period, which is impossible by CEMA method.

Another advantage of the proposed algorithm is that the computation effort can be significantly reduced. Therefore, it might be applied for the real control processing.

The proposed SWLSE method is also verified on a laboratory beam system, where the stiffness and damping can be independently adjusted by changing the dynamic behaviors of the beam system. Through stationary and instationary tests, the result shows that the actual modal parameters can be identified using this proposed method. In comparison with CEMA method, the changes of natural frequency are recovered effectively. The maximum error between SWLSE and CEMA by the damping ratio identification has about 50% deviation. Generally, the frequency identification is better than damping ratio identification for the proposed method.

Finally, it can be concluded that the proposed SWLSE method can clearly indicate the frequency differences with time, and extract it with high resolution that cannot be obtained by using the time-domain signal or FFT technique. It is more suitable for the identification of the actual modal parameters in short time window. For extended application, it can be applied on the real-time control system, processing monitoring or online fault diagnosis.

Field of application

The SWLSE analysis is a powerful tool for estimating a structure's modal parameters during operating conditions. With this method, it is possible to estimate the system modal parameters from an output signal without knowing the input signal, which is needed in real-time monitoring.

There are three types of engineering applications in this work. First, the proposed SWLSE method has investigated for the actual modal parameters in parameters in real machine tools with machining conditions. In the experimental verification, attention is given to the changes of dominant eigenmode of the structure, while the geometry of machine tools is changing. In chapter 6.1, the SWLSE has been applied on the identification of the actual modal parameters during the vertical movement of machine spindle. Due to the more complex geometry and high damping of a high-speed milling center, the results can be observed that the estimated modal parameters have more deviation in comparison with CEMA method. The maximum deviation of the estimated frequency between SWLSE and CEMA method is about 3%, and the deviation of damping ratio is about 35%. Other result shows that the identification accuracy of the mode shapes depends on the identification accuracy of the estimated frequency and damping ratio related FRFs.

Secondly, the process damping ratios have been identified using proposed SWLSE method during machining process. The experimental measurements have been executed on a Hermle U630T universal machining center and a micro rotary swaging machine. (see chapter 6.2) It is found that the damping ratio has a rising trend with an increased spraying in cooling lubricant by a milling process. The process damping ratios are increased with increasing incremental deformation degree and with decreasing revolution speed by a swaging process.

Finally, As mentioned in chapter 6.3, the proposed SWLSE algorithm can also be extended to identify the transient dynamic behavior of a nonlinear feed drive system in short time. The transfer function of the system based on the windowed input/output inverse modeling has been successfully predicted. The experimental results show that the proposed method can provide more accuracy of command response than the simulation model.

Suggestions for future Work

In the further work, a pass-band filter could be implemented as pre-processing, in order to filter out the noise. Secondly, an evaluation method for SWLSE algorithm (like coherence function in classical modal analysis) could be studied in order to validate the identification results. Thirdly, the mathematical model for this method might be improved to multi-degree of freedom, so that the system's double mode can be more accurately estimated. Fourthly, the accuracy of the estimated mode shapes could be more investigated in future work. Besides of the applications in field of identification actual modal parameters, the proposed method can be used in real-time control system and in prediction of transfer function of the feed drive system, like in chapter 6. The relationship of process damping ratio with other machining parameters could be more studied. In order to improve the real trajectory of the nonlinear feed drive system, the periodic ripples of estimated model, which are mentioned in chapter 6.3, could be also investigated in future work. The development of a complete methodology for applying the SWLSE method for machining processes has a great benefit.

REFERENCE

[AHM12] K. Ahmadi and F. Ismail, Investigation of Finite Amplitude Stability Due to Process Damping in Milling, *Procedia CIRP,* 2012*,* vol. 1, pp. 60-65.

[ALT04] Y. Altintas and M. Weck, Chatter Stability of Metal Cutting and Grinding, *CIRP Annals - Manufacturing Technology,* 2004*,* vol. 53, pp. 619-642.

[AMI08] G. Amirian, “Transformation of tracking error in parallel kinematic machining,” Ph.D. dissertation, bime institute, Universität Bremen, Bremen, Germany, 2008.

[ASH99] M. R. Ashory, "HIGH QUALITY MODAL TESTING METHODS,": University of London, 1999.

[ASM97] J. C. Asmussen, *Modal Analysis Based on the Random Decrement Technique: application to civil engineering structrures*: Aalborg University. Department of Mechanical Engineering, 1997.

[AU11] S. Au, Assembling mode shapes by least squares, *Mechanical Systems and Signal Processing,* 2011*,* vol. 25, pp. 163-179.

[BAD05] R. Badeau, G. Richard and B. David, "Fast adaptive esprit algorithm," in Statistical Signal Processing, 2005 IEEE/SP 13th Workshop on, 2005, pp. 289-294.

[BEN00] J. S. Bendat and A. G. Piersol, Random Data: Analysis & Measurement Procedures: Wiley-Interscience, 2000.

[BEN05] J. Benesty, C. Jingdong and H. Yiteng, A generalized MVDR spectrum, Signal Processing Letters, IEEE, 2005, vol. 12, pp. 827- 830.

[BEN06] J. Benesty, C. Jingdong and H. Yiteng, "Estimation of the Coherence Function with the MVDR Approach," in Acoustics, Speech and Signal Processing, 2006.ICASSP 2006 Proceedings.2006 IEEE International Conference on, 2006, p. III-III.

[BJÖ96] A. Björck, Numerical Methods for Least Squares Problems. Philadelphia: SIAM, 1996.

[BOA92] B. Boashash, Time-frequency signal analysis--methods and applications: Longman Cheshire, 1992.

[BOA03] B. Boashash, Time frequency Signal Analysis and Processing. Amsterdam: Elsevier, 2003.

[BRI82] E. O. Brigham and S. A. Azizi, FFT: schnelle Fourier-Transformation: Oldenbourg, 1982.

[BRI92] R. Brincker, S. Krenk, P. H. Kirkegaard, and A. Rytter, Identification of Dynamical Properties from Correlation Function Estimates, 1 ed. vol. 63: Danish Society for Structural Science and Engineering, 1992.

[BRI07] R. Brinker, L. Zhang and P. Andersen, "Modal identification from ambient responses using frequency domain decomposition," in Proceedings of 18th International Modal Analysis Conference San Antonio: Texas, 7.

[BRO79] D. L. Brown and R. J. A. R, Parameter Estimation Techniques for Modal Analysis, SAE Technical Paper, doi:10.4271/790221, 1979,

[BUD96] E. Budak, Y. Altinta and E. Armarego, Prediction of Milling Force Coefficients From Orthogonal Cutting Data, ASME J. Manuf. Sci. Eng., 1996, vol. 118, pp. 216-224.

[BUT04] J. H. L. B. John BUTTERWORTH, "Experimental Determination of Modal Damping from Full Scale Testing," in 13th World Conference on Earthquake Engineering Vancouver, B.C., Canada, 2004.

[CAR73] G. Carter, C. Knapp and A. Nuttall, Estimation of the magnitude-squared coherence function via overlapped fast Fourier transform processing, Audio and Electroacoustics, IEEE Transactions on, 1973, vol. 21, pp. 337- 344.

[CHE05] C. Chen, and C. Cheng, “Integrated design for a mechatronic feed drive system of machine tools,” in proc. IEEE/ASME International Conference on Advanced Intelligent Mechatronics, pp. 588-593, 2005.

[CHE09] B. Chen, X. Chen, Z. He, and J. Tan, Mechanical Fault Diagnosis Based on Local Mean Decomposition Method, Measuring Technology and Mechatronics Automation, International Conference on, 2009, vol. 1, pp. 681-684.

[COH89] L. Cohen, Time-frequency distributions-a review, Proceedings of the IEEE, 1989, vol. 77, pp. 941-981.

[COH95] L. Cohen, Time-frequency analysis: theory and application. Englewood Cliffs, N J: Prentice Hall, 1995.

[COL68] H. A. Cole, "On-the-line analysis of random vibrations," in 9TH Structural dynamics and materials conference; APR. 1-3; PALM SPRINGS, CA; US, 1968.

[COL73] H. A. Cole, N. E. Research and A. R. Center, On-line failure detection and damping measurement of aerospace structures by random decrement signatures: National Aeronautics and Space Administration, 1973.

[COO65] J. Cooley and J. Tukey, An Algorithm for the Machine Calculation of Complex Fourier Series, Mathematics of Computation, 1965, vol. 19, pp. 297-301.

[CUR88] Mills-Curran and W. C., Calculation of eigenvector derivatives for structures with repeated eigenvalues, AIAA Journal, 1988, vol. 26, pp. 867-871.

[DAM07] A. N. Damir, A. Elkhatib and G. Nassef, Prediction of fatigue life using modal analysis for grey and ductile cast iron, International Journal of Fatigue, 2007, vol. 29, pp. 499-507.

[DHA07] N. R. Dhar, M. T. Ahmed and S. Islam, "An experimental investigation on effect of minimum quantity lubrication in machining AISI 1040 steel", International Journal of Machine Tools and Manufacture, 2007, vol. 47, pp. 748-753.

[DIN10] Y. Ding, L. Zhu, X. Zhang, and H. Ding, A full-discretization method for prediction of milling stability, International Journal of Machine Tools and Manufacture, 2010, vol. 50, pp. 502-509.

[DIN12] Y. Ding, L. Li, A. Krause, and O. Riemer, "Frequency response prediction of spindle-workpiece assemblies for ultra-precision diamond turning based on substructure analysis," in Proc. of the 12th euspen International Conference, Stockholm Sweden, 2012, pp. P4.32.

[EWI00] D. J. Ewins, Modal Testing: Theory, Practice and Application, 2nd Edition ed. Baldock: Research Studies Press, 2000.

[FLA99] P. Flandrin, Time-Frequency/Time-Scale Analysis: Academic Press, 1999.

[FLA04] P. Flandrin, G. Rilling and P. Goncalves, Empirical mode decomposition as a filter bank, Signal Processing Letters, IEEE, 2004, vol. 11, pp. 112- 114.

[GAB46] D. Gabor, "Theory of Communication," in J. Inst. Electr. Eng. vol. Vol. 93, 1946, pp. 429-457.

[GER70] W. Gersch, Estimation of the autoregressive parameters of a mixed autoregressive moving-average time series, Automatic Control, IEEE Transactions on, 1970, vol. 15, pp. 583- 588.

[GRO90] A. Grossmann and J. Morlet, Decompositions of functions into wavelets of constant shape and related transforms, Mathematics and physics, Lecture on Recent Results, 1990, vol. 135-65,

[GRÖ00] K. Gröchenig, Foundations of Time-Frequency Analysis: Birkhäuser Boston, 2000.

[GU02] S. Gu, J. Ni and J. Yuan, Non-stationary signal analysis and transient machining process condition monitoring, International Journal of Machine Tools and Manufacture, 2002, vol. 42, pp. 41-51.

[HAM96] P. W. J. Hammond, The analysis of non-stationary signals using time–frequency methods, Journal of Sound and Vibration, 1996, pp. 419-447.

[HE11] X. H. He, X. G. Hua, Z. Q. Chen, and F. L. Huang, EMD-based random decrement technique for modal parameter identification of an existing railway bridge, Engineering Structures, 2011, vol. 33, pp. 1348-1356.

[HEI89] C. E. Heil and D. F. Walnut, Continuous and Discrete Wavelet Transforms, SIAM Review, 1989, vol. 31, pp. 628-666.

[HER99] L. Hermans and H. Van Der Auweraer, Modal Testing and Analysis of Structures under Operational Conditions: Industrial Applications, Mechanical Systems and Signal Processing, 1999, vol. 13, pp. 193-216.

[HEY98] W. Heylen, S. Lammens and P. Sas, Modal analysis theory and testing, 1998.

[HUA98] N. E. Huang, Z. Shen, S. R. Long, M. C. Wu, H. H. Shih, Q. Zheng, N. C. Yen, C. C. Tung, and H. H. Liu, The empirical mode decomposition and the Hilbert spectrum for nonlinear and non-stationary time series analysis, Proceedings of the Royal Society of London. Series A: Mathematical, Physical and Engineering Sciences, 1998, vol. 454, pp. 903-995.

[HUA03] N. E. Huang, M. C. Wu, S. R. Long, S. S. P. Shen, W. Qu, P. Gloersen, and K. L. Fan, A confidence limit for the empirical mode decomposition and Hilbert spectral analysis, Proceedings of the Royal Society of London. Series A: Mathematical, Physical and Engineering Sciences, 2003, vol. 459, pp. 2317-2345.

[HUA07] F. Huang, X. Wang, Z. Chen, X. He, and Y. Ni, A new approach to identification of structural damping ratios, Journal of Sound and Vibration, 2007, vol. 303, pp. 144-153.

[IBR77] S. Ibrahim and E. Mikulcik, A Method for the Direct Indentifikation of Vibration Parameters from the Free Responses, Shock and Vibration Bulletin, 1977, vol. 47, pp. 183-198.

[IBR01] Ibrahim and S. R., Efficient random decrement computation for identification of ambient responses, Proceedings of SPIE - The International Society for Optical Engineering, 2001, vol. 4359, p. 6.

[INM01] D. J. Inman, Engineering Vibration: Prentice Hall, 2001.

[JAM95] G. H. James, T. G. Carne and J. P. Lauffer, The natural excitation technique (NExT) for modal parameter extraction from operating structures, Journal of Analytical and Experimental Modal Analysis, 1995, vol. 10, pp. 260-277.

[JEO92] J. Jeong and W. J. Williams, Kernel design for reduced interference distributions, Signal Processing, IEEE Transactions on, 1992, vol. 40, pp. 402-412.

[JIM01] Z. F. Jimin He, Modal Analysis: Butterworth-Heinemann, 2001.

[JUA85] J. N. Juang and R. S. Pappa, An eigensystem realization algorithm for modal parameter identification and modal reduction, VA Journal of Guidance, Control, and Dynamics, 1985, vol. 0731-5090 vol.8, pp. (620-627).

[KAK96] Y. Kakino and A. Mutsubara, “High speed and high acceleration feed drive system for NC machine tools,” The Japan Society for Precision Engineering Journal, vol. 30, pp. 295-298, 1996.

[KAN13] B. Kanning, “Instationary Vibrational Analysis for Impulse-type Stimulated Structures”, in Logos Verlag Berlin, Verlag für wissenschaftliche Publikationen, 2013, pp. 127, ISBN 978-3-8325-3326-7.

[KIM05] M. S. Kim, and S. C. Chung, “A systematic approach to design high performance feed drive system,” International Journal of Machine tools and Manufacture, vol. 45, pp.1421-1435, 2005.

[KJA88] B. Kjaer, "Structural Testing Part 2 - Modal Analysis and Simulation,", 1988.

[KLO97] F. Klocke and G. Eisenblätter, "Dry Cutting", CIRP Annals - Manufacturing Technology, 1997, vol. 46, pp. 519-526.

[KOR03] P. Korba, M. Larsson and C. Rehtanz, "Detection of oscillations in power systems using Kalman filtering techniques," in Control Applications, 2003.CCA 2003.Proceedings of 2003 IEEE Conference on, 2003, pp. 183-188 vol.1.

[KUH08a] B. Kuhfuß and C. Schenck, "Einsatzmöglichkeiten von Hybridkinematiken für die Hochgeschwindigkeitsbearbeitung von Großbauteilen," in Fertigungsmaschinen mit Parallelkinematiken- Forschung in Deutschland-Aachen: Shaker-Verlag, 2008, pp. 409-430.

[KUH08b] B. Kuhfuß, B. Orlik, S. Schädlich, and H. Groke, "Wavelet basiertes Echtzeitsystem zur Überwachung von Prozess- und Maschinenzustandsänderungen," in SPS/IPC/Drives Elektrische Automatisierung - Systeme und Komponenten - Fachmesse & Kongress, Berlin, 2008, pp. 131-139.

[KUH11a] L. Li, C. Schenck and B. Kuhfuss, "Short Time Identification of Modal Parameters," in Proc. 22nd International Conference on Computer-Aided Production Engineering (CAPE) Edinburgh Scotland, 2011.

[KUH11b] B. Kuhfuss, E. Moumi and V. Piwek, "Load measurement during rotary swaging of micro components using strain gauges," in ICOMM, 2011.

[KUH11c] M. G. A. Nassef, L. Li, C. Schenck, and B. Kuhfuss, Short Time Identification of Feed Drive Systems using Nonlinear Least Squares Method, World Academy of Science, Engineering and Technology, 2011, vol. 59, pp. 1643-1648.

[KUH11d] L. Linghan, B. Kanning, C. Schenck, and B. Kuhfuss, "Comparing different approaches for model parameters identification in short time," in Signal Processing and Information Technology (ISSPIT), 2011 IEEE International Symposium on, 2011, pp. 426-431.

[KUH11e] L. Li, C. Schenck and B. Kuhfuss, Modal Paramters Identification Accuracy with a Short Time Paramtric Algorithm, Key Engineering Materials, 2011, vol. 486, pp. 221-224.

[KUT04] M. Kutner, C. Nachtsheim and J. Neter, Applied Linear Regression Models: McGraw-Hill/Irwin, 2004.

[LED06] Y. Ledoux, S. Samper, H. Favreliere, F. Formosa, E. Pairel, and R. Arrieux, Optimisation of a stamping process by a design of experiment linked to a modal analysis of geometric defects, Archives of Civil and Mechanical Engineering, 2006, vol. 6, pp. 5-17.

[LIT95] J. D. Littler and B. R. Ellis, "Measuring the dynamic characteristics of prototype structures," in A State of the Art in Wind Engineering New Delhi: Wiley Eastern Limited, 1995, pp. 133-154.

[LIU06] Y. B. Liu, Q. Wu, Z. Y. Ma, and K. G. Yan, "An Improved Hilbert-Huang Transform and Its Application in Faults Signal Analysis," in Mechatronics and Automation, Proceedings of the 2006 IEEE International Conference on, 2006, pp. 2426-2431.

[MAL99] S. Mallat, A Wavelet Tour of Signal Processing: Academic Press, 1999.

[MAI97] N. Maia and J. Silva, Theoretical and Experimental Modal Analysis. Taunton: Research Studies Press, 1997.

[MCL70] V. R. McLamore and G. C. H. I, Ambient Vibration of Two Suspension Bridges, Journal of the Structural Division, 1970, vol. 10, pp. 2567-2582.

[MEY93] Y. Meyer and R. D. Ryan, Wavelets: Society for Industrial and Applied Mathematics, 1993.

[MOH04] P. Mohanty and D. J. Rixen, Operational modal analysis in the presence of harmonic excitation, Journal of Sound and Vibration, 2004, vol. 270, pp. 93-109.

[NAG09] NAGHIPOUR, M., MEHRZADI, M., TAHERI, F., ZOU, and G. P., Polynomial correction function for half-power bandwidth (HPB) method of damping of glulam beams reinforced with e-glass reinforced epoxy polymer (GRP), 2009, vol. 36, p. 12.

[NAS11] M. G. Nassef, Mechanical Properties Prediction of Engineering Materials: LAP Lambert Academic Publishing AG & Co KG, 2011.

[OUY07] H. Ouyang, Stationary and non-stationary vibration of atomising discs, Journal of Sound and Vibration, 2007, vol. 308, pp. 699-708.

[PAD04] L. R. Padovese, Hybrid time-frequency methods for non-stationary mechanical signal analysis, Mechanical Systems and Signal Processing, 2004, vol. 18, pp. 1047-1064.

[PAP81] R. S. Pappa and S. R. Ibrahim, A Parametric Study of the Ibrahim Time Domain Modal Identification Algorithm, Shock and Vibration Information Center The Shock and Vibration Bull., 1981, vol. 3, pp. 43-72.

[PET00] K. A. Petsounis and S. D. Fassois, Non-staionary functional series tarma vibration modelling and analysis in a planer manipulator, Journal of Sound and Vibration, 2000, vol. 231, pp. 1355-1376.

[PET01] A. Peter, Experimental Modal Analysis: A Simple Non-Mathematical Presentation, Sound and Vibration, 2001, vol. 35, pp. 20-31.

[PIN06] D. Pines and L. Salvino, Structural health monitoring using empirical mode decomposition and the Hilbert phase, Journal of Sound and Vibration, 2006, vol. 294, pp. 97-124.

[POO07] C. W. Poon and C. C. Chang, Identification of nonlinear elastic structures using empirical mode decomposition and nonlinear normal modes, Smart structures and systems, 2007, vol. 3, pp. 423-437.

[POU06] A. G. Poulimenos and S. D. Fassois, Parametric time-domain methods for non-stationary random vibration modelling and analysis -- A critical survey and comparison, Mechanical Systems and Signal Processing, 2006, vol. 20, pp. 763-816.

[ROU01] S. Rouquette and M. Najim, Estimation of frequencies and damping factors by two-dimensional ESPRIT type methods, Signal Processing, IEEE Transactions on, 2001, vol. 49, pp. 237-245.

[ROY89] R. Roy and T. Kailath, ESPRIT-estimation of signal parameters via rotational invariance techniques, Acoustics, Speech and Signal Processing, IEEE Transactions on, 1989, vol. 37, pp. 984-995.

[SAV64] Savitzky, A.; Golay, M.J.E. "Smoothing and Differentiation of Data by Simplified Least Squares Procedures". Analytical Chemistry 36 (8): 1627–39. doi:10.1021/ac60214a047,1964.

[SCH01] T. L. Schmitz, M. A. Davies and M. D. Kennedy, Tool Point Frequency Response Prediction for High-Speed Machining by RCSA, Journal of Manufacturing Science and Engineering, 2001, vol. 123, pp. 700-707.

[SCH13] S. Schädlich, Potentiale prozessangepasster Wavelets für signalbasierte Condition Monitoring Systeme, Dissertation Dr.-Ing., Universität Bremen, Juli 2013, Berichte aus dem Institut für Strukturmechanik und Produktionsanlagen, Universität Bremen, Hrsg. R. Kienzler, B. Kuhfuß, K. Tracht, ISBN 978-3-8440-1976-6.

[SDT12] SDTools, Structural Dynamics Toolbox User's Guide: SDTools, 2012.

[SEL12] V. Sellmeier and B. Denkena, High speed process damping in milling, CIRP Journal of Manufacturing Science and Technology, 2012, vol. 5, pp. 8-19.

[SER00] O. Sergeyev and Z. Mroz, Derivative analysis and optimal design of 3d frame structure for stress and frequency constraints, 2000, vol. 75, pp. 167-185.

[SIS69] T. R. Sisson, R. L. Kegg and A. S. O. M. Engineers, An Explanation of Low-speed Chatter Effects: ASME, 1969.

[SMI05] J. S. Smith, The local mean decomposition and its application to EEG perception data, J R Soc Interface, 2005, vol. 2, pp. 443-54.

[SOK01] M. Soković and K. Mijanović, "Ecological aspects of the cutting fluids and its influence on quantifiable parameters of the cutting processes", Journal of Materials Processing Technology, 2001, vol. 109, pp. 181-189.

[SPI09] M. D. Spiridonakos and S. D. Fassois, Parametric identification of a time-varying structure based on vector vibration response measurements, Mechanical Systems and Signal Processing, 2009, vol. 23, pp. 2029-2048.

[THA09] Y. T. Thai-Hoa Le, "Modal identification ambient vibration structure using frequency domain decompostition and wavelet transform," in The 7th Asia-Pacific Conference on Wind Engineering Taipei, Taiwan, 8.

[TLU78] J. Tlusty, Analysis of the State of Research in Cutting Dynamics, Annals of the CIRP, 1978, vol. 27, pp. 583-589.

[TLU00] T. J., Manufacturing Processes and Equipment. New Jersey USA: Prentice Hall, 2000.

[TUN12] L. T. Tunç and E. Budak, Effect of cutting conditions and tool geometry on process damping in machining, International Journal of Machine Tools and Manufacture, 2012, vol. 57, pp. 10-19.

[VAN82] J. K. Vandiver, A. B. Dunwoody, R. B. Campbell, and M. F. Cook, A Mathematical Basis for the Random Decrement Vibration Signature Analysis Technique, Journal of Mechanical Design, 1982, vol. 104, pp. 307-313.

[WAN05] D. Wang, W. H. Zhang and J. S. Jiang, What are the repeated frequencies? Journal of Sound and Vibration, 2005, vol. 281, pp. 1186-1194.

[WAN12] Y. Wang, Z. He, J. Xiang, and Y. Zi, Application of local mean decomposition to the surveillance and diagnostics of low-speed helical gearbox, Mechanism and Machine Theory, 2012, vol. 47, pp. 62-73.

[WEC90] M. Weck, Werkzeugmaschinen Band 4. Messtechnische Untersuchung und Beurteilung: VDI Verlag, 1990.

[WEL67] P. D. Welch, The Use of Fast Fourier Transform for the Estimation of Power Spectra: A Method Based on Time Averaging Over Short, Modified Periodograms, IEEE Trans. Audio &Electroacoust, 1967, vol. AU-15, pp. 70-73.

[WÖL05] H. P. Wölfel, Maschinendynamik, Umdruck zur Vorlesung ed.: Technische Universität Darmstadt Fachgebiet Maschinendynamik, 2005.

[YAN84] YANG, J. C. S., CHEN, J., DAGALAKIS, and N. G., Damage detection in offshore structures by the random decrement technique, Journal of energy resources technology, 1984, vol. 106,

[YAN05] S. L. J. Yang, Identification of parametric variations of structures based on least squares estimation and adaptive tracking technique, Journal of Engineering Mechanics, 2005, pp. 290-298.

[YAN08] J. Z. Yang, C. W. Liu and W. G. Wu, "A hybrid method for the estimation of power system low-frequency oscillation parameters," in Power and Energy Society General Meeting - Conversion and Delivery of Electrical Energy in the 21st Century, 2008 IEEE, 2008, p. 1-1.

[YIN08] H. P. Yin, A new theoretical basis for the bandwidth method and optimal power ratios for the damping estimation, Mechanical Systems and Signal Processing, 2008, vol. 22, pp. 1869-1881.

[YON11] Y. J. S. M. He Yong, "Milling Experimental Investigation on Titanium Alloy Ti6Al4V under Different Cooling/Lubrication Conditions," in Advanced Materials Research, 2011, pp. 406-411.

[ZAG09] I. Zaghbani and V. Songmene, Estimation of machine-tool dynamic parameters during machining operation through operational modal analysis, International Journal of Machine Tools and Manufacture, 2009, vol. 49, pp. 947-957.

[ZEN12] M. Zeng, J. Liu, X. Zhang, T. Shi, and G. Liao, Fault Diagnosis of Flip Chip Using Vibration and Modal Analysis, IERI Procedia, 2012, vol. 1, pp. 87-93.

[ZHO07] Z. Zhou, Mechefske, C. K., and F. Xi, Nonstationary vibration of a fully flexible parallel kinematic machine, Journal of vibration and acoustics, 2007, vol. 129, p. 8.

[ZHO10] W. Zhong, D. Zhao and X. Wang, A comparative study on dry milling and little quantity lubricant milling based on vibration signals, International Journal of Machine Tools and Manufacture, 2010, vol. 50, pp. 1057-1064.

[ZUB00] A. Zubaydi and M. R. H. A, Damage identification in stiffened plates using the random decrement technique, Oceanic Engineering International, 2000, vol. 1, pp. 20-30.

Student work

Results which have arisen in the context of the support of the following student work are contained in the work in hand:

N. Thöne, "Sensorbasierte Überwachung der KSS-Effektivität in der Zerspanzone,". vol. Masterthesis Bremen Germany: Bremen of University, 2012.

J. Carrillo Garcia, „Force measurement in micro rotary swaging“. Vol. Masterthesis Bremen Germany: Bremen of University, 2012.

Appendix

A Data Processing

A.1 Eigenvalue and eigenvector

For an $n \times n$ square matrix A, this matrix can be expressed as follows:

$$Ax = \lambda x \tag{A.1}$$

where λ is a real value, and x is a nonzero vector. They are called eigenvalue and eigenvector of matrix A, respectively. x is the eigenvector corresponding to the eigenvalue λ.

Eq. (A.1) can be using a identity matrix I written in:

$$(A - \lambda I)x = 0 \tag{A.2}$$

There is a nontrivial solution to the equation (A.2). This happens if and only if the matrix $A - \lambda I$ is not invertible. That means if only the determinant of $A - \lambda I$ is 0. So the eigenvalue λ can be obtained to solve the equation:

$$\det(A - \lambda I) = 0 \tag{A.3}$$

where

$$\det(A - \lambda I) = \begin{vmatrix} a_{11} - \lambda & a_{12} & \cdots & a_{1m} \\ a_{21} & a_{22} - \lambda & \cdots & a_{2m} \\ \vdots & \vdots & \ddots & \vdots \\ a_{m1} & a_{m2} & \cdots & a_{mm} - \lambda \end{vmatrix} = P_n(\lambda) \tag{A.4}$$

The $\det(A - \lambda I)$ can be expressed as a n-degree polynomial with the variable λ. This polynomial is called characteristic polynormial of matrix A.

Now, to find the eigenvalue λ is simplified as solving the roots of this polynomial. The n roots are the n eigenvalues of matrix A that make $A - \lambda I$ singular. For each eigenvalue λ, the eigenvector x can be obtained by solving the equation $(A - \lambda I)x = 0$.

A.2 Frequency domain quadratic integral

There are various implementations of the frequency response functions depending on the response parameters. According to physical means the displacement, velocity and acceleration as system response can be specified [EWI00].

Usually, accelerometers are used for the experimental modal testing. The acceleration signal as a function of time is in complex notation expressed as:

$$\ddot{x} = A\sin(\omega t) \tag{A.5}$$

Expressions for velocity and displacement can be obtained by simple integral:

$$\dot{x} = -A/\omega * \cos(\omega t) + C \tag{A.6}$$

$$x = -A/\omega^2 * \sin(\omega t) + Ct + D \tag{A.7}$$

Considering the equation in frequency domain, the other type of FRF which is called receptance of FRF can be obtained from accelerance of FRF:

$$X(\omega) = -\frac{\ddot{X}(\omega)}{\omega^2} \tag{A.8}$$

A.3 Half power bandwidth method

It is well known that half power bandwidth is one of the damping calculation methods applying to well-separated modes of multi degree of freedom systems. It is based on interpreting three values of frequency, which are three characteristic points corresponding to extreme of the magnitude frequency response function (by f_{res}) and the points (by f_1 and f_2) of amplitude of resonance frequency, also $f_{res}/\sqrt{2}$.

For a small damping ratio can be expressed approximately:

$$\xi = \frac{f_2 - f_1}{2 f_{res}} \tag{A.9}$$

Alternatively if ξ is not assumed small, the relationship becomes [BUT04]:

$$\xi = \sqrt{0.5 - \sqrt{0.0625(\frac{f_2 - f_1}{f_{res}})^2 (\frac{f_2 + f_1}{f_{res}})^2}} \quad \text{(A.10)}$$